

PRESSURE DROP DURING FORCED CONVECTION LOCAL BOILING
OF WATER CONTAINING AN ORGANIC ADDITIVE

By

Reid Robinson June

Bachelor of Science
Oklahoma State University
Stillwater, Oklahoma
1954

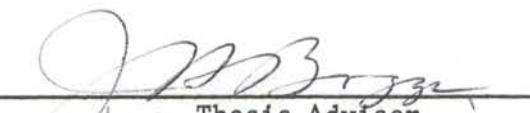
Master of Science
Oklahoma State University
Stillwater, Oklahoma
1959

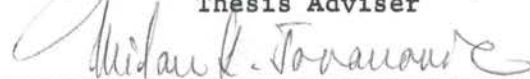
Submitted to the Faculty of the Graduate School of
the Oklahoma State University
in partial fulfillment of the requirements
for the degree of
DOCTOR OF PHILOSOPHY
May, 1961

OCT 10 1961


PRESSURE DROP DURING FORCED CONVECTION LOCAL BOILING
OF WATER CONTAINING AN ORGANIC ADDITIVE


Thesis Approved:



Thesis Adviser


Michael K. Torrance





O. H. Hamilton



Dean of the Graduate School

472400

ACKNOWLEDGEMENT

The author wishes to acknowledge the financial assistance provided by the National Science Foundation. This assistance was in the form of a fellowship awarded the author and sponsorship of the research.

The guidance and assistance of Dr. J. H. Boggs throughout the author's entire graduate program was greatly appreciated.

The following persons contributed materially to the success of the investigation and their assistance is gratefully acknowledged: Dr. J. B. West, Dr. M. K. Jovanovic, Dr. O. H. Hamilton, P. A. Butler, M. H. Sabet, Prof. William Granet, Prof. B. S. Davenport, J. A. McCandless, G. M. Cooper, and Mrs. Sonya Giddens.

Recognition is due the personnel of the Oklahoma State University Computing Center for their able assistance during the data reduction phase of the research.

Gratitude is expressed to the author's family, and especially to his wife, Jeanne, for their many sacrifices during the course of the research.

TABLE OF CONTENTS

Chapter	Page
I. INTRODUCTION	1
II. SUMMARY OF PREVIOUS INVESTIGATIONS	3
III. ANALYSIS OF PRESSURE DROP WITH HEAT TRANSFER	12
IV. EXPERIMENT APPARATUS	19
V. EXPERIMENTAL PROCEDURE	33
VI. EXPERIMENTAL RESULTS AND CORRELATION OF DATA	43
VII. ANALYSIS OF EXPERIMENTAL ERRORS	65
VIII. CONCLUSIONS AND RECOMMENDATIONS	71
SELECTED BIBLIOGRAPHY	73
APPENDICES	75
A. Calibration and Performance Curves for Experimental Apparatus	75
B. Representative Pressure Profiles and Gradients	80
C. Properties of Mixtures	85
D. Generalized Least Squares Method of Correlating Experimental Data	102
E. Nomenclature	107

LIST OF TABLES

Table	Page
I. The Effect of Additives on the Pressure Gradient When Compared to Water	49
II. Test Data	55
III. Summary of Experimental Errors in Flow Measurement . .	68
IV. Summary of Constants in Bingham's Equation	88
V. For Transit Statements for Data Correlation Program . .	106

LIST OF FIGURES

Figure	Page
1. Temperature Variation Along the Length of a Heated Tube	9
2. Forced Convection Heat Transfer Coefficient	17
3. Schematic Diagram of Test Apparatus	21
4. Test Section	23
5. Instrument and Control Identification	32
6. Isothermal Friction Factor	34
7. Isothermal Pressure Drop	35
8. Typical Reproduction Run	37
9. Gas Removed From System Fluid	40
10. Typical Pressure Gradient Along Test Section	44
11. Variation of the Pressure Gradient for Water Along a Heated Tube	47
12. Variation of the Pressure Gradient Ratio with the Temperature Ratio for Water	52
13. Correlation of Data	54
14. Moyno Pump Characteristics	76
15. Orifice Calibration Curve	77
16. Thermocouple Calibration Curve	78
17. Voltage Drop Along Test Section	79
18. Experimental Pressure Profile---Run No. 0008	81
19. Experimental Pressure Profile---Run No. 2214	82

LIST OF FIGURES (Continued)

Figure	Page
20. Experimental Pressure Profile---Run No. 1310	83
21. Experimental Pressure Gradients	84
22. Viscosity Ratio for Mixtures	89
23. Viscosity of Pure Liquids	90
24. Thermal Conductivity Ratio for Mixtures	92
25. Thermal Conductivity of Pure Liquids	93
26. Density Ratio for Mixtures	95
27. Density of Pure Liquids	96
28. Heat Capacity Ratio for Mixtures	97
29. Heat Capacity of Pure Liquids	98
30. Saturation Temperature Ratio for Mixtures	100
31. Variation of Saturation Temperature with Pressure for Pure Liquids	101

LIST OF PLATES

Plate	Page
I. Bare Test Section	24
II. Insulated Test Section	25
III. Transformers	26
IV. Rear View of Test Apparatus	27
V. Front View of Test Apparatus	31

CHAPTER I

INTRODUCTION

The current trend in modern heat technology is toward higher and higher rates of energy release per unit volume and area of apparatus. If the thermal energy released by such devices as nuclear reactors, high performance electronic tubes, and rocket engines is not removed from the apparatus, a temperature so high as to make the device inoperable will soon occur. For this reason, an effective means of heat removal or transfer is necessary for the operation of such devices.

The boiling of a liquid in contact with a superheated surface has long been recognized as an effective means of transferring heat. Local boiling is a particular type of boiling in which the bulk or average temperature of the fluid is below the saturation temperature corresponding to the absolute pressure of the fluid.

Heat transfer in local boiling has been the subject of considerable research (1), (2), (3), (4). Pressure drop associated with forced convection local boiling has been less thoroughly investigated (5), (6), (7). The purpose of this investigation was to determine the effect of an organic additive in distilled water on pressure drop during forced convection local boiling.

The stimulus for this investigation was provided by free convection boiling studies on water containing an organic additive (8), (9). These

studies indicated that water containing a small percentage of certain additives had markedly different heat transfer characteristics than pure water. Information on the effect of additives on pressure drop during forced convection local boiling is desirable for a more complete understanding of the process and for the prediction of pressure drop occurring during the process.

Experimental measurements of pressure drop were made in nonboiling and local boiling forced convection flow in an electrically heated horizontal tube. Experimental data were collected with the following combinations of fluids as the heat transfer medium: distilled water; distilled water containing methanol; distilled water containing butanol; and distilled water containing methyl ethyl ketone. The experimental data were correlated in terms of the nonboiling pressure gradient for water, the viscosity of water and the mixture, additive concentration, and the following temperatures: bulk temperature at a particular point, bulk temperature at the start of local boiling, and the saturation temperature corresponding to the system pressure. The resulting correlation was compared with previously published correlations for distilled water.

The range of variables covered in this investigation was:

Heat Flux: 60,000 to 250,000 Btu/hr-ft²

System Pressure: 50 to 250 psia

Mass Velocity: 190 to 400 lb/ft²-sec

Additives and Concentrations:

Methanol: 1.00%, 2.00% and 2.99% by weight

Butanol: 1.00%, 2.08% and 3.12% by weight

Methyl Ethyl Ketone: 1.00%, 2.03% and 3.00% by weight.

CHAPTER II

SUMMARY OF PREVIOUS INVESTIGATIONS

A survey of the literature revealed that little information was available on pressure drop during forced convection local boiling. According to Leppert, Costello and Hoglund (1) the effect of an additive on pressure drop in local boiling had not been explored prior to 1958. Private correspondence with Leppert (10) revealed no knowledge of work in this area since that time. No analytical method for predicting pressure drop in local boiling was found in the literature.

A literature survey on this subject might be logically divided into two parts: (A) information concerning pressure drop in local boiling for water, and (B) information concerning the effect of additives in water upon boiling characteristics which would in turn affect pressure drop.

Two correlation equations for predicting local boiling pressure drop for water were found. Reynolds (6) presents the following equation for the range of variables indicated:

$$(\Delta P)_{LB} = \left(\frac{dP}{dL} \right)_0 \frac{G' D C_p (\Delta t_{sub})_0}{4 a q''} \sinh \left[\frac{4 a q'' L}{G' D C_p (\Delta t_{sub})_0} \right] \quad \text{II-1}$$

where

system pressure varied from 45 to 100 psia;

mass velocity varied from 343 to 652 lb/sec-ft²;

heat flux varied from 130,000 to 300,000 Btu/hr-ft².

The terms in Reynolds' equation are:

$(\Delta P)_{LB}$ = local boiling pressure drop, in. of H_2O ;

$(\frac{dP}{dL})_o$ = isothermal liquid pressure gradient at average bulk water temperature, in. of H_2O/ft ;

G' = mass velocity of fluid through tube, $lb/hr-ft^2$;

D = inside diameter of tube, ft;

C_p = heat capacity of water, $Btu/lb^\circ F$;

$(\Delta t_{sub})_o$ = subcooling of fluid at point where local boiling starts, or the difference between saturation temperature and bulk temperature at this point, $^\circ F$;

a = parameter related to heat flux (q'') by $a = 4.6 \times 10^{-6} q'' + 1.2$, dimensionless;

q'' = heat flux, $Btu/hr-ft^2$;

L = distance from the point where local boiling starts to any point in question (along the length of local boiling), up to a point where net boiling starts, ft.

Reynolds' equation correlated his experimental data within $\pm 20\%$.

Tanger (5) presents the following equation for predicting pressure drop for the range of variables indicated:

$$(\Delta P)_{LB} = \left(\frac{dP}{dL}\right)_{NB} \left[\frac{G D C_p (\Delta t_{sub})_o}{4 q''} \right] \left[\frac{L}{L_B} + \left\{ e^{0.2(1-P/200)} \right\} \right. \\ \left. \left\{ \frac{q''}{40,000} - 2 \right\} \left\{ 0.04332 \left(\frac{L}{L_B} \right) + 1.25293 \left(\frac{L}{L_B} \right)^2 - \right. \right. \quad II-2 \\ \left. \left. 7.27288 \left(\frac{L}{L_B} \right)^3 + 9.30486 \left(\frac{L}{L_B} \right)^4 \right\} \right]$$

where

system pressure varied from 50 to 250 psia;

heat flux varied from 100,000 to 300,000 $Btu/hr-ft^2$;

mass velocity varied from 194 to 347 $lb/sec-ft^2$.

The variables in Tanger's equation are:

$(\Delta P)_{LB}$ = local boiling pressure drop, in. of H_2O ;

$\left(\frac{dP}{dL}\right)_{NB}$ = pressure gradient at the start of local boiling, in. H_2O/ft ;

G = mass velocity, $lb/hr-ft^2$;

C_p = heat capacity of water, $Btu/lb-^{\circ}F$;

$(\Delta t_{sub})_o$ = fluid subcooling at the start of local boiling, $^{\circ}F$;

q'' = heat flux, $Btu/hr-ft^2$;

(L/L_B) = ratio of length of test section from start of local boiling to any point in the local boiling length, dimensionless;

p = system pressure, psia.

The primary difference in the above two equations resulted from an attempt by Tanger to account for the effects of system pressure and to account for the plateaus found in the pressure profiles in the first half of the local boiling length. Tanger's equation correlated his experimental data within $\pm 25\%$ and the data of Reynolds within $\pm 40\%$.

Bonilla (7) gives the following relation for approximating local boiling pressure drop if the local boiling heat transfer coefficient is known:

$$(\Delta P)_{LB} = (\Delta P)_{NB} \left(\frac{h_{LB}}{h_{NB}} \right)^{2.3} \quad \text{II-3}$$

where

ΔP_{LB} = pressure drop in local boiling;

ΔP_{NB} = pressure drop for nonboiling;

h_{LB} = local boiling heat transfer coefficient;

h_{NB} = nonboiling heat transfer coefficient.

Both Tanger's and Reynolds' equations contain the parameters of local boiling length, L_B , and distance from the point of start of local boiling to another point in the local boiling length, L . It is apparent that in order to use these relations the point of the start of local boiling along the tube length must be established. Several methods were found for determining the location of this point. Jens and Lottes (11), from an analysis of MIT, UCLA, and Purdue data, present the following relation for the difference in inside wall temperature and saturation temperature at the start of local boiling for water in contact with stainless steel or nickel surfaces:

$$(\Delta t)_{sat} = \frac{60 \left(\frac{q''}{10^6} \right)^{1/4}}{e^{p/900}} \quad \text{II-4}$$

where

Δt_{sat} = wall superheat, °F;

q'' = heat flux, Btu/hr-ft²;

p = system pressure, psia.

The range of variables considered in the development of this equation was:

q'' : up to 3,650,000 Btu/hr-ft²;

p : up to 2,000 psia;

G : up to 7,650,000 lb/hr-ft².

The equation predicted the temperature difference within $\pm 14^\circ\text{F}$.

A second expression for Δt_{sat} has been given by McAdams, Addoms, and Kennel (12). This expression is:

$$(\Delta t)_{sat} = C' (q'')^{0.26} \quad \text{II-5}$$

where

Δt_{sat} = wall superheat, °F;

q'' = heat flux, Btu/hr-ft²;

$C' = 0.189$ for 0.30 cubic centimeters of air per liter;

$C' = 0.074$ for 0.06 cubic centimeters of air per liter.

If the inside wall temperatures in the nonboiling region of the tube are plotted as a function of length along the tube, the intersection with the temperature predicted by Equation II-4 or II-5 should indicate the point where local boiling starts. The following relation of McAdams (13) may be used in determining wall temperature in the nonboiling region:

$$\frac{hd}{k_b} = 0.023 \left(\frac{Gd}{\mu_b} \right)^{0.8} \left(\frac{\mu C_p}{k} \right)_b^{0.4} \quad \text{II-6}$$

where the subscript b indicates evaluation at bulk temperature; and

h = heat transfer film coefficient;

d = tube diameter;

k = thermal conductivity;

G = mass velocity;

μ = dynamic viscosity;

C_p = heat capacity.

Solving for h from Equation II-6 and substituting into the fundamental relation $q'' = h(t_w - t_b)$ permits evaluation of the inside wall temperature t_w , at a particular bulk temperature t_b , and a particular heat flux q'' . The value of the coefficient h may also be found from Colburn's (14) relation

$$\frac{h}{(C_p)_b G} \left(\frac{\mu C_p}{k} \right)_F^{2/3} = \frac{0.023}{(dG/\mu_F)^{0.2}} \quad \text{II-7}$$

where the subscript F indicates property evaluation at a "film" temperature equal to $\frac{t_w + t_b}{2}$.

Equation II-7 has some preference over Equation II-6 in that the temperature at which a particular property is evaluated is based on the process occurring at that temperature. Figure 1 is a plot of inside wall temperature and bulk temperature as a function of distance along the tube for the nonboiling and local boiling regions of the tube. Point A denotes the start of local boiling.

Another method of determining the start of local boiling has as its basis the shape of the pressure profile along the tube length. Tanger (5) found that the pressure drop in the nonboiling region of the tube was a linear function of distance along the tube. A change in the shape of the pressure profiles was due to a change in the flow or heat transfer process. This change was the transition from heat transfer in forced convection to heat transfer by local boiling. Tanger (5) was able to predict the start of local boiling within $1\frac{1}{2}$ inches by examining the shape of the pressure profiles.

Once the start of local boiling has been determined, the local boiling length may be found in the manner described by Reynolds (6) and Tanger (5). If a knowledge of fluid bulk temperature at inlet and outlet of the tube is assumed, with no net vapor generation, the familiar relation $q = \dot{m} C_p (\Delta t)_b$ may be used to find the amount of subcooling at the start of local boiling. In this relation,

q = heat flow, Btu/hr;

\dot{m} = mass flow rate, lb/hr;

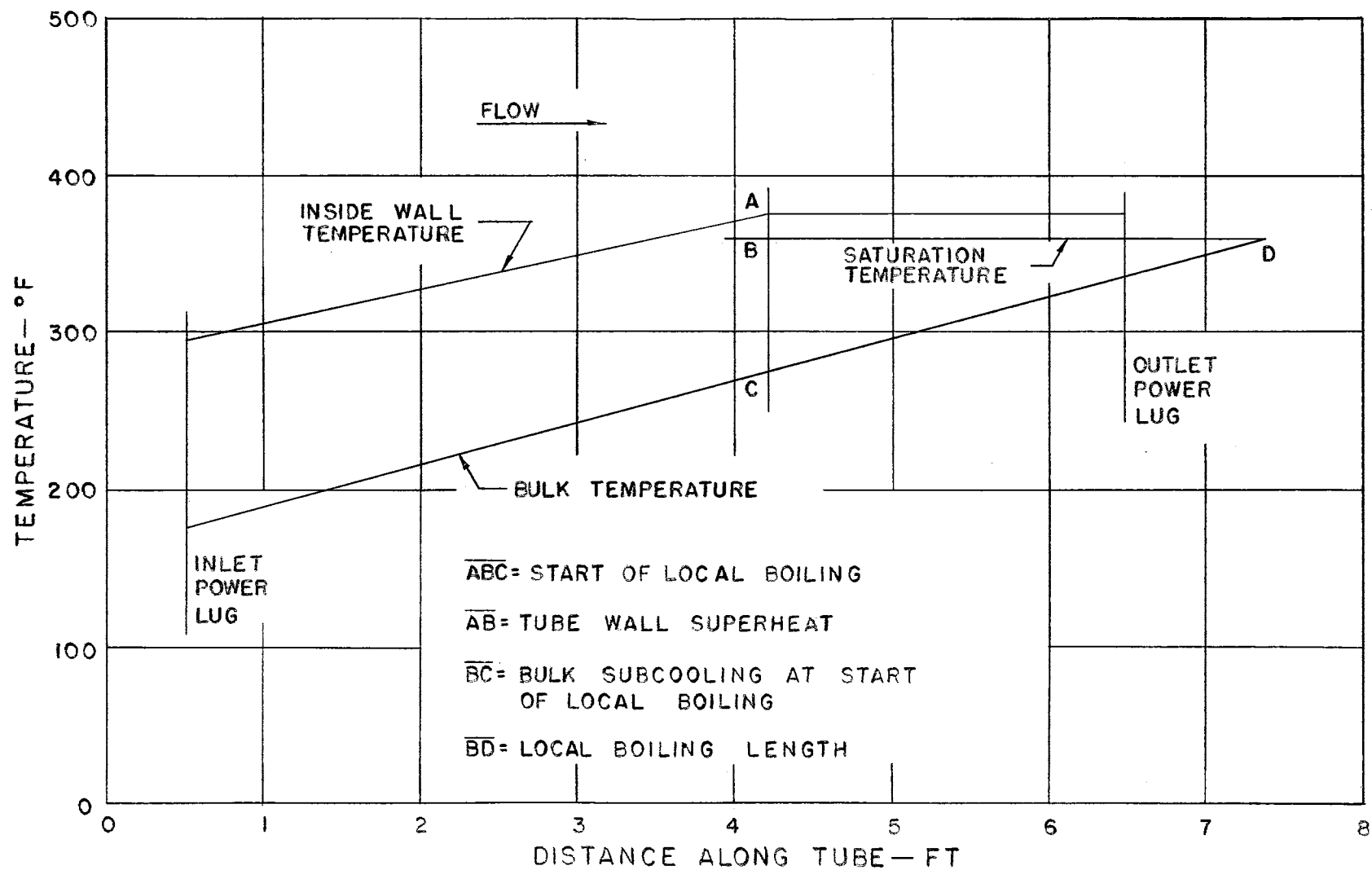


Figure 1. Temperature Variation Along the Length of a Heated Tube

C_p = heat capacity, Btu/lb°F;

$(\Delta t)_b$ = change of bulk temperature, °F.

The subcooling at the start of local boiling is denoted by \overline{BC} in Figure 1.

Since local boiling occurs until the bulk temperature is equal to the saturation temperature for a given system pressure, or until $(\Delta t)_{sub} = 0$, the length of tube required to increase the bulk temperature to the saturation temperature may be found for a particular value of the heat flux. This length of tube is the local boiling length and is denoted by \overline{BD} in Figure 1.

The results of Leppert et al (1) revealed that small amounts of certain organic fluids in distilled water decreased average bubble size and produced much smoother boiling than could be obtained with pure water. Photographs from this study revealed a marked decrease in bubble size and increased smoothness of boiling for water-alcohol mixtures, compared with pure water at the same values of heat flux and fluid velocity. The additives used in this study were propanol in concentrations of 0.5 and 1.5% by weight and methanol in concentrations of 1.4 and 2.65% by weight. It was concluded in this investigation that the undesirable conditions of density fluctuation, lower average density, and higher static pressure drop associated with local boiling of water should be alleviated to some extent by the smaller bubble size produced by the additive.

Van Wijk, Vos and van Stralen (8) have investigated the influence of concentration in binary mixtures upon the maximum heat flux attainable in nucleate boiling. Mixtures of water with ethanol, 1-propanol, tert-butanol, n-butanol, 1-pentanol, 1-octanol, acetone, methyl ethyl ketone,

and ethyleneglycol, respectively, were investigated. These were free convection experiments conducted at atmospheric pressure, using an electrically heated platinum wire 0.02 cm in diameter and 6 cm long immersed in the fluid contained in a glass vessel. Photographs from this study revealed that the bubbles formed in a mixture of water containing 2% n-butanol by weight were much smaller than the bubbles formed in either pure component at the same heat flux. It was also found for a mixture of 4.2% by weight of methyl ethyl ketone in water that the size of the bubbles leaving the heating surface was smaller than for either of the pure components. It was of interest to note that the advantage of an additive in water upon $(q/A)_{\max}$, i.e., the attainability of a higher maximum heat flux than with pure water, occurred at relatively low concentrations, less than 10% by weight in most cases.

The effect of pressure on bubble size for water containing organic additives was investigated by van Stralen (9). The studies were in free convection at pressures less than atmospheric. It was found that the bubble size increased with decreasing pressure, but that the size of bubbles found in the mixtures remained smaller than those of either pure component at the same conditions. Mixtures considered in this investigation were water with 1-pentanol, methyl ethyl ketone, n-butanol, acetone, 1-propanol and ethanol, respectively. Concentration of the additives was from 0 to 20% by weight. As noted in the investigation by van Wijk et al (8), at atmospheric pressure, the maximum value of (q/A) for a given pressure occurred at a relatively low concentration. The concentration for $(q/A)_{\max}$ appeared essentially independent of pressure. The range of pressures considered in this investigation was from 10 cm Hg to 76 cm Hg.

CHAPTER III

ANALYSIS OF PRESSURE DROP WITH HEAT TRANSFER

The problem of predicting static pressure drop during the flow of a fluid in a heated tube is complicated by temperature variation along the tube length and across the tube cross section at any axial location. A relation between heat transfer and fluid friction was derived by Reynolds in 1874. This relation, known as Reynolds' Analogy, was first derived for flow over a flat plate of fluids for which the Prandtl number was unity. Subsequent modification, to allow the application of the analogy to fluids of Prandtl number other than unity and to configurations other than a flat plate, led to the general form of Reynolds' Analogy. The application of the general form in predicting nonboiling pressure gradients will be described in this chapter. Other methods of predicting nonboiling pressure gradients will be discussed and compared to the experimental gradients found in this investigation.

Reynolds' Analogy was originally expressed in mathematical form for turbulent flow in a tube of constant wall temperature. The analogy may be applied in the case of variable tube wall temperature if variations of fluid property values with temperature are considered. Quantitative results may be obtained by a stepwise method if the rate of temperature change along the tube length is not great.

The general form of Reynolds' Analogy may be written as:

$$St Pr^{2/3} = \frac{C_f}{2} \quad \text{III-1}$$

where

$$St = \text{Stanton number} = \frac{h}{\rho_u C_p};$$

$$Pr = \text{Prandtl number} = \frac{\mu C_p}{k};$$

C_f = the skin friction coefficient for a flat plate.

A friction coefficient f for flow inside a tube may be derived in terms of the average skin friction coefficient for a flat plate by the following steps. The drag force D on the inside surface of a tube of diameter d due to pressure drop ΔP in length L may be written as

$$D = \Delta P \left(\frac{\pi}{4} \right) d^2. \quad \text{III-2}$$

The drag force is usually written in terms of the average skin friction coefficient as

$$D = C_f A \left(\frac{\rho u^2}{2 g_c} \right) \quad \text{III-3}$$

where

A = the surface area over which the force acts, or $\pi d \cdot L$.

The pressure drop for flow in a tube is usually written as

$$\Delta P = f \left(\frac{L}{d} \right) \left(\frac{\rho u^2}{2 g_c} \right). \quad \text{III-4}$$

Eliminating the drag force D from Equations III-2 and III-3 and substituting for ΔP from Equation III-4 yields:

$$f \left(\frac{L}{d} \right) \frac{\rho u^2}{2 g_c} \frac{\pi}{4} d^2 = C_f \pi d \cdot L \left(\frac{\rho u^2}{2 g_c} \right)$$

or

$$f = 4C_f. \quad \text{III-5}$$

Equation III-4 may be written in terms of the skin friction coefficient as

$$\Delta P = 4C_f \left(\frac{L}{d} \right) \left(\frac{\rho u^2}{2g_c} \right). \quad \text{III-6}$$

Differentiating Equation III-6 with respect to L yields:

$$\frac{dP}{dL} = 4C_f \left(\frac{1}{d} \right) \left(\frac{\rho u^2}{2g_c} \right). \quad \text{III-7}$$

Substituting the value of C_f from Equation III-1 in Equation III-6 results in

$$\frac{dP}{dL} = \frac{8}{d} (St Pr^{2/3}) \left(\frac{\rho u^2}{2g_c} \right). \quad \text{III-8}$$

Substituting

$$(dP)_h = 12 \left(\frac{dP}{dL} \right)$$

in Equation III-8 yields an expression for (dP/dL) with units of inches of fluid per foot length:

$$\left(\frac{dP}{dL} \right)_h = \frac{96}{d} (St Pr^{2/3}) \left(\frac{u^2}{2g_c} \right) \quad \text{III-9}$$

where the subscript h indicates a head of fluid.

Since $G = \rho u$, Equation III-9 may be written as

$$\begin{aligned} \left(\frac{dP}{dL} \right)_h &= \frac{48}{d} (St Pr^{2/3}) \left(\frac{G^2}{\rho^2 g_c} \right) \\ &= \frac{48}{d} \left(\frac{G h Pr^{2/3}}{C_p \rho^2 g_c} \right). \end{aligned} \quad \text{III-10}$$

Upon substituting the value for the heat transfer coefficient from Equation II-7 in Equation III-10 one obtains

$$\left(\frac{dP}{dL}\right)_h = \frac{48}{d} \left[\frac{0.023 G}{C_p \rho^2 g_c} \left(\frac{dG}{\mu_F}\right)^{-0.2} \left(\frac{\mu C_p}{k}\right)^{-2/3} C_{p_b} G \text{Pr}^{2/3} \right]. \quad \text{III-11}$$

Since $\text{Pr} = \frac{\mu C_p}{k}$, Equation III-11 may be written as

$$\left(\frac{dP}{dL}\right)_h = \frac{1.104 G^{1.8} (\mu_F)^{0.2}}{d^{1.2} \rho_b^2 g_c}. \quad \text{III-12}$$

The value of the film temperature needed to evaluate the dynamic viscosity in Equation III-12 may be found in the manner described below.

From Newton's law of cooling,

$$q'' = h(t_w - t_b). \quad \text{III-13}$$

The heat transfer coefficient is a function of the film temperature, and consequently a function of the wall and bulk temperatures. For a given heat flux q'' , mass velocity G , and bulk temperature t_b , the film temperature may be found by a graphical method in the following steps:

1. Assume values of $t_w - t_b$;
2. Solve for h_1 from Equation III-13;
3. Solve for h_2 from Equation II-7 for assumed values of t_b , G and t_F ;
4. Plot h_1 and h_2 against $t_w - t_b$.

The correct value of $t_w - t_b$ lies at the intersection of h_1 and h_2 for a given heat flux, mass velocity and bulk temperature.

Since

$$t_F = \frac{t_w + t_b}{2} = \frac{t_w - t_b}{2} + t_b$$

the film temperature may be found for the evaluation of the viscosity in Equation III-12.

The procedure of steps 1 through 3 was programmed for an IBM 650 computer. The results are plotted in Figure 2 for a mass velocity of 299 lb/sec-ft². It was found that the pressure gradients predicted by Equation III-12 were consistently higher than those found experimentally in the nonboiling region of the tube. Since the density is definitely a bulk property, it was apparent that the viscosity should be evaluated at a higher temperature than the film temperature. Previous experiments (5), (15) have indicated that the viscosity should be evaluated at the wall temperature. It was found that a film temperature defined by $t_F = t_b + 2/3(t_w - t_b)$ resulted in calculated nonboiling pressure gradients in best agreement with experimental values.

Other methods exist for calculating the pressure gradient in non-boiling heat transfer. A stepwise method, using isothermal friction factors evaluated from Blasius' Law, was given by Tanger (5). Blasius' Law is

$$f = \frac{0.316}{(Re)^{1/4}} .$$

It was found in the present investigation that the method based on Reynolds' Analogy gave pressure gradients which agreed more closely with experimental values.

Previous studies in local boiling pressure drop resulted in the correlation equations presented in Chapter II. Because of the lack of analytical means for predicting local boiling pressure gradients, the experimental gradients have been expressed as functions of some reference

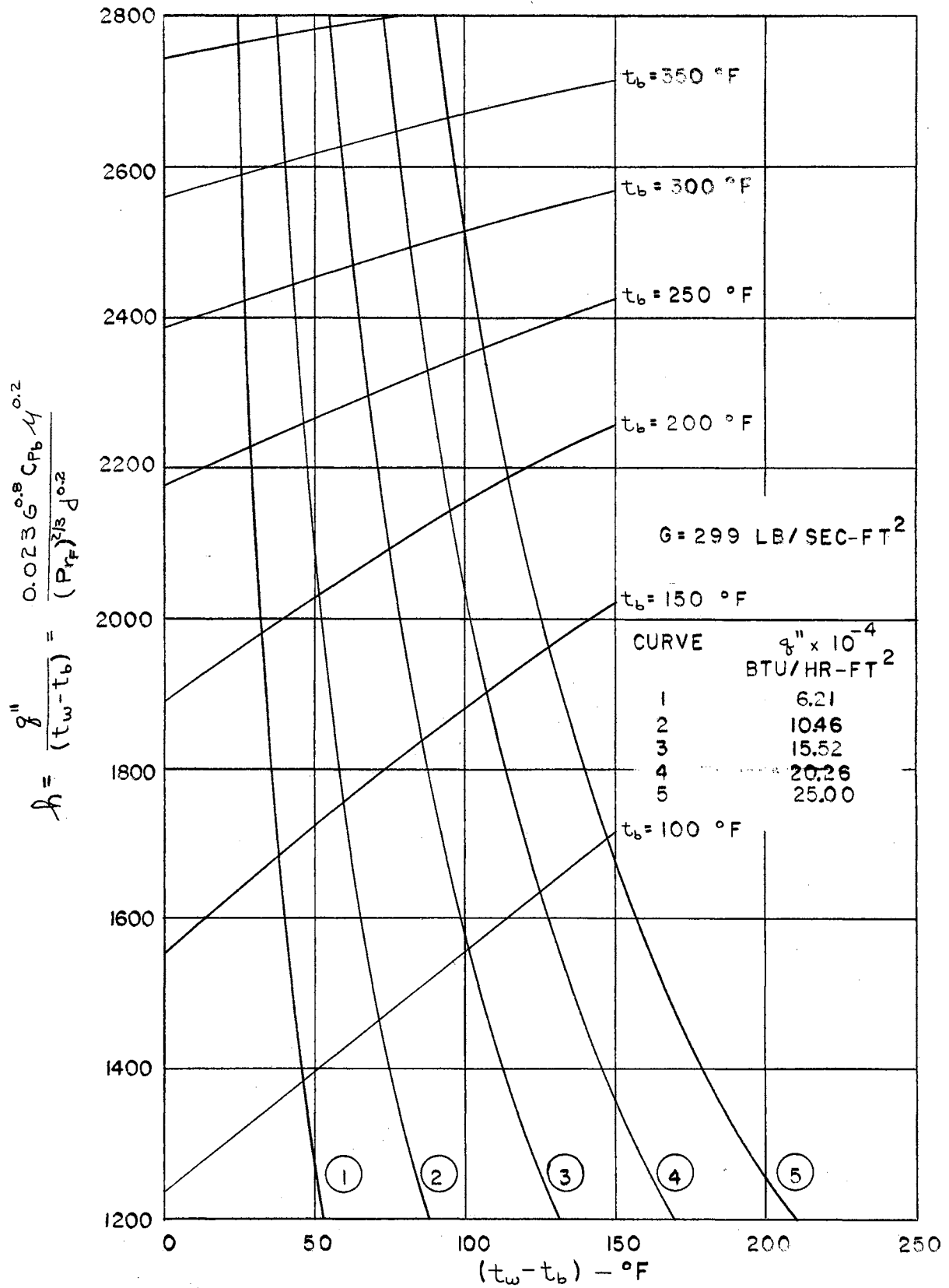


Figure 2. Forced Convection Heat Transfer Coefficient

pressure gradient. The reference used by Tanger (5) was the pressure gradient in the nonboiling region calculated from Blasius' Law. Reynolds (6) used the isothermal liquid pressure gradient at the average bulk water temperature as the reference. It was felt by the author that the effect of local boiling on the pressure gradient was best shown by referencing the local boiling pressure gradient to the nonboiling gradient which would exist for the same heat flux, mass velocity and bulk temperature if local boiling were not occurring. It should be noted that the gradients calculated from Reynolds' Analogy for a given heat flux and mass velocity were essentially independent of bulk temperature for the ranges of pressure and temperature of this investigation. The effect of considerably higher pressures and temperatures on property values should be best reflected in a reference gradient that contains, or was derived from relations which contained, the basic properties describing the flow. Such is the case with the reference gradient used in the present investigation.

CHAPTER IV

EXPERIMENTAL APPARATUS

The apparatus used in this investigation was also used by Tanger (5) in the study of local boiling pressure drop for forced circulation of water. Several refinements in the apparatus were made to better suit it for a study of pressure drop during forced convection local boiling of water containing an additive (16). The changes made included the following.

1. An automatic system pressure controller was installed for better maintenance of steady state conditions.
2. A manometer fluid with a specific gravity of 1.75 was used to allow greater accuracy in pressure drop data.
3. Bypass lines were installed on the manometers to insure positive zeroing and removal of air from the manometer system.
4. An auxiliary system for bleeding the manometers was installed to avoid contacting the manometer fluid with water containing an additive.
5. A transfer line was installed between the supply tank and the holdup tank to facilitate the introduction of an additive and to allow thorough mixing of the fluids.
6. Temperatures were measured by use of a Leeds and Northrup portable precision potentiometer.

The principal components of the apparatus are shown in figures and

plates in this chapter. A brief description of these components is given in subsequent paragraphs. For a more detailed description, the reader is referred to Reference (5). Figure 3 is a schematic diagram of the loop.

System fluid was taken from the supply tank and increased in pressure by a stainless steel Robbins and Myers "Moyno" pump. This pump was of the positive displacement type, and consequently the volumetric rate of discharge was nearly independent of discharge pressure for the range of pressures considered in this investigation. Figure 14, Appendix A, is a plot of volumetric discharge rate with discharge pressure for constant pump speed.

The flow was then directed through a flow-measuring orifice with a throat diameter of 0.353 inches. The pressure drop across the orifice was measured on a Meriam, Model 30 FE 50, 60-in. manometer mounted on the control panel. The fluid employed in this manometer was Meriam No. D-8325 with a specific gravity of 1.75. The manometer fluid worked under water. Figure 15, Appendix A, is a calibration curve for the orifice.

The system fluid then passed through the preheater where heat was added to bring the temperature to a desired level. The preheater consisted of six Cromalox MT-201, 240-volt, 10,000-watt two-element heaters enclosed in a stainless steel tube six inches in diameter. Six single elements were directly connected to switches on the control panel; the other six elements were controlled through a 45-KW Powerstat transformer.

The flow then entered the test section. The test section consisted of an AISI type 304 welded stainless steel tube with an inside diameter of 0.399 inches and an outside diameter of 0.502 inches. The overall

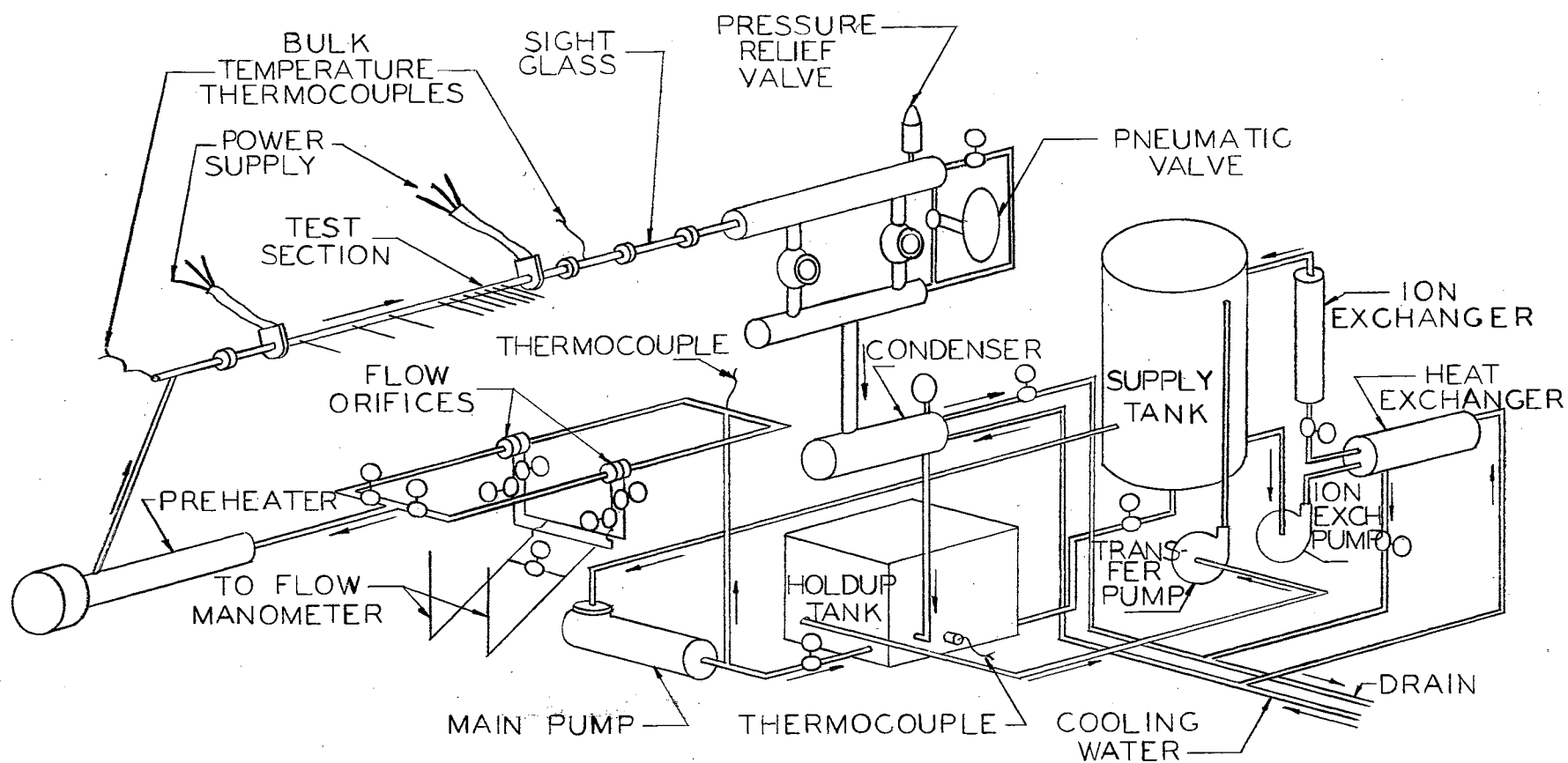


Figure 3. Schematic Diagram of Test Apparatus

length was 84 inches, and the heated length was 72 inches. The test section was instrumented to allow the following data to be gathered:

1. fluid bulk temperature at inlet and outlet of the test section,
2. outside wall temperatures in the local boiling and nonboiling regions of the tube,
3. static pressure drop at nine sections along the tube length,
4. voltage drop at five sections along the tube length.

Figure 4 is a schematic diagram of the test section. The instrumented test section was insulated with a 1/8-in. layer of strip asbestos and a 1-in. thickness of 85% magnesia.

Plate 1 is a view of the bare test section. Plate 2 is a view of the insulated test section.

Energy was supplied to the test section by three Lincoln 400 "Fleet-welder Special Transformers" connected in parallel. It was possible with this arrangement to transmit a maximum of 48-KW to the test section. Plate 3 shows the transformer installation.

Visual observation of the flow was afforded by a Pyrex sight glass located immediately downstream from the test section.

The flow next entered the exhaust manifold. A pneumatically operated valve, manufactured by Minneapolis-Honeywell, was located at the manifold outlet and was used to control the system pressure. This valve operated on a signal transmitted by a Minneapolis-Honeywell Tel-O-Set Two-Mode adjustable band controller. Plate 4 shows the location of this valve in the exhaust manifold.

The system fluid was cooled to approximately 70°F in a Ross type BCF-501-2 two-pass tube and shell heat exchanger. Tap water was used on

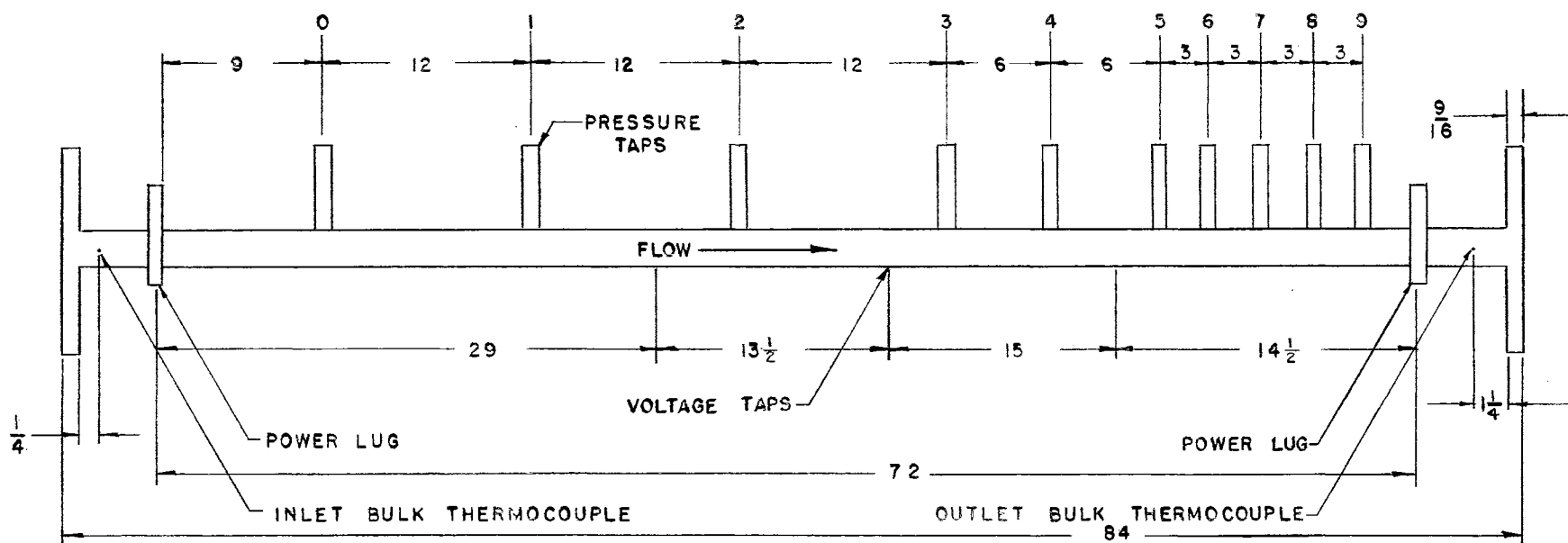


Figure 4. Test Section

PLATE I. BARE TEST SECTION

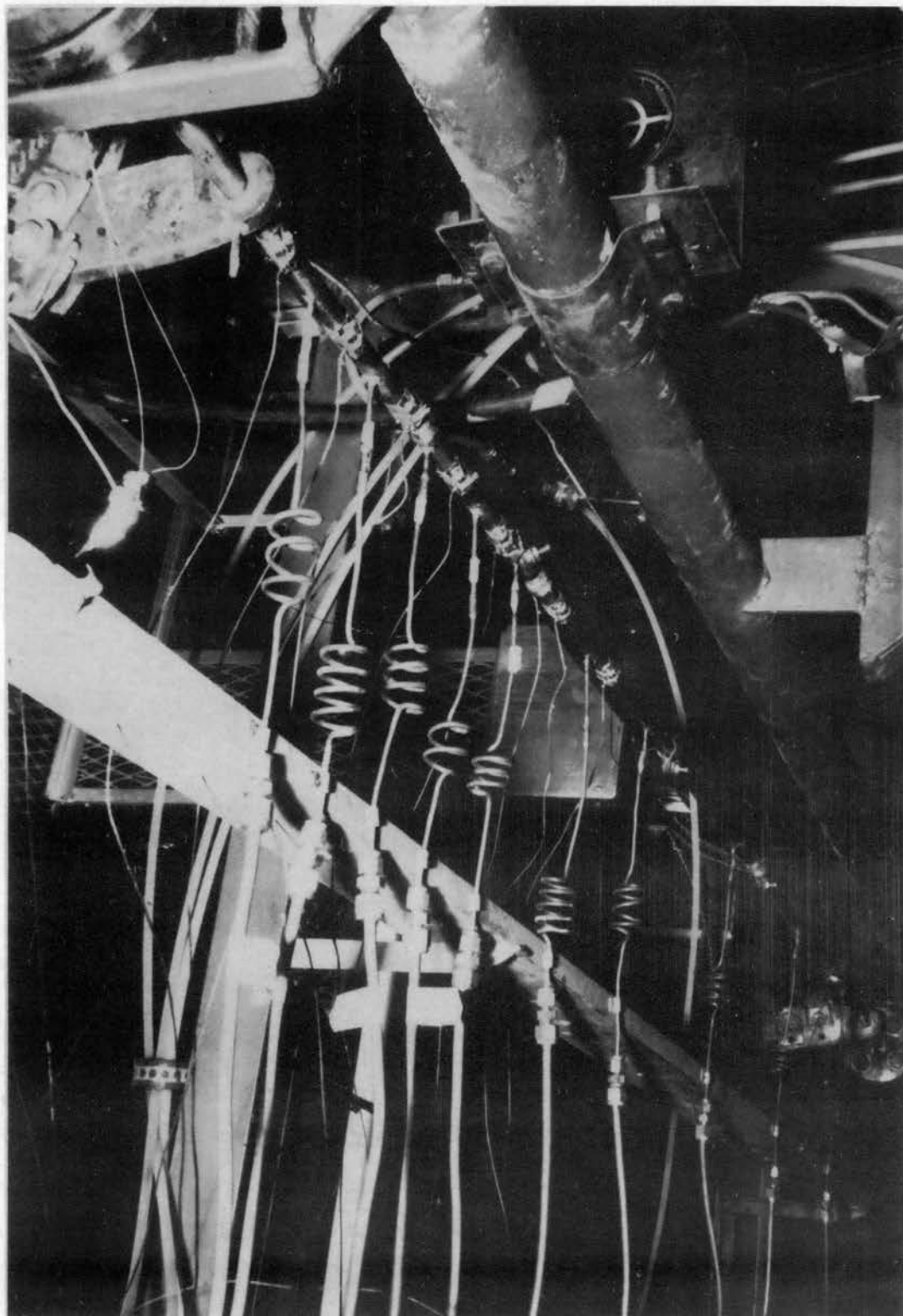


PLATE II. INSULATED TEST SECTION

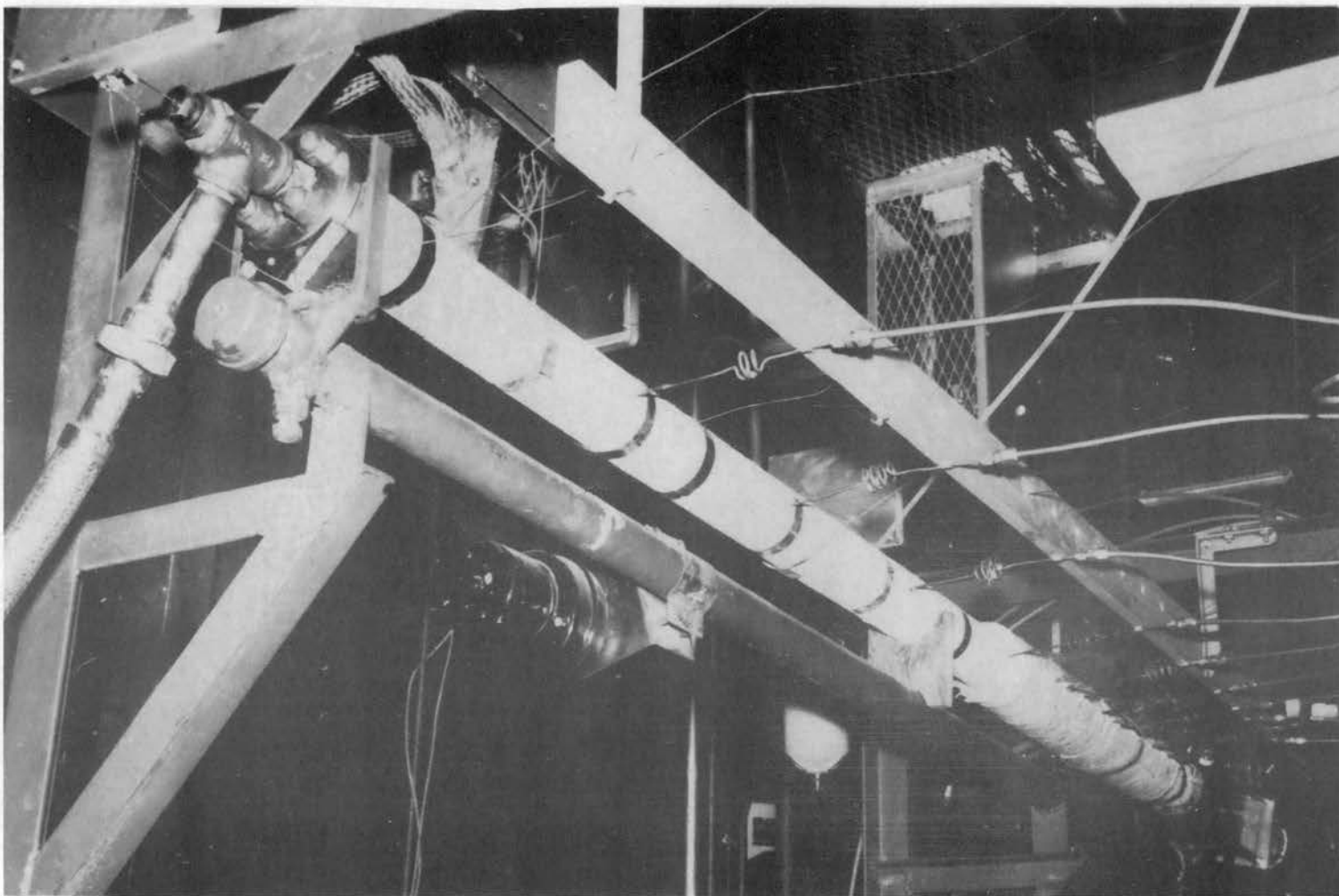


PLATE III. TRANSFORMERS

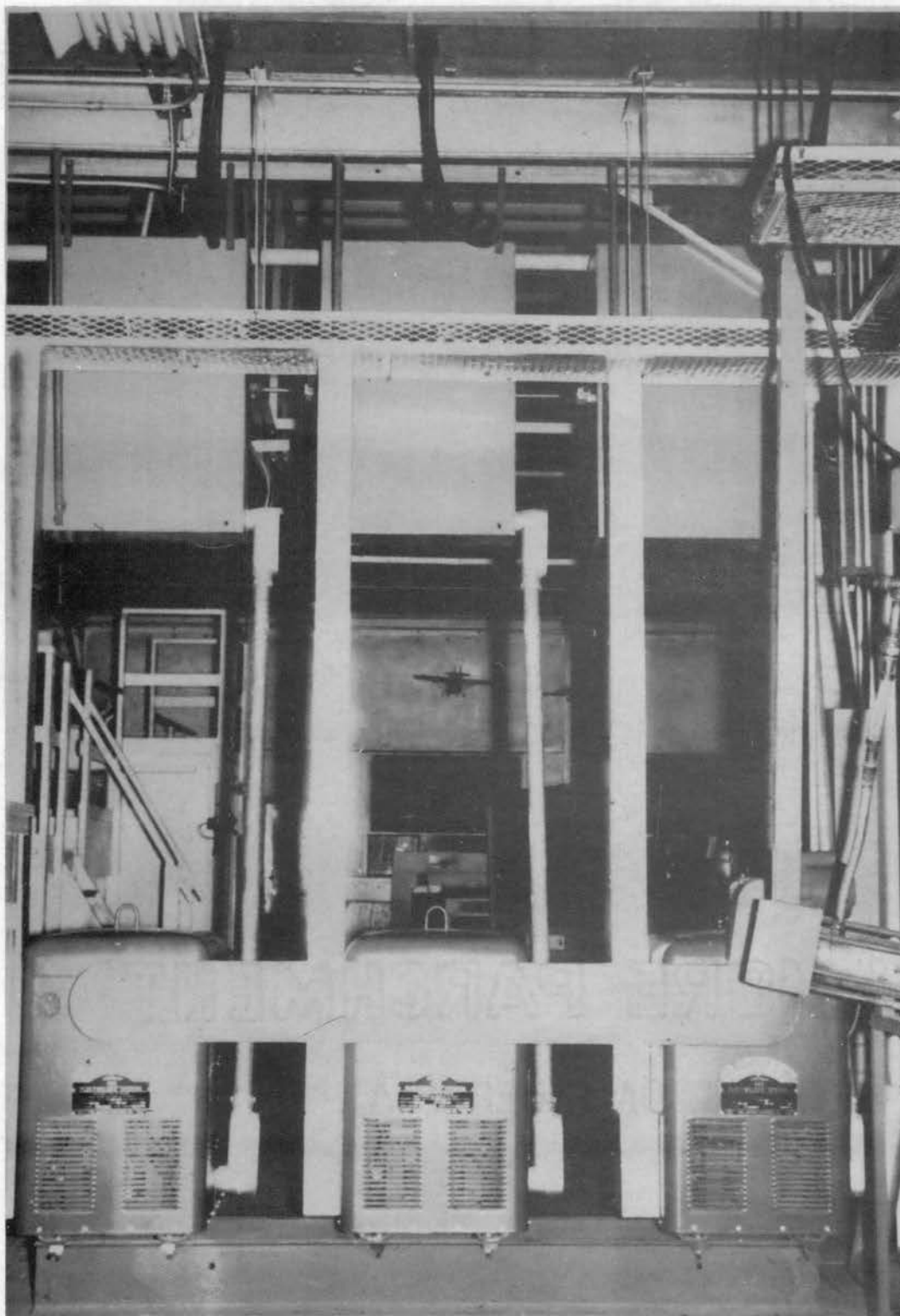
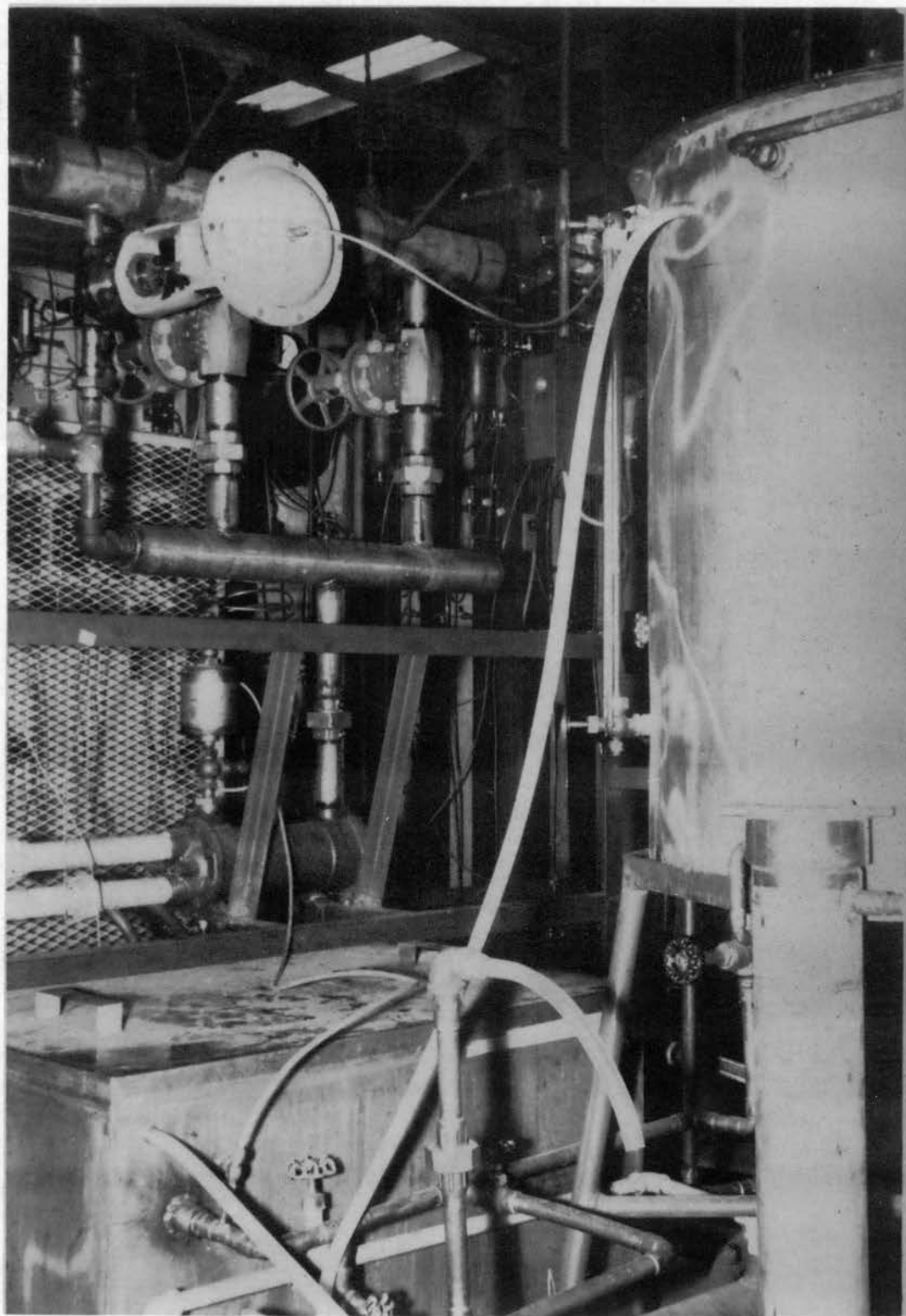


PLATE IV. REAR VIEW OF TEST APPARATUS



the tube side of this exchanger.

The flow then entered the holdup tank and was pumped into the supply tank by a Yeomans Brothers centrifugal pump driven by a 1/3-hp General Electric motor. Plate 4 is a rear view of the loop showing the holdup and supply tanks.

Auxiliary equipment on the loop included an ion exchange system, a degassing system, and a manometer bleeding system.

The ion exchange system consisted of a Yeomans Brothers centrifugal pump and a column charged with "Amberlite" resin. Fluid was pumped from the supply tank through the column of resin and discharged back into the supply tank. An examination of the resin after several hours operation indicated that it was removing impurities from the system fluid.

A valve manufactured by the McAlear Company was located on the shell side of the Ross heat exchanger to avoid "air-lock" of the exchanger. The construction and location of this valve was such that it would pass gas and vapor, but not liquid. The gaseous discharge from this valve was measured and an estimate of the degree of degassing of the system fluid obtained.

It was found that the manometer fluid used was affected by the additives employed in the study. This fact made it necessary to avoid contacting the manometer fluid with water containing an additive. A stainless steel column of seven gallons capacity was fabricated and installed. Appropriate valving was installed to allow isolation of the manometer system from the main system. The stainless steel column was filled with distilled water and pressurized with compressed air. Opening bleed valves

on the manometers caused distilled water to circulate in the manometer system and carry to the atmosphere any air trapped in the system.

Instrumentation

Pressure drop was measured at nine sections along the test section length with five Meriam Model 30FE50, 60-in., well type, dual-tube manometers. The manometer fluid employed was Meriam No. D-8325 with a specific gravity of 1.75. The manometer scales were graduated in inches and tenths of an inch.

Precision temperature measurement was accomplished with 30-gage iron-constantan thermocouples connected to a Leeds and Northrup portable precision potentiometer, No. 8663, through a 24-position selector switch. An ice bath was used as the reference junction for this measurement. Figure 16, Appendix A, is the thermocouple calibration curve. A Brown multi-point Elektronik Strip Chart Recorder, Type J, 0-600°F, 10 record, was used with iron-constantan thermocouples for visual indication of temperature at several points along the test section length.

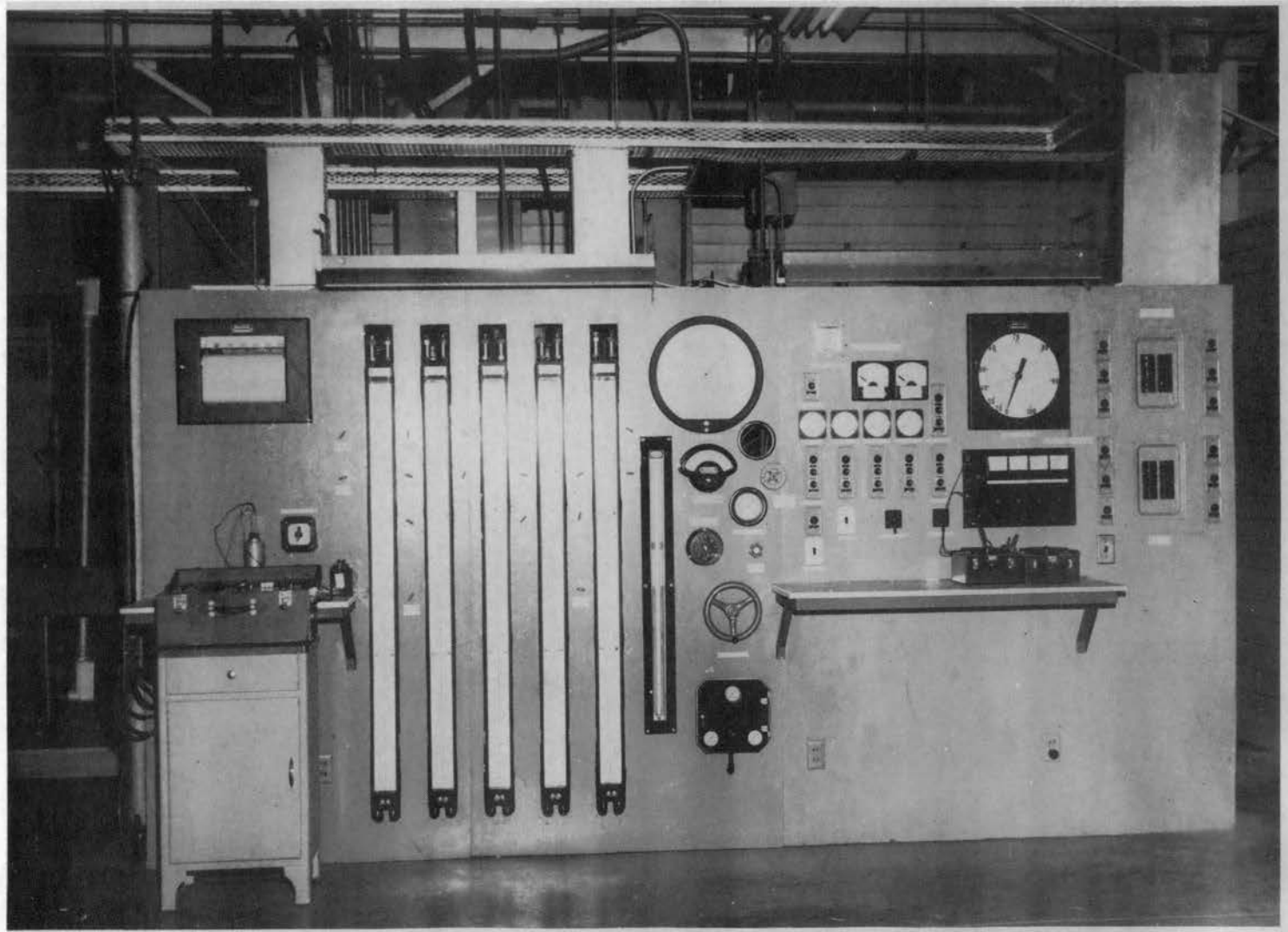
Power input to the test section was measured with a single-phase General Electric P-3 wattmeter, No. 3939252, with a range of 0-200/400/800 watts and an accuracy of 0.2% of full-scale value. Voltage drop along the test section was measured with a General Electric P-3 voltmeter No. 3684998, with a range of 0-15/30 volts and an accuracy of 0.2% of full-scale value. A General Electric JKR-2 current transformer with a ratio of 5:1500 was used to supply current to the wattmeter.

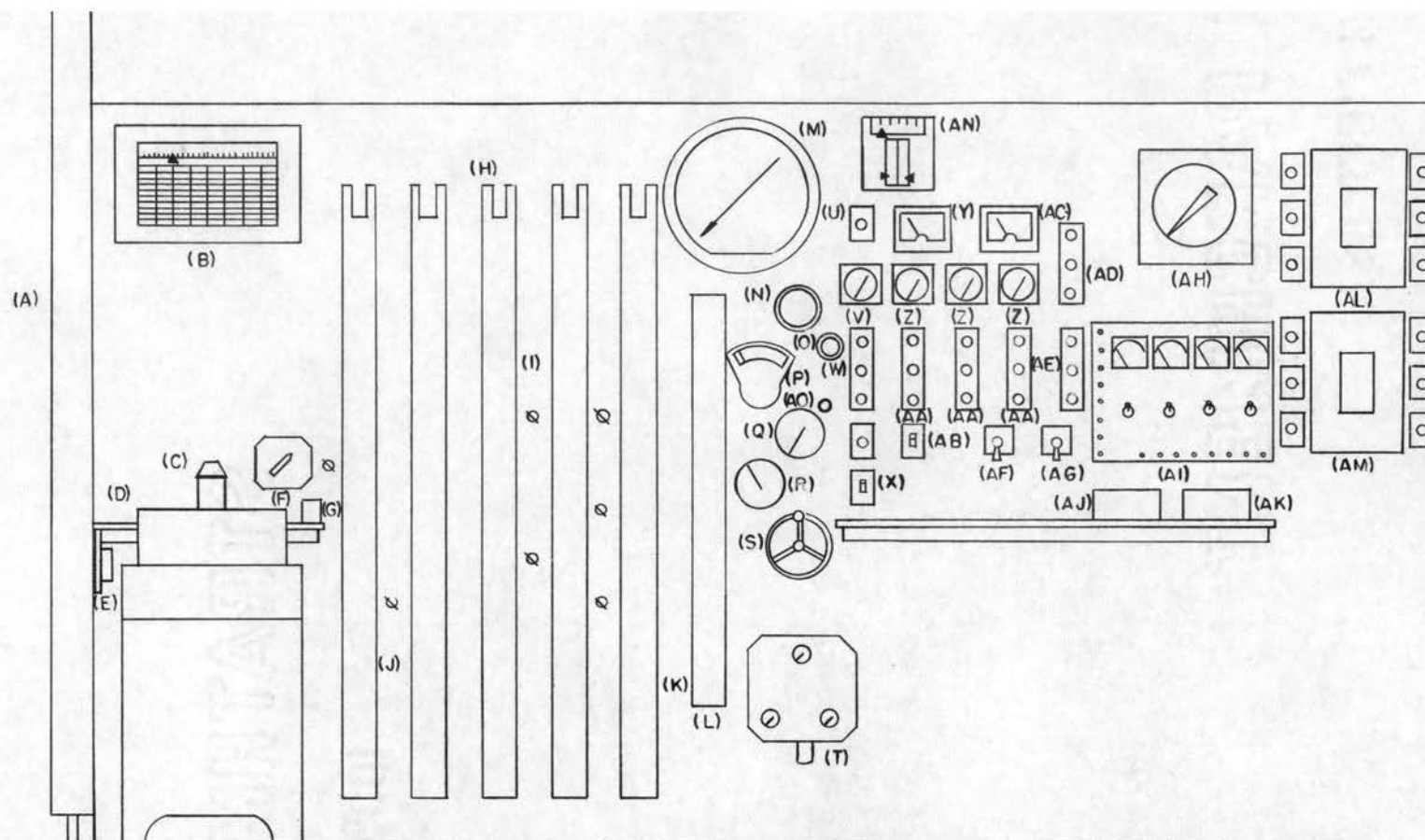
System pressure was measured with a 0-750 psi precision Heise pressure

gage, 16 inches in diameter, graduated in 1-psi increments. Calibration information on this gage was furnished by the manufacturer.

Plate 5 is a view of the control panel, and instruments and controls are identified in Figure 5.

PLATE V. FRONT VIEW OF TEST APPARATUS





(A) MANOMETER BLEED COLUMN
 (B) TEMPERATURE RECORDER
 (C) DEWAR FLASK
 (D) POTENTIOMETER
 (E) VARIAC
 (F) THERMOCOUPLE SELECTOR
 (G) STANDARD CELL
 (H) CHECK VALVES
 (I) SHUTOFF VALVES
 (J) PRESSURE DROP MANOMETERS
 (K) FLOW MANOMETER
 (L) AUXILLARY MANOMETER
 (M) PRECISION PRESSURE GAGE

(N) OBSERVATION PORT
 (O) THROTTLE VALVE
 (P) MAIN PUMP SPEED INDICATOR
 (Q) SYSTEM PRESSURE GAGE
 (R) HOLDUP TANK TEMP INDICATOR
 (S) MAIN PUMP SPEED CONTROL
 (T) SYSTEM PRESSURE SENSOR
 (U) PANIC SWITCH
 (V) TOTAL CURRENT AMMETER
 (W) MAIN PUMP SWITCH
 (X) TRANSFER PUMP SWITCH
 (Y) TEST SECTION VOLTMETER
 (Z) TRANSFORMER AMMETERS

(AA) TRANSFORMER SWITCHES
 (AB) ION EXCH. PUMP SWITCH
 (AC) TEST SECTION WATTMETER
 (AD) DIRECT PREHEATER
 (AE) POWERSTAT PREHEATER
 (AF) TRANSFORMER POWER CONTROL
 (AG) PREHEATER POWERSTAT CONTROL
 (AH) CURRENT RECORDER
 (AI) PREHEATER INST. PANEL
 (AJ) PRECISION WATTMETER
 (AK) PRECISION VOLTMETER
 (AL) PREHEATER JUNCTION BOX
 (AM) POWERSTAT JUNCTION BOX
 (AN) PRESSURE CONTROL
 (AO) BYPASS VALVE

Figure 5. Instrument and Control Identification

CHAPTER V

EXPERIMENTAL PROCEDURE

Before starting runs with additives, several calibration and check-out runs were made using distilled water in the loop. It was determined from these preliminary runs that a rather definite experimental procedure should be followed in order to obtain best results.

The preliminary runs included a number of isothermal runs. These runs served the purpose of insuring that the pressure drop measurements along the test section length were reproducible, and that the experimental friction factors found compared favorably with those predicted for smooth tubes by a Moody diagram. Figure 6 is a plot of experimental friction factors and friction factors predicted by a Moody diagram with Reynolds number. Figure 7 is a plot of measured pressure drop and predicted pressure drop along the length of the tube.

Previous studies in boiling heat transfer have indicated that the condition of the heat transfer surface plays an important role in the boiling phenomenon. Previous investigators have found it necessary to clean the heat transfer surface after a relatively short running time, in some cases as little as three hours (17), in order to obtain reproducible data. Such was found to be the case in the present investigation. Small amounts of deposits were formed on the test section wall, even though the heat transfer loop was constructed throughout of stainless steel or non-ferrous materials, distilled water was used, and an ion exchange system was employed to remove ionic impurities from the fluid.

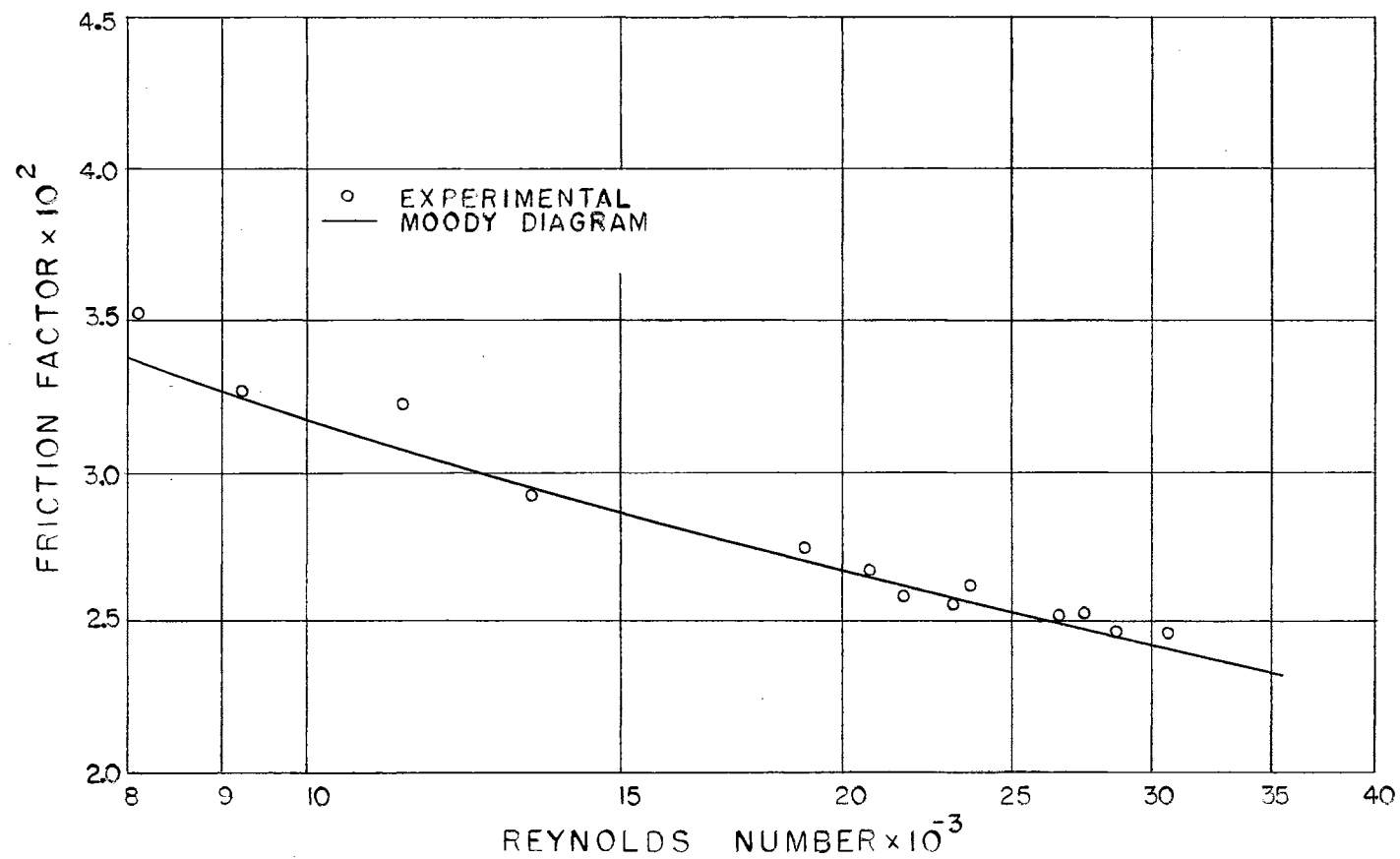


Figure 6. Isothermal Friction Factor

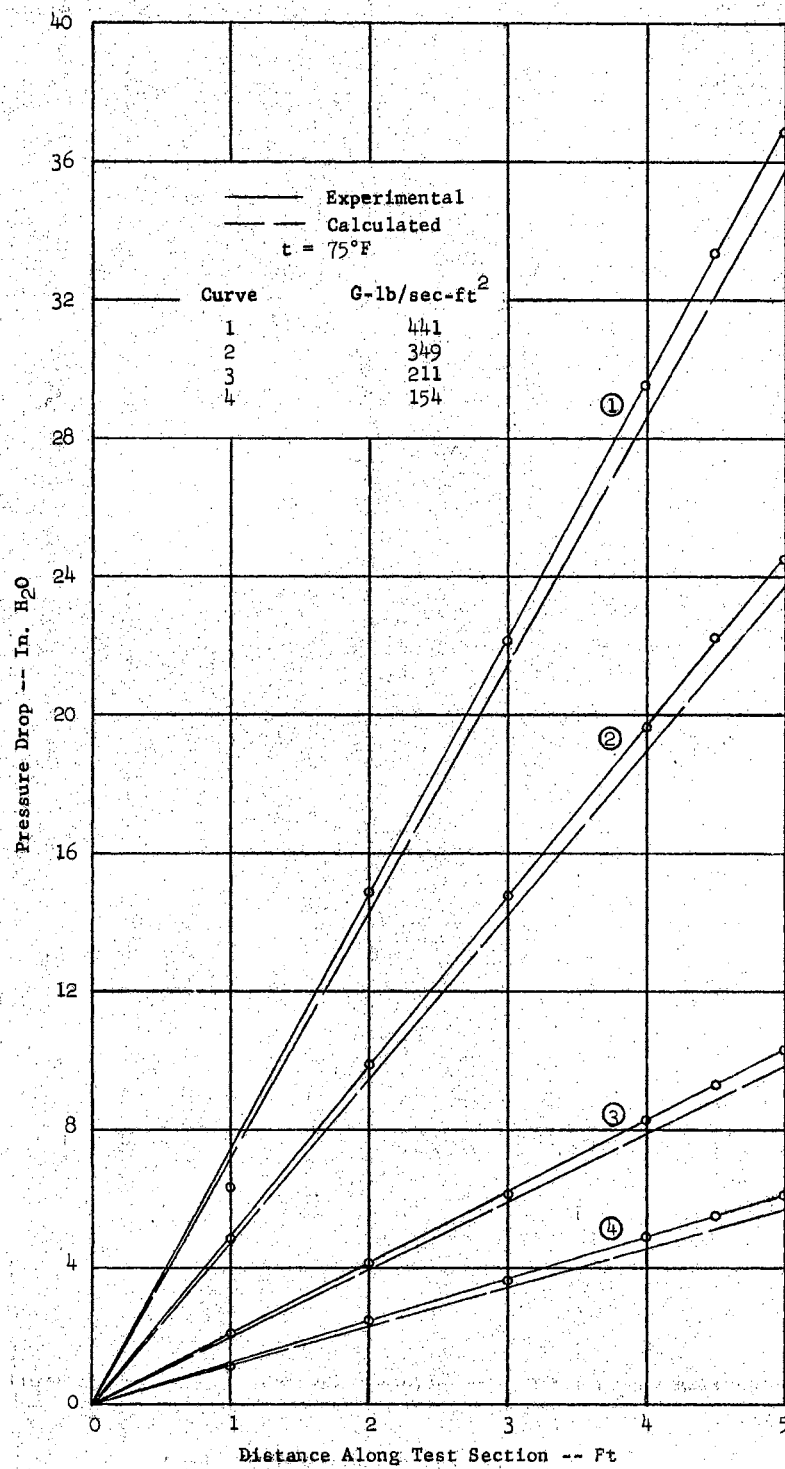


Figure 7. Isothermal Pressure Drop

The presence of such deposits could be detected by an increase of the test section wall temperature with time, all other system variables remaining constant. An increase of tube wall temperature indicated that a film of high resistance to heat transfer was forming. To insure that all additive runs with a particular combination of system variables were made with as near as possible the same surface condition, the following procedure was used.

1. The test section was cleaned with a dilute solution of nitric acid and flushed with distilled water before starting each sequence of runs with a particular additive.
2. Runs with particular combinations of system variables were made in the same order for each additive and each additive concentration.
3. Approximately one run in ten was reproduced on another day to insure consistency of the experimental data. Figure 8 shows a representative pressure profile with original and reproduced data points indicated.

A range of system variables consistent with the physical limitations of the loop was selected. The influence of system pressure, flow rate, and heat flux on pressure drop in local boiling of water was studied. Combinations of these variables were selected to investigate thoroughly the effects of the most predominant variables. Sixteen combinations of system pressure, flow rate, and heat flux were established, and runs were made using distilled water as the heat transfer medium.

Since available correlations for predicting heat transfer and pressure drop for water in forced convection local boiling correlate experimental data only within some 25%, it was felt that the changes in these

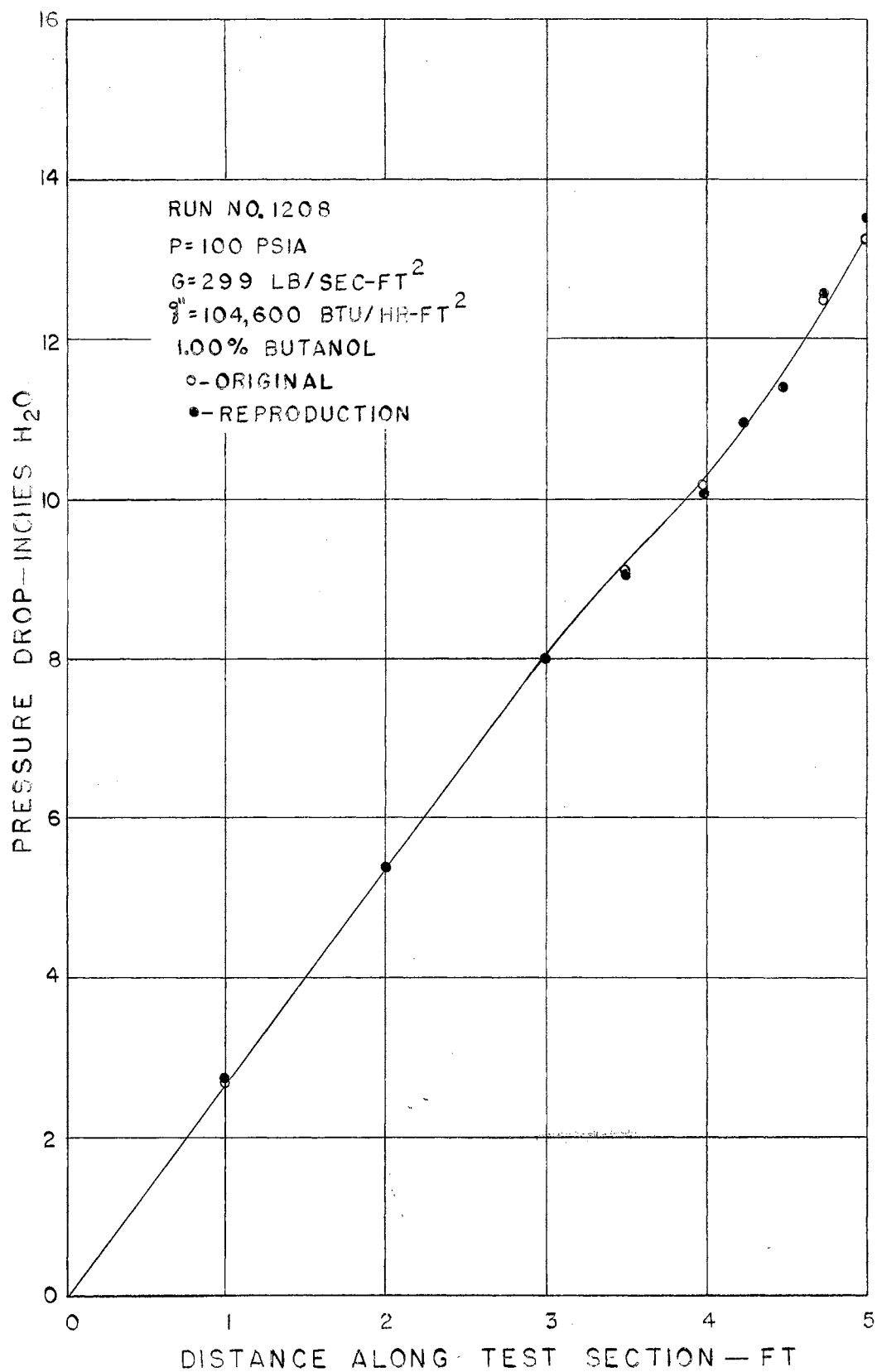


Figure 8. Typical Reproduction Run

parameters produced by an additive might be masked out by the use of such correlations. For this reason it was decided to make all additive runs at the same combinations of system variables as used for the water runs. This procedure made it possible to compare runs made with varying concentrations of different additives with runs made with water at the same values of system pressure, flow rate and heat flux without resorting to empirical relations.

After the test section was cleaned in the manner previously described, the unit was filled with a known weight of distilled water and all openings in the system sealed. The loop was started and allowed to run for approximately ten minutes to displace any air present in the flow system. During this period the manometer system was bled to remove any air which might have collected in the system. The flow was bypassed from the test section by closing the system pressure control valve and opening the bypass valve in the main pump discharge line. A moderate pressure was established in the manometer system under conditions of no flow and the zero of each manometer was checked. It was found that the zero settings of the manometer scales did not change during the course of the experimental runs.

The effect of dissolved gases on local boiling heat transfer has been found to be appreciable in previous boiling studies, particularly at lower pressures (12). The variation found in $(\Delta t)_{\text{sat}}$ with time in this investigation agreed qualitatively with the variation predicted by Equation II-5 for decreasing amounts of dissolved air. Experiments were made to determine the amount of gas removed through the McAlear valve described in Chapter IV. A plot of volume of air removed with time was made. This plot

indicated that a running time of approximately one hour at a moderate heat flux and flow rate was sufficient to remove 80 to 90% of the gas dissolved in the water. Figure 9 is a plot of volume of gas removed with time. The portion of this curve with the greater slope indicates a net removal of gas from the system. The portion of the curve with the smaller and nearly constant slope represents a rate of gas removal equal to the rate of gas absorption by the system fluid. At the beginning of each day of data taking, the loop was run for approximately one hour at a moderate flow rate and heat flux before any useable data were taken.

Sufficient additive to give a concentration of 1% by weight was weighed and added to the known weight of water in the system. The additive was introduced into the system through an aspirator located in the 1-in. line between the supply and holdup tanks. This line was left open for approximately one hour and the system fluid was circulated between the holdup and supply tanks by the transfer pump. The purpose of this step was to insure thorough mixing of the additive in the water.

At the beginning of an experimental run the flow rate, system pressure, and heat flux were set. Experience gained in the preliminary runs indicated values of preheater power required to obtain a reasonable length of local boiling for various combinations of flow rate, pressure, and heat flux.

Steady state was reached after approximately fifteen to thirty minutes. During this time fine adjustments were made to bring system variables to the desired values. Once a steady state was reached, no change in variable settings was necessary to maintain this condition. Steady state conditions were assumed to exist when several consecutive readings of pressure drop

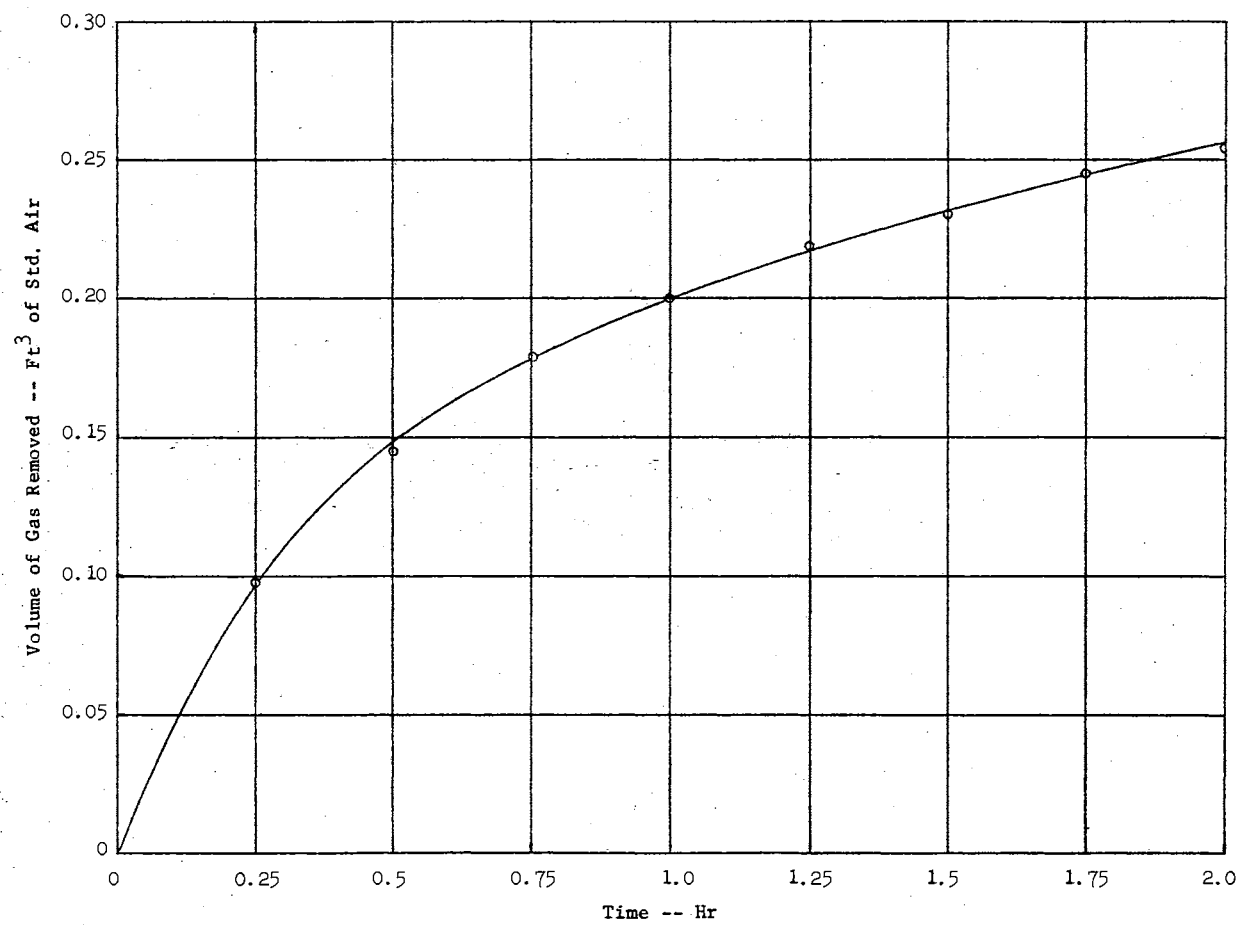


Figure 9. Gas Removed From System Fluid

were the same. Due to the inherent instability of boiling, a variation with time was found in some runs. All data points were read twice and an average of the two values was used in subsequent calculations. The data recorded on a particular run included:

1. run number,
2. additive used,
3. concentration of additive by weight,
4. barometric pressure,
5. ambient temperature,
6. system pressure,
7. pressure drop across the flow-measuring orifice,
8. static pressure drop at nine sections along the test section,
9. fluid temperatures at the orifice, test section inlet and outlet,
10. voltage drop along the test section,
11. current in the test section, and
12. power input to the test section.

After sixteen runs were made with an additive concentration of 1%, sufficient additive was introduced to bring the concentration to 2% by weight. The procedure outlined above was followed for concentrations of 2% and 3%. After completing runs at 3%, the system was drained and flushed. The test section was cleaned and the procedure repeated with different additives. Samples of system fluid were taken periodically and analyzed as a check on the weighing procedure and possible losses by evaporation or leakage of system fluid. The analysis was made by a commercial laboratory through use of a modified form of the Heise

oxidation-reduction method, and revealed no loss.

To determine the effect of progressively increasing the additive concentration on the heat transfer surface, the following procedure was followed: (1) runs were made using 1%, 2% and 3% methanol in the manner previously described; (2) the test section was drained and acid-cleaned; (3) data were taken using the same fluid as used in the previous methanol run. The experimental data obtained by the two methods of testing agreed within the normal limits of reproducibility of previous data. From this it was concluded that it was satisfactory to increase the concentration of the additive progressively, as previously described.

CHAPTER VI

EXPERIMENTAL RESULTS AND CORRELATION OF DATA

The experimental pressure drop data were plotted as functions of distance along the test section. Representative plots are shown in Figures 18 through 20, Appendix B. Since the bulk temperature at a particular location along the test section varied among runs made with different mixtures at the same pressure, flow rate, and heat flux, it was necessary to replot the data to allow comparison at a particular bulk temperature. The slope of the pressure profiles was measured at 12-in. intervals in the nonboiling region and at 3-in. intervals in the local boiling region. Plots of the measured pressure gradients were made with bulk temperature as the independent variable. These curves permitted analysis of the data at common values of bulk temperature. Representative plots are shown in Figure 21, Appendix B.

Some general remarks can be made concerning the behavior of the pressure gradient as a function of bulk temperature. It was noted that the pressure gradient in the nonboiling region was essentially independent of bulk temperature. Uncertainty of pressure drop data was greatest in the nonboiling region due to small values of manometer readings, but it was felt that in general the dependence on bulk temperature was small. Region AB in Figure 10 represents the nonboiling region.

A decrease in the pressure gradient before the start of local boiling

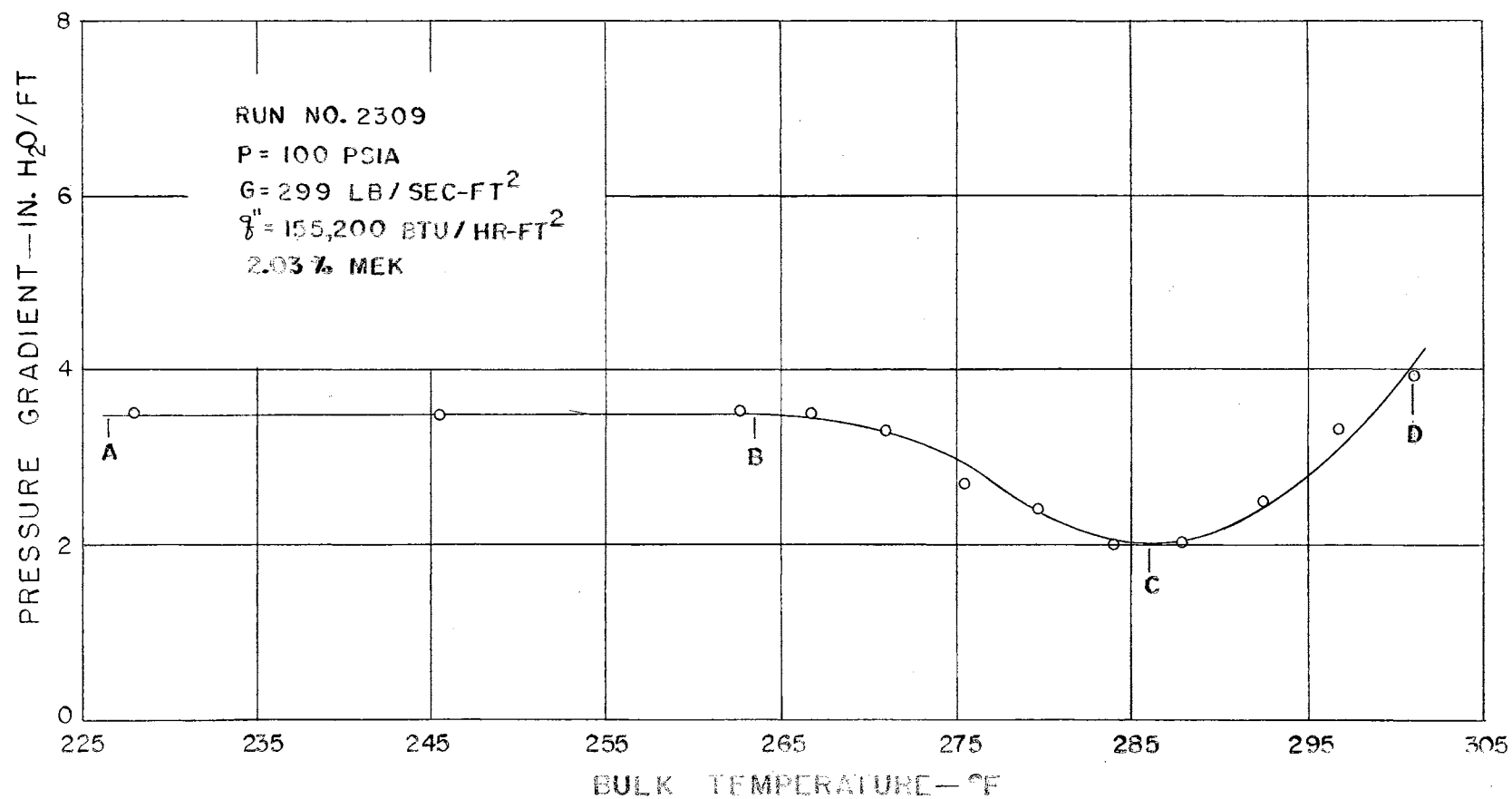


Figure 10. Typical Pressure Gradient Along Test Section

was noted in virtually all runs. This result is contrary to the results of Tanger (5) and Reynolds (6) for water. In the previous studies, an increase in the gradient was noted as the first deviation from the essentially constant gradient in the nonboiling region. The average decrease in the gradients obtained in the present investigation was about 30% of the value in the nonboiling region. Region BC in Figure 10 represents the region of decreasing pressure gradient discussed above.

A qualitative explanation for the behavior of the pressure gradients in region BC may be given by considering the mechanism of pressure drop and boiling heat transfer. It was found that the tube wall temperatures in region BC were above the saturation temperature corresponding to the system pressure. As the bulk temperature increased, the degree of superheat (i.e., the difference between wall temperature and saturation temperature) also increased. This is to be expected because in order for boiling to occur, the liquid must be slightly superheated to provide a potential for the flow of heat from the liquid to a bubble of vapor at the saturation temperature (18). The region of decreasing pressure gradient represents, then, a region of increasing tube wall superheat which ends only when the degree of superheat is high enough to cause boiling.

The pressure gradient is strongly dependent on the fluid viscosity in the laminar sublayer near the tube wall. The viscosity is in turn strongly dependent on temperature. It would appear that a rapid decrease in viscosity is experienced with increasing temperature of a superheated liquid. The effect of other properties must be considered in a quantitative analysis, but the effect of viscosity should predominate.

As soon as the tube wall superheat is high enough to cause boiling, bubbles of vapor begin forming and collapsing in the fluid stream. This point is denoted by C in Figure 10 and is ordinarily referred to as the start of local boiling. The life of the bubbles increases with increasing distance along the test section since the bulk temperature is proportional to distance along the tube. The turbulence and decrease in average fluid density caused by the presence of increasing numbers of bubbles increases the pressure gradient for a given mass velocity. This region is denoted by CD in Figure 10. The experimental data of this investigation ended at point D. Local boiling occurs until the bulk temperature equals the saturation temperature; at this point, "net" or "bulk" boiling occurs.

Figure 11 is a plot of the pressure gradient as a function of distance along a heated tube. The nonboiling, local boiling and net boiling regions are denoted by AB, BC and CD, respectively. The method proposed by Martinelli and Nelson (19) was used to obtain pressure gradients in the net boiling region. A discontinuity was noted at the start of local boiling when the experimental data obtained in this investigation were extrapolated to that point. The discrepancy was greatest at the start of net boiling but decreased rapidly with increasing distance along the tube. It was felt by the author that the proposed curve shown in Figure 11 better represented the transition from local boiling to net boiling.

An analysis of the pressure drop data was made considering the effect of a particular additive and the effect of additive concentration. Although some scattering of data was noted, it was possible to make the observations indicated in subsequent paragraphs.

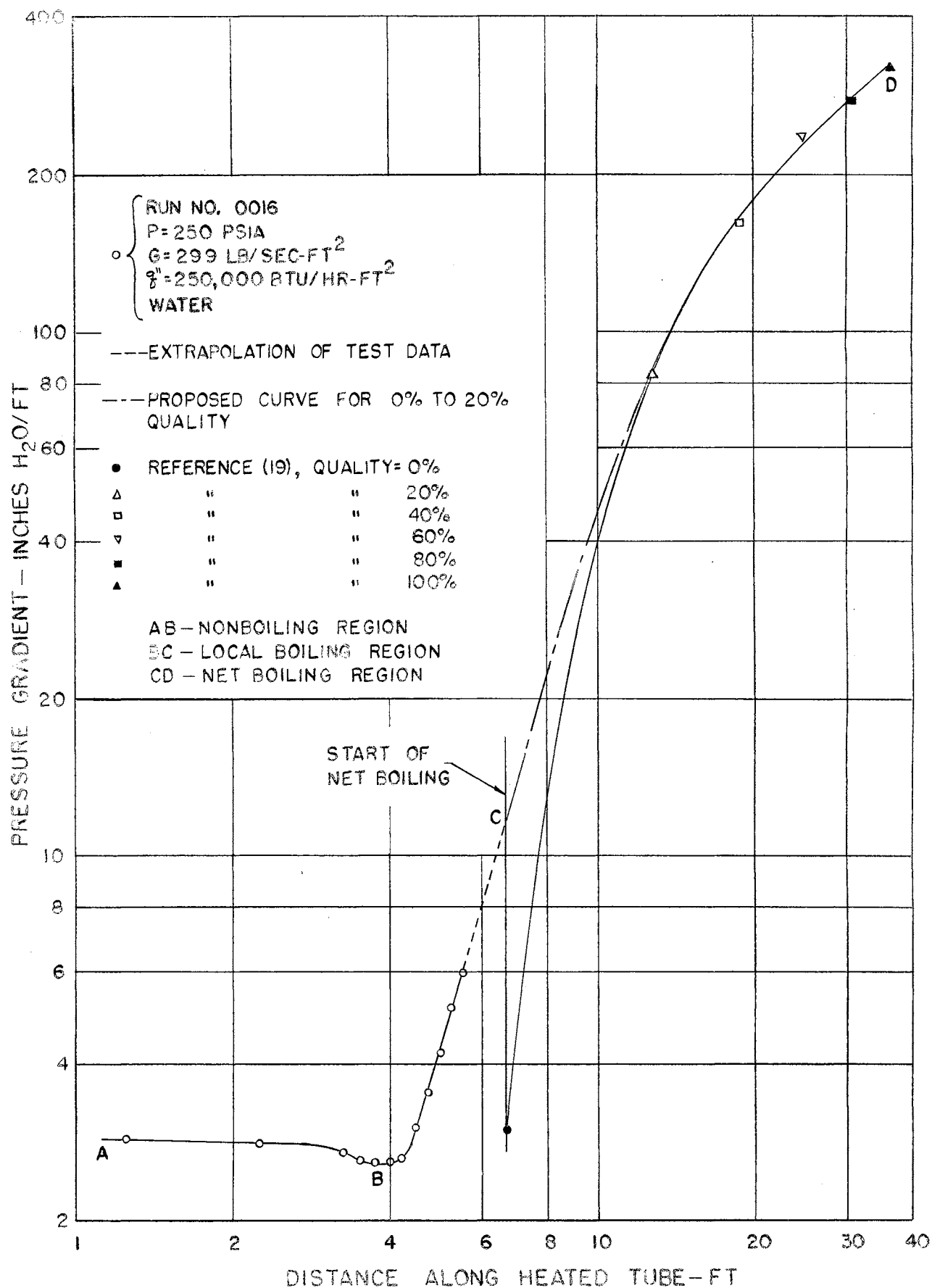


Figure 11. Variation of the Pressure Gradient for Water in the Nonboiling, Local Boiling and Net Boiling Regions of a Heated Tube

The effects of particular additives on the following parameters were considered:

1. the pressure gradient in the nonboiling region,
2. the bulk temperature at which the pressure gradient started to decrease,
3. the value of the pressure gradient at the start of local boiling,
4. the bulk temperature at the start of local boiling, and
5. the rate of change of the pressure gradient in the local boiling region.

The effects of the various additives are tabulated in Table I.

Considerable scattering of data was noted in the analysis for the effect of additive concentration. The following comments may be made.

1. The deviation of nonboiling pressure gradients from those for pure water generally increased with increased concentration of methyl ethyl ketone. The effect of increased concentrations of butanol and methanol varied and was, in general, much smaller than for methyl ethyl ketone.

2. The bulk temperature at the start of local boiling was generally greatest for concentrations of 1% and decreased with increased concentration.

3. No relation between the value of the pressure gradient at the start of local boiling and additive concentration was noted.

4. The rate of increase of the pressure gradient in the local boiling region generally increased with increased concentration of additive.

Correlation of Data

It was felt that the influence of the following variables should be considered in any relation correlating the experimental data:

TABLE I
THE EFFECT OF ADDITIVES ON THE PRESSURE GRADIENT
WHEN COMPARED TO WATER

Additive	Nonboiling Pressure Gradient	Bulk Temperature At Start of Decrease Of Pressure Gradient	Pressure Gradient At Start of Local Boiling	Bulk Temperature At Start of Local Boiling	Rate of Increase Of Pressure Gradient In Boiling Region
Butanol	Decrease	Increase	Decrease	Increase	Increase
MEK	Increase	Increase	Decrease	Increase	Increase
Methanol	Increase	Decrease	Decrease	Increase	No Change

1. the additive present in the mixture,
2. the concentration of additive in the mixture,
3. heat flux,
4. flow rate, and
5. system pressure.

A dimensionless pressure gradient ratio was defined by

$$R = \frac{(dP/dL)_{LB}}{(dP/dL)_{NB}} \quad \text{VI-1}$$

where

$(dP/dL)_{LB}$ = the experimental pressure gradient in the local boiling region at a particular bulk temperature;

$(dP/dL)_{NB}$ = the calculated nonboiling reference pressure gradient defined in Chapter III, and evaluated for water at the bulk temperature of the boiling gradient.

A dimensionless temperature ratio was defined by

$$\Theta = \frac{t_b - t_s}{t_{sat} - t_s} \quad \text{VI-2}$$

where

t_b = bulk temperature at a particular location in the local boiling region;

t_s = the bulk temperature at the start of local boiling;

t_{sat} = the saturation temperature corresponding to the system pressure (saturation temperatures were obtained from Figures 30 and 31, Appendix C).

The effects of heat flux, flow rate, and system pressure on the pressure gradient ratio were thought to be accounted for by the temperature ratio defined by Equation VI-2. The saturation temperature is obviously dependent on the system pressure. An examination of the pressure gradients revealed that the bulk temperature at the start of local boiling

increased with increased rate of flow for constant values of other variables; t_s is thus a function of the flow rate. The preceding is to be expected, since an increase in velocity increases the effectiveness of forced convection heat transfer, decreases the surface temperature at a given heat flux, and thereby delays the start of local boiling. Other investigators (7) have correlated the influence of heat flux and mass velocity with the degree of subcooling, $t_{sat} - t_b$, at the start of local boiling; the effect of heat flux is thus reflected.

That the suppositions made in the preceding paragraph are correct is shown in Figure 12 where the pressure gradient ratio is plotted logarithmically as a function of the temperature ratio for the water runs.

A logarithmic plot of the pressure gradient ratio as a function of the temperature ratio was made with data from all runs. A curve of the following form represented a good fit of the data:

$$R = a + b(\theta)^c \quad \text{VI-3}$$

where a , b , and c are coefficients to be determined.

It was seen that the effect of the additives on the pressure gradient ratio was greater than that reflected by the temperature ratio. A dimensionless viscosity ratio was defined by

$$V = \left(\frac{\mu_M}{\mu_W} \right)^{d(\text{conc.})}$$

where

μ_M = the viscosity of a mixture at a particular temperature;

μ_W = the viscosity of water at the same temperature;

d = a coefficient to be determined;

conc. = additive concentration in the mixture in percent by weight (nominally, 1, 2 and 3 in this investigation).

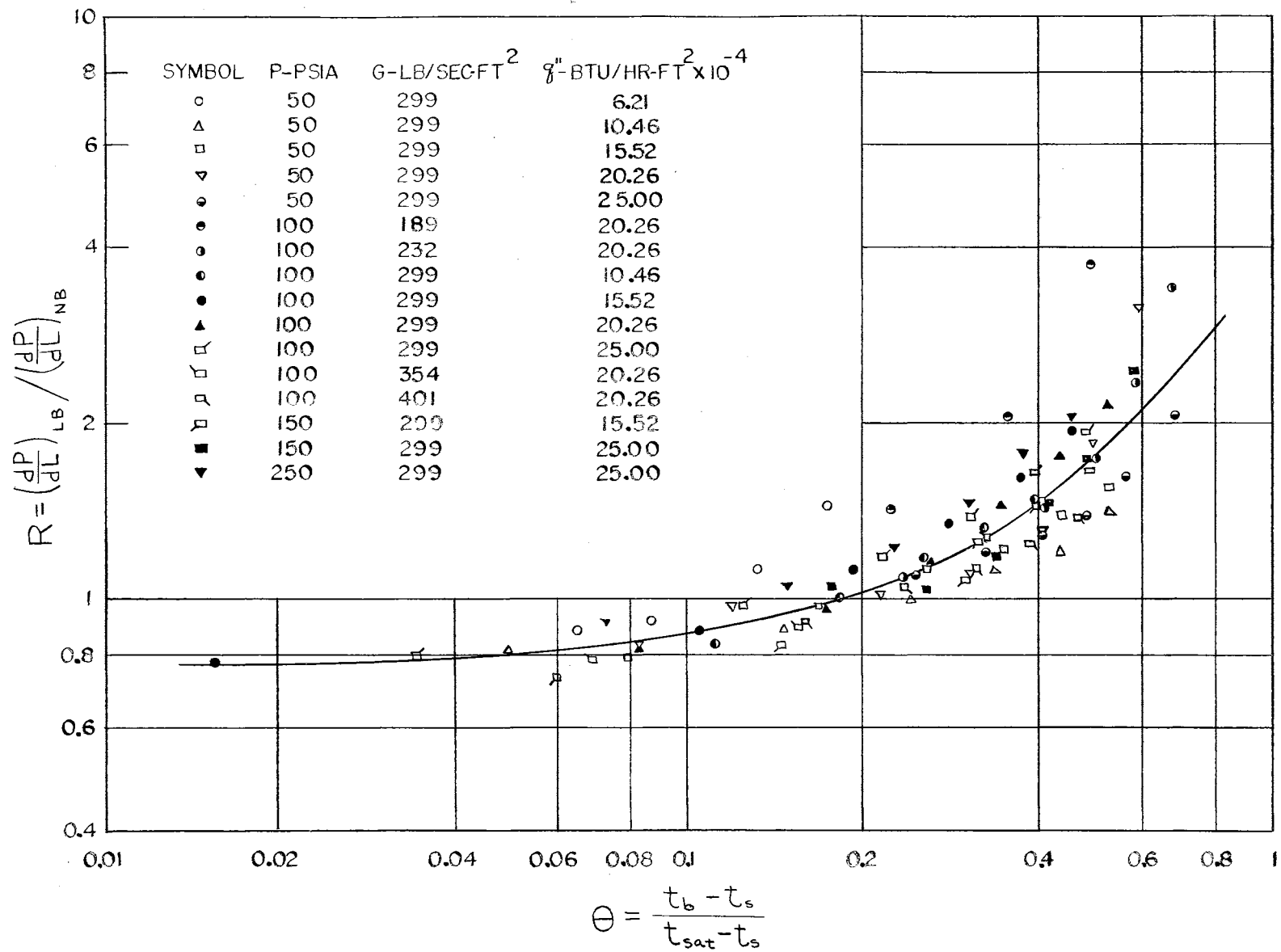


Figure 12. Variation of the Pressure Gradient Ratio with the Temperature Ratio for Water

Viscosity was chosen for this parameter as the property best reflecting the effect of an additive on pressure drop. Although the viscosity exerts its strongest influence in the laminar boundary layer and should therefore be evaluated at a film temperature, the ratio evaluated at the bulk temperature is essentially equal to the ratio evaluated at the film temperature.

The final form of the correlation equation was

$$R = \left[a + b(\theta)^c \right] \left(\frac{\mu_M}{\mu_w} \right)^{d(\text{conc.})} \quad \text{VI-4}$$

The generalized least squares method described in Appendix D was used to evaluate the coefficients a , b , c , and d in Equation VI-4. Substituting individual terms for the ratios and the values of the coefficients gave the final result,

$$\left(\frac{dP}{dL} \right)_{LB} = \left(\frac{dP}{dL} \right)_{NB} \left[0.682 + 2.46 \left(\frac{t_b - t_s}{t_{sat} - t_s} \right)^{1.28} \right] \left(\frac{\mu_M}{\mu_w} \right)^{-0.657(\text{conc.})} \quad \text{VI-5}$$

Equation VI-5 correlated the local boiling data within $\pm 25\%$, with a standard deviation of 0.312. Figure 13 is a logarithmic plot of Equation VI-5 with the experimental pressure gradient ratio.

It is recommended that Equation VI-5 be applied in a stepwise manner for predicting pressure drop over a given length of tube. The variation of bulk temperature with length will depend upon the particular system under consideration.

The data of Tanger (5) for water was correlated with $\pm 100\%$ by Equation VI-5; the data of Reynolds (6) for water was correlated within $\pm 60\%$.

The experimental data obtained in this investigation are tabulated in Table II.

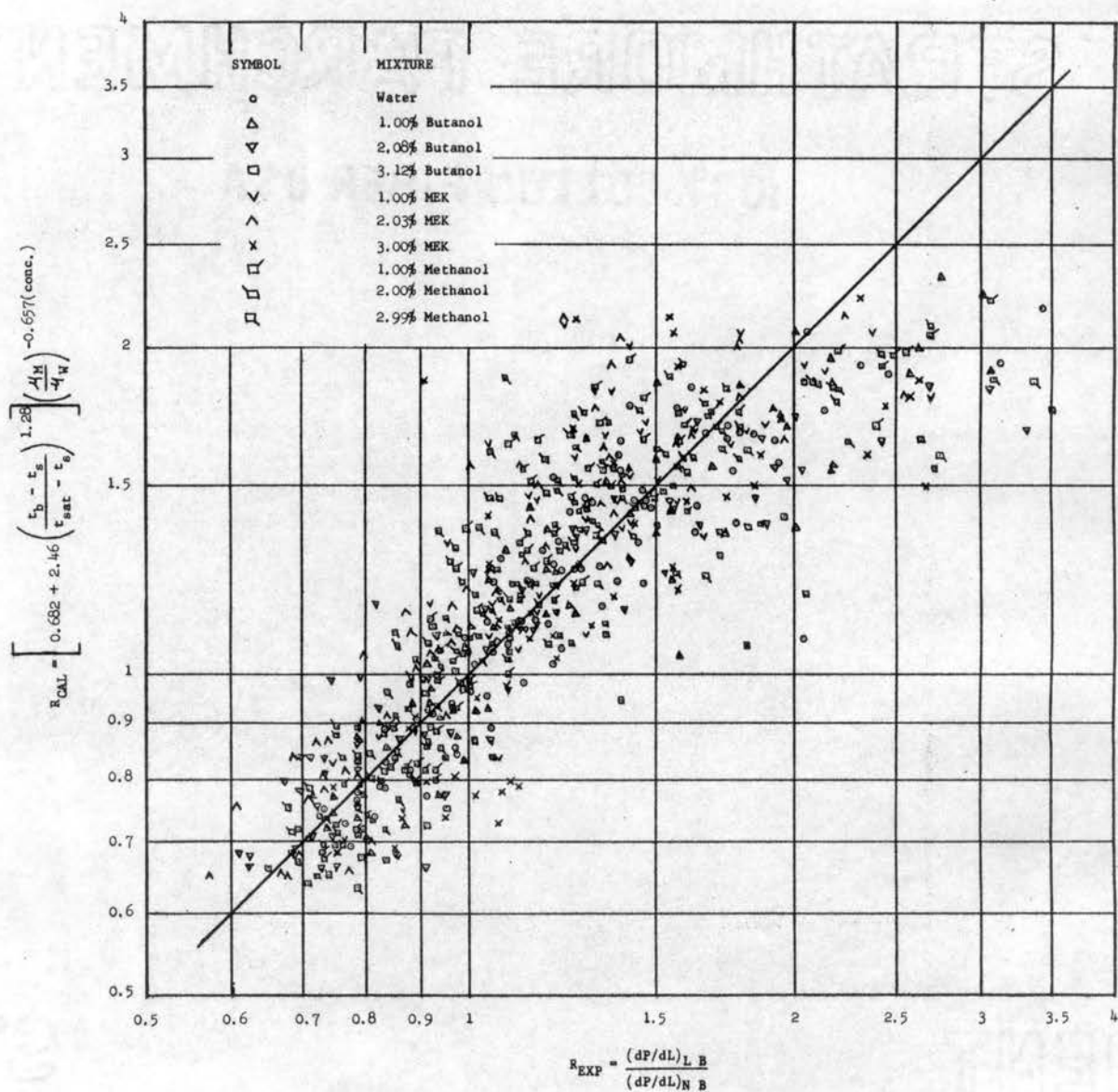


Figure 13. Correlation of Data

TABLE II

TEST DATA

Run No. ^a	Pressure psia	Mass Velocity lb/ft ² -sec	Heat Flux Btu/hr-ft ²	BULK TEMPERATURE °F			PRESSURE DROP ^b Inches of Water								
				Inlet	Outlet	Start of Local Boiling	1	2	3	4	5	6	7	8	9
0001	50	299	62,100	235	274	263	3.13	6.09	8.88	10.00	11.32	12.07	12.52	13.55	14.03
0002	50	299	104,600	204	273	251	3.11	6.00	8.75	9.89	11.09	11.99	12.51	13.50	13.99
0003	50	299	155,200	164	267	233	2.98	5.83	8.48	9.60	10.85	11.83	12.49	13.58	14.96
0004	50	299	202,600	132	268	221	2.76	5.48	8.10	9.45	10.88	11.46	12.86	14.46	16.86
0005	50	299	250,000	95	263	190	2.62	5.21	7.82	9.22	10.88	11.92	12.70	13.97	15.79
0006	100	189	202,600	96	312	261	1.01	2.02	3.18	3.83	4.64	4.93	5.56	6.52	7.48
0007	100	232	202,600	139	316	246	1.67	3.30	4.97	5.85	6.86	7.67	8.32	9.75	11.36
0008	100	299	104,600	250	311	292	3.08	5.93	8.70	9.75	11.06	11.93	12.60	13.74	14.74
0009	100	299	155,200	213	311	282	2.94	5.78	8.47	9.59	10.88	11.87	12.64	13.91	15.44
0010	100	299	202,600	178	309	266	2.92	5.72	8.32	9.49	10.88	12.00	12.73	14.12	15.75
0011	100	299	250,000	138	303	252	2.72	5.42	8.01	9.26	10.65	11.78	12.38	13.74	15.05
0012	100	354	202,600	196	309	272	3.88	7.50	11.03	12.49	14.25	15.54	16.59	18.09	19.55
0013	100	401	202,600	208	307	274	4.84	9.38	13.85	15.79	17.89	19.35	20.66	22.31	23.78
0014	150	299	155,200	244	341	310	3.00	5.83	8.54	9.60	10.91	11.91	12.64	13.80	14.96
0015	150	299	250,000	175	336	275	2.81	5.48	8.06	9.41	10.84	12.04	12.86	14.44	16.16
0016	250	299	250,000	219	383	318	2.87	5.66	8.25	9.60	11.14	12.26	13.20	14.79	16.14

TABLE II (Continued)

Run No. ^a	Pressure psia	Mass Velocity lb/sec-ft ²	Heat Flux Btu/hr-ft ²	BULK TEMPERATURE °F			PRESSURE DROP ^b Inches of Water								
				Inlet	Outlet	Start of Local Boiling	1	2	3	4	5	6	7	8	9
1201	50	299	62,100	233	272	264	3.08	5.92	8.78	9.90	11.21	12.08	12.28	13.49	13.64
1202	50	299	104,600	198	265	249	3.00	5.81	8.55	9.68	10.73	11.68	11.92	13.12	13.31
1203	50	299	155,200	158	259	235	2.92	5.70	8.42	9.52	10.58	11.38	11.76	12.90	13.50
1204	50	299	202,600	126	259	215	2.76	5.40	8.04	9.30	10.65	11.49	12.04	13.25	14.29
1205	50	299	250,000	84	248	213	2.62	5.10	7.58	8.93	9.92	10.95	11.32	12.75	13.28
1206	100	189	202,600	96	311	261	0.73	1.58	2.66	3.38	4.22	4.42	5.06	5.85	6.82
1207	100	232	202,600	140	318	272	1.54	3.09	4.65	5.44	6.15	6.81	7.48	8.64	10.20
1208	100	299	104,600	249	317	300	2.72	5.38	7.99	9.11	10.14	10.97	11.36	12.49	13.09
1209	100	299	155,200	216	320	292	2.68	5.28	7.79	8.94	9.94	10.94	11.66	13.38	15.08
1210	100	299	202,600	177	312	270	2.62	5.23	7.65	8.75	9.82	10.85	11.48	12.90	14.04
1211	100	299	250,000	147	316	264	2.51	4.99	7.35	8.68	9.82	10.95	11.78	13.55	15.38
1212	100	354	202,600	195	308	278	3.62	7.16	10.58	12.00	13.37	14.62	15.38	16.95	18.00
1213	100	401	202,600	208	307	283	4.59	8.98	13.24	15.08	16.88	18.28	19.20	20.90	21.82
1214	150	299	155,200	246	348	323	2.72	5.32	7.91	9.05	10.24	11.19	11.85	13.28	14.70
1215	150	299	250,000	183	348	275	2.68	5.21	7.70	9.11	10.66	11.89	12.82	14.65	16.84
1216	250	299	250,000	228	394	337	2.55	5.10	7.58	9.00	10.50	11.59	12.69	14.59	16.80

TABLE II (Continued)

Run No. ^a	Pressure psia	Mass Velocity lb/sec-ft ²	Heat Flux Btu/hr-ft ²	BULK TEMPERATURE °F			PRESSURE DROP ^b Inches of Water								
				Inlet	Outlet	Start of Local Boiling	1	2	3	4	5	6	7	8	9
2201	50	299	62,100	228	269	262	2.94	5.78	8.59	9.75	11.06	11.78	12.12	13.35	13.35
2202	50	299	104,600	194	263	241	2.92	5.70	8.51	9.56	10.58	11.32	11.70	12.94	13.14
2203	50	299	155,200	153	258	232	2.78	5.49	8.18	9.30	10.31	10.99	11.38	12.45	13.16
2204	50	299	202,600	117	254	222	2.66	5.29	7.88	9.00	10.05	10.89	11.12	12.11	13.12
2205	50	299	250,000	79	247	213	2.48	4.95	7.46	8.62	9.82	10.91	11.20	12.00	12.79
2206	100	189	202,600	78	292	239	0.93	1.96	3.08	3.57	4.01	4.29	4.59	5.07	5.41
2207	100	232	202,600	133	308	262	1.54	3.08	4.72	5.46	6.00	6.64	7.05	8.14	9.08
2208	100	299	104,600	246	315	298	2.92	5.70	8.44	9.68	10.58	11.51	11.85	12.94	13.28
2209	100	299	155,200	214	319	294	2.85	5.53	8.08	9.30	10.12	11.06	11.51	13.72	15.96
2210	100	299	202,600	174	310	274	2.78	5.45	8.00	9.05	9.90	10.82	11.42	13.05	14.50
2211	100	299	250,000	134	302	259	2.53	5.04	7.48	8.68	9.59	10.59	11.18	12.54	13.54
2212	100	354	202,600	195	308	279	3.66	7.22	10.66	12.02	13.33	14.49	15.38	17.26	18.65
2213	100	401	202,600	212	312	282	4.58	9.08	13.42	15.30	17.02	18.45	19.35	22.01	23.98
2214	150	299	155,200	241	344	318	2.76	5.40	7.99	9.09	10.04	10.88	11.36	12.68	13.76
2215	150	299	250,000	173	341	297	2.62	5.21	7.66	8.85	9.98	11.00	11.78	13.31	14.72
2216	250	299	250,000	221	387	345	2.62	5.25	7.76	9.00	10.40	11.40	12.26	13.84	15.64

TABLE II (Continued)

Run No. ^a	Pressure psia	Mass Velocity lb/sec-ft ²	Heat Flux Btu/hr-ft ²	BULK TEMPERATURE °F			PRESSURE DROP ^b Inches of Water								
				Inlet	Outlet	Start of Local Boiling	1	2	3	4	5	6	7	8	9
3201	50	299	62,100	228	269	261	3.22	6.38	9.56	11.10	12.22	13.01	13.42	14.68	14.75
3202	50	299	104,600	198	267	252	3.15	6.19	9.28	10.42	11.48	12.64	12.94	14.10	14.48
3203	50	299	155,200	156	260	235	2.91	5.85	8.75	9.94	11.06	11.75	12.19	13.22	13.59
3204	50	299	202,600	114	251	226	2.85	5.70	8.55	9.77	10.95	12.09	11.98	13.05	13.74
3205	50	299	250,000	80	248	213	2.53	5.26	7.85	9.08	10.28	11.57	11.59	12.69	13.46
3206	100	189	202,600	78	291	253	1.01	2.08	3.23	3.75	4.16	4.46	4.65	5.38	5.64
3207	100	232	202,600	116	291	250	1.61	3.26	4.95	5.70	6.21	6.75	6.98	7.84	8.14
3208	100	299	104,600	245	313	297	3.12	6.08	8.93	10.3	11.23	12.24	12.62	13.70q	14.02
3209	100	299	155,200	205	307	282	3.04	5.92	8.70	9.82	10.84	11.78	12.08	13.32	14.49
3210	100	299	202,600	173	309	274	2.89	5.72	8.36	9.45	10.42	11.38	12.00	14.02	15.84
3211	100	299	250,000	139	307	262	2.70	5.44	8.06	9.26	10.28	11.53	12.27	14.06	15.56
3212	100	354	202,600	189	302	271	3.75	7.46	11.06	12.60	13.88	15.08	15.64	17.14	18.16
3213	100	401	202,600	205	305	276	4.69	9.28	13.70	15.60	17.32	18.79	19.75	21.69	23.08
3214	150	299	155,200	240	343	318	2.92	5.82	8.70	9.98	11.02	11.89	12.41	13.54	14.62
3215	150	299	250,000	176	344	303	2.81	5.62	8.32	9.52	10.72	11.89	12.80	14.81	16.91
3216	250	299	250,000	224	392	339	2.83	5.66	8.42	9.68	11.08	12.15	13.20	15.39	18.00

TABLE II (Continued)

Run No. ^a	Pressure psia	Mass Velocity lb/sec-ft ²	Heat Flux Btu/hr-ft ²	BULK TEMPERATURE °F			PRESSURE DROP ^b Inches of Water								
				Inlet	Outlet	Start of Local Boiling	1	2	3	4	5	6	7	8	9
1301	50	299	62,100	229	271	261	3.09	6.08	9.00	10.18	11.32	12.30	12.60	13.55	13.65
1302	50	299	104,600	198	269	252	3.04	6.00	8.94	10.14	11.23	12.32	12.62	13.59	13.88
1303	50	299	155,200	158	264	237	2.98	5.96	8.92	10.18	11.44	12.52	12.88	14.00	14.96
1304	50	299	202,600	123	260	223	2.83	5.81	8.75	10.09	11.40	12.38	12.84	14.04	15.19
1305	50	299	250,000	87	258	215	2.69	5.53	8.44	9.92	11.48	11.92	13.24	14.23	15.19
1306	100	189	202,600	91	305	261	1.16	2.40	3.75	4.20	4.80	5.25	5.48	6.08	6.75
1307	100	232	202,600	129	305	262	1.80	3.73	5.70	6.45	6.98	7.72	7.95	8.85	9.58
1308	100	299	104,600	248	318	302	3.17	6.42	9.82	11.08	12.14	13.04	13.50	14.42	14.92
1309	100	299	155,200	210	313	288	3.15	6.34	9.76	10.99	12.02	13.03	13.35	14.44	15.26
1310	100	299	202,600	172	309	277	3.11	6.24	9.68	10.89	11.90	12.95	13.29	14.59	15.90
1311	100	299	250,000	141	309	268	3.00	6.15	9.64	10.88	11.98	13.06	13.69	15.34	17.21
1312	100	354	202,600	201	315	287	4.59	9.26	13.86	15.52	16.91	18.16	18.87	20.53	22.76
1313	100	401	202,600	215	316	289	5.89	11.89	17.81	19.89	21.73	23.25	24.11	25.91	28.31
1314	150	299	155,200	244	346	321	3.40	6.96	10.72	12.05	13.05	14.10	14.44	15.6	16.66
1315	150	299	250,000	176	342	301	3.30	6.75	10.42	11.70	12.76	13.84	14.55	16.16	17.92
1316	250	299	250,000	222	387	343	3.45	7.12	10.91	12.22	13.28	14.32	15.08	16.66	18.45

TABLE II (Continued)

Run No. ^a	Pressure psia	Mass Velocity lb/sec-ft ²	Heat Flux Btu/hr-ft ²	BULK TEMPERATURE °F			PRESSURE DROP ^b Inches of Water								
				Inlet	Outlet	Start of Local Boiling	1	2	3	4	5	6	7	8	9
2301	50	299	62,100	224	267	257	3.39	6.73	10.05	11.30	12.60	13.40	13.68	14.70	14.92
2302	50	299	104,600	192	262	246	3.32	6.59	9.82	11.12	12.15	13.10	13.34	14.38	14.63
2303	50	299	155,200	153	259	234	3.21	6.40	9.59	10.72	11.62	12.81	12.91	14.12	15.13
2304	50	299	202,600	116	255	220	3.06	6.16	9.35	10.47	11.37	12.34	12.74	14.05	15.41
2305	50	299	250,000	80	250	212	2.85	5.92	9.04	10.20	11.49	12.45	12.79	13.54	15.00
2306	100	189	202,600	83	299	246	1.09	2.31	3.47	3.98	4.45	4.88	5.10	5.66	6.32
2307	100	232	202,600	126	301	257	1.80	3.64	5.46	6.19	6.66	7.37	7.58	8.44	9.30
2308	100	299	104,600	245	315	297	3.52	7.07	10.63	11.98	12.95	13.96	14.40	15.38	15.69
2309	100	299	155,200	207	310	286	3.49	7.01	10.58	11.94	12.88	13.99	14.30	15.28	16.20
2310	100	299	202,600	171	306	272	3.49	7.01	10.50	11.75	12.75	13.91	14.14	15.58	17.08
2311	100	299	250,000	135	304	263	3.39	6.84	10.31	11.55	12.56	13.61	14.06	15.68	17.40
2312	100	354	202,600	195	309	281	4.59	8.89	12.73	14.34	15.62	16.91	17.55	19.05	21.20
2313	100	401	202,600	210	310	285	5.78	11.18	16.01	18.09	19.72	21.30	22.31	23.96	26.51
2314	150	299	155,200	238	341	317	3.79	7.52	11.08	12.46	13.55	14.54	14.94	15.88	16.76
2315	150	299	250,000	168	334	294	3.54	7.14	10.55	11.86	12.82	13.82	14.21	15.56	16.85
2316	250	299	250,000	219	383	342	3.77	7.46	10.82	12.08	13.12	14.10	14.75	16.28	18.05

TABLE II (Continued)

Run No. ^a	Pressure psia	Mass Velocity lb/sec-ft ²	Heat Flux Btu/hr-ft ²	BULK TEMPERATURE °F			PRESSURE DROP ^b Inches of Water								
				Inlet	Outlet	Start of Local Boiling	1	2	3	4	5	6	7	8	9
3301	50	299	62,100	220	262	252	3.47	6.73	9.68	11.02	12.19	13.12	13.42	14.45	14.98
3302	50	299	104,600	188	259	246	3.36	6.52	9.46	10.82	11.83	12.90	13.01	14.18	14.30
3303	50	299	155,200	145	251	227	3.28	6.47	9.49	10.84	11.86	12.82	13.10	14.36	14.74
3304	50	299	202,600	112	251	218	3.19	6.38	9.34	10.72	11.68	12.80	13.24	14.81	16.06
3305	50	299	250,000	81	251	203	3.00	6.11	9.13	10.54	11.83	12.76	13.46	15.15	17.02
3306	100	189	202,600	85	302	253	1.58	3.26	4.76	5.45	5.74	6.34	6.54	7.52	8.60
3307	100	232	202,600	124	300	258	2.49	5.06	7.14	8.12	8.64	9.41	9.56	10.63	11.72
3308	100	299	104,600	240	310	294	4.05	7.93	11.59	13.33	14.62	15.73	16.12	17.18	17.55
3309	100	299	155,200	203	306	282	4.22	8.32	12.09	13.95	15.34	16.52	16.93	18.05	19.20
3310	100	299	202,600	165	301	270	4.20	8.32	12.15	13.99	15.41	16.61	16.96	18.20	19.42
3311	100	299	250,000	133	302	261	4.20	8.38	12.24	14.14	15.54	16.78	17.14	18.86	20.78
3312	100	354	202,600	189	303	276	6.06	11.90	16.33	18.46	19.93	21.24	21.95	23.26	24.82
3313	100	401	202,600	206	306	281	7.70	15.02	20.55	23.29	25.28	26.86	27.82	29.48	31.46
3314	150	299	155,200	234	336	312	4.65	9.11	13.28	15.34	16.93	18.05	18.49	19.46	20.04
3315	150	299	250,000	168	335	304	4.58	9.15	13.28	15.22	16.58	17.70	18.19	19.72	21.75
3316	250	299	250,000	216	380	342	4.88	9.62	13.55	15.41	16.59	17.66	18.15	19.66	21.49

TABLE II (Continued)

Run No. ^a	Pressure psia	Mass Velocity lb/sec-ft ²	Heat Flux Btu/hr-ft ²	BULK TEMPERATURE °F			PRESSURE DROP ^b Inches of Water								
				Inlet	Outlet	Start of Local Boiling	1	2	3	4	5	6	7	8	9
1401	50	299	62,100	235	278	266	3.96	7.12	9.90	11.02	12.19	13.01	13.55	14.44	14.96
1402	50	299	104,600	203	274	252	3.90	6.96	9.79	10.84	11.90	12.75	13.31	14.44	15.24
1403	50	299	155,200	161	267	237	3.68	6.73	9.43	10.48	11.59	12.48	13.10	14.38	15.79
1404	50	299	202,600	128	268	221	3.64	6.62	9.26	10.34	11.56	12.68	13.31	14.78	16.72
1405	50	299	250,000	86	257	190	3.49	6.30	8.89	9.98	11.70	12.30	13.16	14.14	15.08
1406	100	189	202,600	87	298	235	1.20	2.29	3.50	3.99	4.56	5.14	5.30	5.97	6.51
1407	100	232	202,600	131	308	260	2.00	3.62	5.32	6.03	6.79	7.58	7.91	8.84	9.86
1408	100	299	104,600	250	320	300	4.01	7.05	9.86	10.88	12.00	12.82	13.42	14.36	15.31
1409	100	299	155,200	215	320	290	3.94	6.94	9.68	10.80	11.92	13.01	13.72	15.34	17.36
1410	100	299	202,600	178	317	270	3.82	6.82	9.46	10.58	11.92	13.06	13.78	15.39	17.56
1411	100	299	250,000	135	304	254	3.71	6.71	9.30	10.39	11.59	12.71	13.31	14.44	15.60
1412	100	354	202,600	198	312	282	4.95	8.68	12.18	13.63	15.19	16.49	17.36	18.88	20.45
1413	100	401	202,600	214	314	283	6.38	11.11	15.49	17.39	19.31	20.72	21.97	23.80	25.62
1414	150	299	155,200	241	344	314	3.98	7.05	9.75	10.80	11.98	12.98	13.46	14.51	15.60
1415	150	299	250,000	173	341	285	3.81	6.79	9.43	10.58	11.92	13.05	13.74	15.22	16.82
1416	250	299	250,000	219	384	325	3.90	6.86	9.50	10.70	12.11	13.07	13.96	15.50	17.21

TABLE II (Continued)

Run No. ^a	Pressure psia	Mass Velocity lb/sec-ft ²	Heat Flux Btu/hr-ft ²	BULK TEMPERATURE °F			PRESSURE DROP ^b Inches of Water								
				Inlet	Outlet	Start of Local Boiling	1	2	3	4	5	6	7	8	9
2401	50	299	62,100	234	276	263	3.73	6.54	9.28	10.36	11.55	12.38	12.88	13.78	14.36
2402	50	299	104,600	198	270	252	3.69	6.46	9.28	10.33	11.36	12.30	12.66	13.58	13.99
2403	50	299	155,200	157	262	227	3.56	6.32	8.92	9.98	11.04	11.96	12.38	13.33	14.06
2404	50	299	202,600	120	258	210	3.38	6.08	8.59	9.41	10.85	11.65	12.22	13.33	14.23
2405	50	299	250,000	87	256	197	3.04	5.55	7.95	9.04	10.72	11.22	12.15	13.12	14.32
2406	100	189	202,600	90	306	243	1.14	2.16	3.38	3.88	4.46	4.95	5.23	5.96	6.73
2407	100	232	202,600	136	311	240	1.82	3.36	4.65	5.72	6.49	7.31	7.69	8.28	10.09
2408	100	299	104,600	250	320	299	3.59	6.31	9.04	10.04	11.20	12.04	12.61	13.57	14.78
2409	100	299	155,200	210	313	283	3.56	6.22	8.89	9.98	11.06	12.08	12.45	13.46	14.32
2410	100	299	202,600	178	315	269	3.49	6.08	8.66	9.79	11.04	12.08	12.82	14.32	16.29
2411	100	299	250,000	136	305	246	3.34	5.92	8.40	9.52	10.80	11.50	12.50	13.74	15.04
2412	100	354	202,600	201	315	279	4.48	7.95	11.42	12.86	14.38	15.71	16.70	18.56	21.08
2413	100	401	202,600	214	312	286	5.76	10.22	14.64	16.44	18.30	19.72	20.89	22.55	24.32
2414	150	299	155,200	241	343	312	3.66	6.34	9.04	10.05	11.21	12.08	12.64	13.65	14.62
2415	150	299	250,000	173	341	283	3.49	6.06	8.64	9.79	11.10	12.15	12.98	14.40	16.18
2416	250	299	250,000	222	386	336	3.60	6.26	8.81	9.98	11.32	12.38	13.22	14.79	16.54

TABLE II (Continued)

Run No. ^a	Pressure psia	Mass Velocity lb/sec-ft ²	Heat Flux Btu/hr-ft ²	BULK TEMPERATURE °F			PRESSURE DROP ^b Inches of Water								
				Inlet	Outlet	Start of Local Boiling	1	2	3	4	5	6	7	8	9
3401	50	299	62,100	232	274	264	3.39	6.11	8.78	9.94	11.15	11.96	12.45	13.39	13.80
3402	50	299	104,600	198	269	249	3.26	5.92	8.61	9.68	10.76	11.62	12.08	12.98	13.50
3403	50	299	155,200	156	262	233	3.15	5.79	8.39	9.45	10.51	11.38	11.81	12.78	13.42
3404	50	299	202,600	126	265	219	2.88	5.40	7.90	8.98	10.17	11.06	11.80	13.65	16.15
3405	50	299	250,000	91	261	199	2.51	4.93	7.12	8.08	9.95	10.54	11.55	13.55	16.35
3406	100	189	202,600	87	302	238	1.12	2.12	3.30	3.79	4.38	4.80	5.11	5.67	6.34
3407	100	232	202,600	128	303	254	1.79	3.36	5.02	5.74	6.34	7.09	7.31	8.20	9.02
3408	100	299	104,600	247	317	295	3.22	5.85	8.53	9.60	10.79	11.57	12.08	12.99	13.58
3409	100	299	155,200	207	310	281	3.14	5.74	8.38	9.49	10.55	11.48	11.92	12.90	13.69
3410	100	299	202,600	173	309	267	3.08	5.66	8.23	9.30	10.40	11.46	11.95	13.28	14.81
3411	100	299	250,000	136	305	260	2.91	5.42	8.00	9.08	10.20	11.33	11.91	13.30	14.72
3412	100	354	202,600	196	310	277	4.39	7.87	11.30	12.83	14.29	15.53	16.29	17.95	19.84
3413	100	401	202,600	210	310	285	5.55	9.98	14.29	16.41	18.04	19.58	20.41	22.12	23.78
3414	150	299	155,200	241	345	316	3.21	5.83	8.49	9.58	10.66	11.62	12.15	13.36	14.85
3415	150	299	250,000	172	338	282	3.08	5.66	8.19	9.34	10.54	11.62	12.20	13.72	15.26
3416	250	299	250,000	212	374	329	3.10	5.72	8.24	9.40	10.51	11.48	12.11	13.15	14.06

a. Run numbers are coded as follows:

1. The first digit is nominal concentration of additive in percent by weight.
2. The second digit is additive identification where 0 = water only; 2 = butanol; 3 = methyl ethyl ketone; 4 = methanol.
3. The third and fourth digits together identify runs with common values of pressure, mass velocity and heat flux.

b. Pressure drop data were measured relative to the reference (0) pressure tap.

CHAPTER VII

ANALYSIS OF EXPERIMENTAL ERRORS

The purpose of this chapter is to analyze the errors which may have existed in the experimental measurements made in this investigation. The errors discussed are of three categories: (1) errors in instrument readings due to inherent instrument limitations, (2) the cumulative error existing in a value calculated from imperfect values, and (3) errors introduced through certain assumptions.

Errors in the following measured quantities will be discussed: temperature, power input to the test section, differential pressure across the flow-measuring orifice and along the test section, and system pressure. The maximum error existing in the calculated flow rate will be analyzed. The effect of the following assumptions will be discussed.

1. The heat loss from the test section to the atmosphere is negligible.
2. The axial heat flow along the test section is negligible.
3. The heat flux is uniform along the test section length.

The smallest scale division of the potentiometer used for temperature measurement was 0.01 mv. Since 0.03 mv corresponds to 1°F for iron-constantan wire in the range of temperatures found in this investigation, it was possible to measure temperature within one-sixth of 1°F. Uncertainties in thermocouple calibration and fluid property values which were

evaluated from measured temperatures did not justify the use of a value of this accuracy. For these reasons, temperatures were rounded to the nearest degree Fahrenheit.

The scale of the wattmeter used for measuring the power input to the test section was such that a reading accurate within 0.5 watt was possible. The maximum error occurred at 38 watts, the lowest wattmeter reading used in the experiment. The maximum error in the power measurement was calculated as $\frac{0.5 \times 100}{38} = 1.3\%$.

It was possible to read differential pressures across the flow-measuring orifice and along the test section within ± 0.05 inch of manometer fluid. The surface tension varied among different manometer tubes and along the length of a given tube and resulted in menisci of varying shapes. The specific gravity of the manometer fluid was given by the manufacturer as 1.75 at 55°F. An experiment was conducted to determine the specific gravity of the fluid at temperatures in the range of 70°F to 100°F. The specific gravity was found to vary from 1.745 at 80°F to 1.731 at 100°F. Fluctuation of differential pressure across the orifice was noted in some runs. It is estimated that the cumulative effect of the above factors resulted in differential pressure measurements accurate within ± 0.2 inches of water.

The smallest division of the gage used for measuring system pressure was 1 psi. A calibration curve furnished by the manufacturer of the gage indicated zero correction for the range of pressures used in this investigation. This curve neglected corrections of less than 0.75 psi. It is believed that the system pressure measurement was accurate within ± 1 psi.

An accurate determination of mass flow rate is of prime importance in an experiment of this nature. Extreme care was taken in the calibration of the flow-measuring orifice in order to obtain the best possible accuracy in the flow measurement. The orifice was calibrated by weighing the amounts of fluid delivered through the orifice in a given time for particular values of pressure drop across the orifice. The scale used for weighing the fluid was accurate within ± 0.01 lb and the timer used was accurate within ± 0.001 minute. The equation given in the ASME Power Test Codes (1949), Reference (20), for the gravimetric flow rate of an incompressible fluid, was solved for the coefficient of discharge, K , and experimentally determined values substituted in the right-hand side. The result is

$$K = \frac{W}{0.668 A_2 E \sqrt{\rho \Delta P}} \quad \text{VII-1}$$

where

K = coefficient of discharge, dimensionless;

W = flow rate, lb/sec;

A_2 = throat area of the orifice, sq in.;

E = area multiplier for thermal expansion of the orifice plate, dimensionless;

ρ = density of the fluid, lb/ft³.

ΔP = pressure drop across the orifice, psi;

0.668 = a constant to make the equation dimensionally correct for the units given.

Figure 15, Appendix A, is a plot of the discharge coefficient with Reynolds number based on the throat diameter of the orifice. The maximum

error in the discharge coefficient may be calculated according to the following rules given by Marshall (21).

1. When two inaccurate numbers are multiplied, the error in the product is equal to the algebraic sum of the individual errors.
2. When one inaccurate number is divided by another, the maximum possible fraction of error in the quotient is equal to the sum of the fractions of error in the divisor and dividend.
3. When an inaccurate number is raised to a power, fractional or otherwise, the result will have a percent of error equal to the percent of error in the number multiplied by the power. The maximum fractions of error in the individual terms of Equation VII-1 are tabulated in Table III.

TABLE III
SUMMARY OF EXPERIMENTAL ERRORS IN FLOW MEASUREMENT

Parameter	Maximum Fraction of Error
Weight of Fluid	0.00025
Time	0.0008
Area of Orifice	0.0026
Density	0.0005
Pressure Drop Across Orifice	0.02
Area Multiplier for Thermal Expansion*	Negligible

* This term is 1.000 for stainless steel in the temperature range under consideration.

Combining these errors in the manner indicated by rules 1 through 3 given above yields:

$$\text{Max. error in } K = \left[0.00025 + 0.0008 + 0.0026 + \left(\frac{0.02 + 0.0005}{2} \right) \right] 100 = 1.39\% .$$

It should be noted that the predominant factor in the error in the discharge coefficient is the error in the differential pressure. The fractional error given above, 0.02, occurs at the lowest flow rate considered. This fraction of error decreases rapidly as the flow rate increases. It was assumed for the calculation of the maximum error in the discharge coefficient that the maximum fractional errors tabulated above were in the same algebraic sense; in actuality, the signs of the errors will probably vary and result in a smaller error in the discharge coefficient. It is believed, on the basis of these factors, that the calculated flow rate was accurate within $\pm 1\%$.

The maximum outer surface temperature of the test section insulation was found to be 110°F. The heat loss from the test section may be calculated by assuming a natural convection heat transfer coefficient of 1 Btu/hr-ft² and a temperature difference of 40°F between the insulation and atmosphere:

$$q_{\text{Loss}} = hA(\Delta t) = 1 \cdot \frac{\pi \cdot 3}{12} \cdot 6(40) = 189 \text{ Btu/hr} .$$

The loss is 0.49% of 39,000 Btu/hr, the minimum heat input considered in the investigation, and may be neglected.

The heat loss through the downstream power lug of the test section may be calculated for a maximum temperature difference of 380°F between

the lug surface and the atmosphere as:

$$q_{\text{Loss}} = hA(\Delta t) = 1 \cdot \left[\frac{2(2 \cdot 3 + \frac{3}{8} \cdot 3) + 2(\frac{3}{8})}{144} \right] (380) = 39.6 \text{ Btu/hr.}$$

The loss is 0.1% of the minimum heat input and is negligible.

The axial heat conduction along the test section may be calculated for a temperature difference of 400°F between two points six feet apart as:

$$q = kA \left(\frac{\Delta t}{\Delta x} \right) = 10 \cdot \frac{\pi}{4} \left[\left(\frac{0.502}{12} \right)^2 - \left(\frac{0.399}{12} \right)^2 \right] \left(\frac{400}{6} \right) = 0.334 \text{ Btu/hr.}$$

The axial conduction is negligible compared to the minimum heat input.

The voltage drop was measured at five sections along the test section. A typical set of curves of voltage drop with distance is shown in Figure 17, Appendix A. Although there was some scattering of data, the best curve through the points appeared to be a straight line. Since the current in the test section was constant, a linear voltage drop verified the assumption of uniform heat flux.

CHAPTER VIII

CONCLUSIONS AND RECOMMENDATIONS

The following conclusions were drawn from analysis of the pressure drop data obtained in this investigation.

1. Local boiling pressure drop for water containing an organic additive may be correlated within $\pm 25\%$ for the additives and range of variables considered in this investigation by the following empirical equation relating significant variables:

$$\left(\frac{dP}{dL}\right)_{LB} = \left(\frac{dP}{dL}\right)_{NB} \left[0.682 + 2.46 \left(\frac{t_b - t_s}{t_{sat} - t_s} \right)^{1.28} \right] \left(\frac{\mu_m}{\mu_w} \right)^{-0.657(\text{conc.})}$$

The saturation temperature and viscosities used in the above equation may be found by use of the methods and curves presented in Appendix C.

2. Local boiling pressure drop for distilled water may be correlated within $\pm 25\%$ by the following empirical equation:

$$\left(\frac{dP}{dL}\right)_{LB} = \left(\frac{dP}{dL}\right)_{NB} \left[0.682 + 2.46 \left(\frac{t_b - t_s}{t_{sat} - t_s} \right)^{1.28} \right]$$

3. The presence in water of an additive of the types and concentrations considered in this investigation appears to be detrimental to the local boiling pressure drop beyond the first 20% of the local boiling length.

As a result of this study the following recommendations are made.

1. Further studies of the mechanism of local boiling should be made

and an analytical method developed for predicting local boiling pressure drop.

2. Careful study of the mechanism of local boiling should be made prior to the selection of mixtures for investigation. Further study is recommended on the effect of additives with properties which should, according to the mechanism, reduce pressure drop in local boiling.

3. Knowledge of mixture property values is limited. Selection of particular mixtures for study should be based in part, at least, on the availability or obtainability of accurate property data over a wide range of pressures and temperatures.

4. Studies of local boiling of water with additives should be made at considerably higher pressures than those used in this investigation.

5. Further studies with the object of reducing static pressure drop in local boiling with mixtures of water and additives of the types considered in this investigation are not recommended.

Contrary to the predictions of other investigators, the use in water of additives of the types considered in this investigation appeared to increase static pressure drop in forced convection local boiling. Experimental results in areas which are not yet covered by analytical methods are subject to different interpretation by different investigators. One of the purposes of this study was to contribute experimental data which may be of value in arriving at analytical means for predicting local boiling pressure drop.

It may be stated in conclusion that the mechanism of local boiling is imperfectly understood. The use of organic additives in water, with the object of improving heat transfer characteristics or reducing static pressure drop in forced convection local boiling should be considered with care.

SELECTED BIBLIOGRAPHY

1. Leppert, G., C. P. Costello, and B. M. Hoglund, "Boiling Heat Transfer to Water Containing a Volatile Additive," Trans. Amer. Soc. Mech. Engrs., Vol. 80, pp. 1395-1404, (1958).
2. Forster, K. E. and R. Greif, "Heat Transfer to a Boiling Liquid--- Mechanism and Correlations," Trans. Amer. Soc. Mech. Engrs., JOURNAL OF HEAT TRANSFER, Vol. 81, pp. 43-53, (1959).
3. Rohsenow, W. M., "Method of Correlating Heat Transfer Data for Surface Boiling of Liquids," Trans. Amer. Soc. Mech. Engrs., Vol. 74, pp. 969-975, (1952).
4. Kreith, F. and M. Summerfield, "Pressure Drop and Convective Heat Transfer with Boiling at High Heat Flux," Trans. Amer. Soc. Mech. Engrs., Vol. 72, pp. 869-878, (1950).
5. Tanger, G. E., Local Boiling Pressure Drop for Forced Circulation of Water, (Unpublished Ph.D. dissertation, Oklahoma State University, 1959).
6. Reynolds, J. B., Local Boiling Pressure Drop, ANL-5178, (1954).
7. Bonilla, C. F., Nuclear Engineering, McGraw-Hill, New York, N.Y., (1957).
8. Van Wijk, W. R., A. S. Vos, S. J. D. van Stralen, "Heat Transfer to Boiling Binary Liquid Mixtures," Chem. Engr. Sc., Vol. 5, pp. 68-80, (1956).
9. Van Stralen, S. J. D., "Heat Transfer to Boiling Binary Liquid Mixtures at Atmospheric and Subatmospheric Pressures," Chem. Engr. Sc., Vol. 5, pp. 290-296, (1956).
10. Leppert, G., Stanford University, Stanford, California, (Private Communication dated July 19, 1960).
11. Jens, W. H., P. A. Lottes, Analysis of Heat Transfer, Burnout, Pressure Drop, and Density Data for High-Pressure Water, ANL-4627, (1951).
12. McAdams, W. H., J. N. Addoms, W. E. Kennel, Heat Transfer at High Rates to Water with Surface Boiling, ANL-4268, (1952).
13. McAdams, W. H., Heat Transmission, 2nd Ed., McGraw-Hill, New York, N.Y., (1942).
14. Colburn, A. P., "Method of Correlating Forced Convection Heat Transfer Data and a Comparison with Fluid Friction," Trans. Amer. Inst. Chem. Engrs., Vol. 29, pp. 174-210, (1933).
15. Eckert, E. R. G. and R. M. Drake, Introduction to the Transfer of Heat and Mass, 2nd. Ed. McGraw-Hill, New York, N.Y., (1959).

16. Butler, P. A., Modification of a Forced Convection Heat Transfer Loop for Use With Binary Mixtures, (Unpublished thesis, Oklahoma State University, 1960).
17. Bonilla, C. F. and C. H. Perry, "Heat Transmission to Boiling Binary Liquid Mixtures," Trans. Amer. Inst. Chem. Engrs., Vol. 37, pp. 685-705, (1941).
18. Jakob, M., Heat Transfer, Vol. I, John Wiley & Sons, New York, N.Y., (1949).
19. Martinelli, R. C., and D. B. Nelson, "Prediction of Pressure Drop During Forced-Circulation Boiling of Water," Trans. Amer. Soc. Mech. Engrs., Vol. 70, pp. 695-702, (1948).
20. Power Test Codes 19.5, 4-1949, Amer. Soc. Mech. Engr., (1949).
21. Marshall, R. B., Measurements in Electrical Engineering, Pt. 1, 2nd Ed., John S. Swift Co., Cincinnati, Ohio, (1948).
22. ASTM Standards on Petroleum Products---Committee D-2-1947, Amer. Soc. for Testing Materials, Philadelphia, Pa., (1947).
23. Lottes, P. A., "Physical and Thermodynamic Properties of Light and Heavy Water," The Reactor Handbook, Vol. 3, McGraw-Hill, New York, N.Y., (1955).
24. Perry, J. H., Ed. in Chief, Chemical Engineer's Handbook, 3rd Ed., McGraw-Hill, New York, N. Y., (1950).
25. Handbook of Chemistry and Physics, 39th Ed., Chemical Rubber Publishing Co., Cleveland, Ohio, (1957-1958).
26. Alcohols, Union Carbide Chemicals Co., New York, N. Y., (1958).
27. Sakiadis, B. C. and J. Coates, "Studies of Thermal Conductivity of Liquids, Part I," Amer. Inst. of Chem. Engrs. Journ., Vol. 1, pp. 275-288, (1955).
28. Sakiadis, B. C. and J. Coates, "Studies of Thermal Conductivity of Liquids, Part III," Amer. Inst. of Chem. Engrs. Journ., Vol. 3, pp. 121-126, (1957).
29. Cecil, O. B. and R. H. Munch, "Thermal Conductivity of Some Organic Liquids," Ind. and Eng. Chem., Vol. 48, pp. 437-440, (1956).
30. Methyl Ethyl Ketone, 2nd Ed., Shell Chemical Corp., New York, N.Y., (1950).
31. Keenan, J. H. and F. G. Keyes, Thermodynamic Properties of Steam, John Wiley & Sons, New York, N.Y., (1936).
32. Scarborough, J. B., Numerical Mathematical Analysis, Johns Hopkins Press, Baltimore, Md., (1930).

APPENDIX A

CALIBRATION AND PERFORMANCE CURVES

FOR EXPERIMENTAL APPARATUS

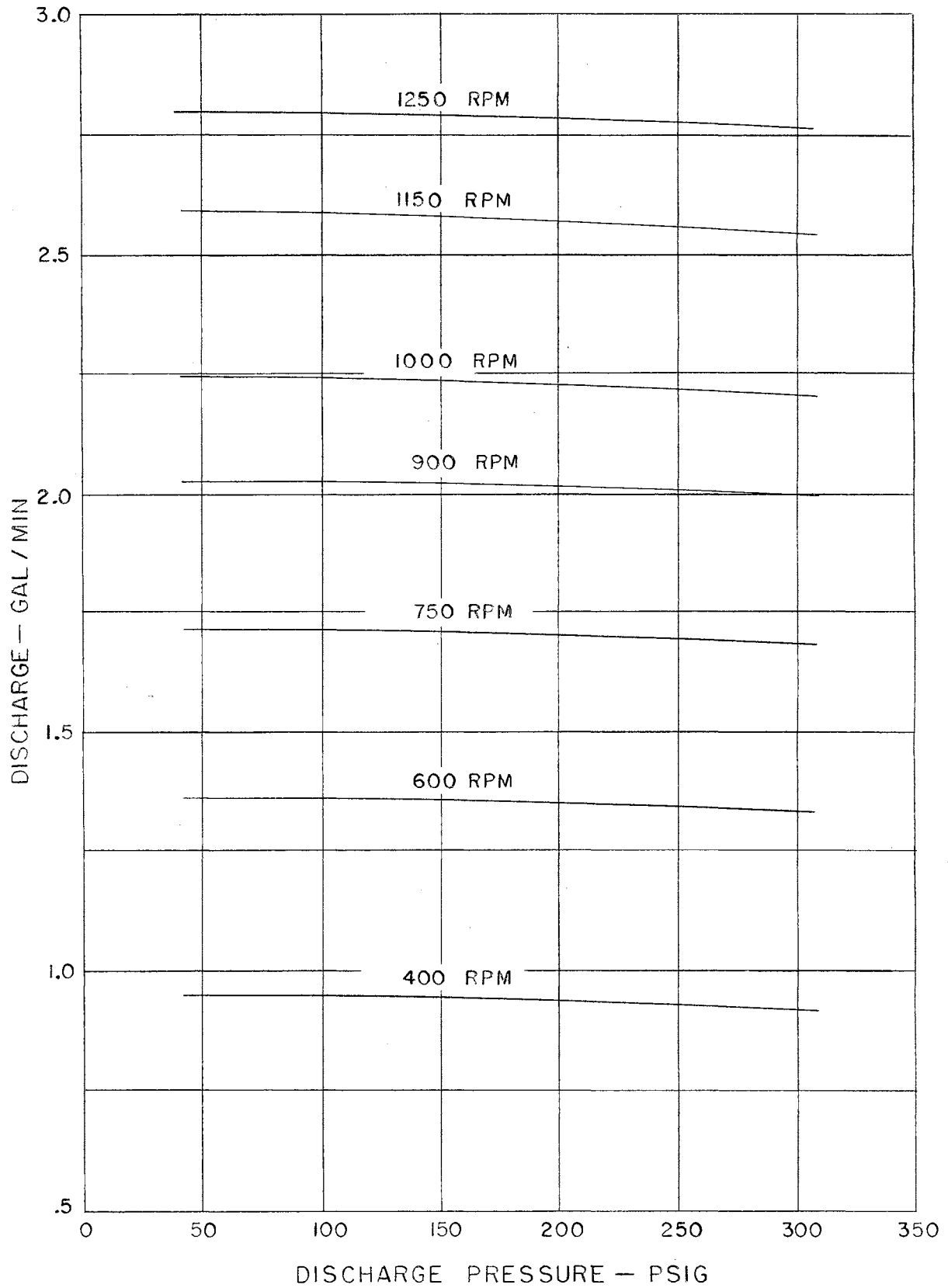


Figure 14. Moyno Pump Characteristics

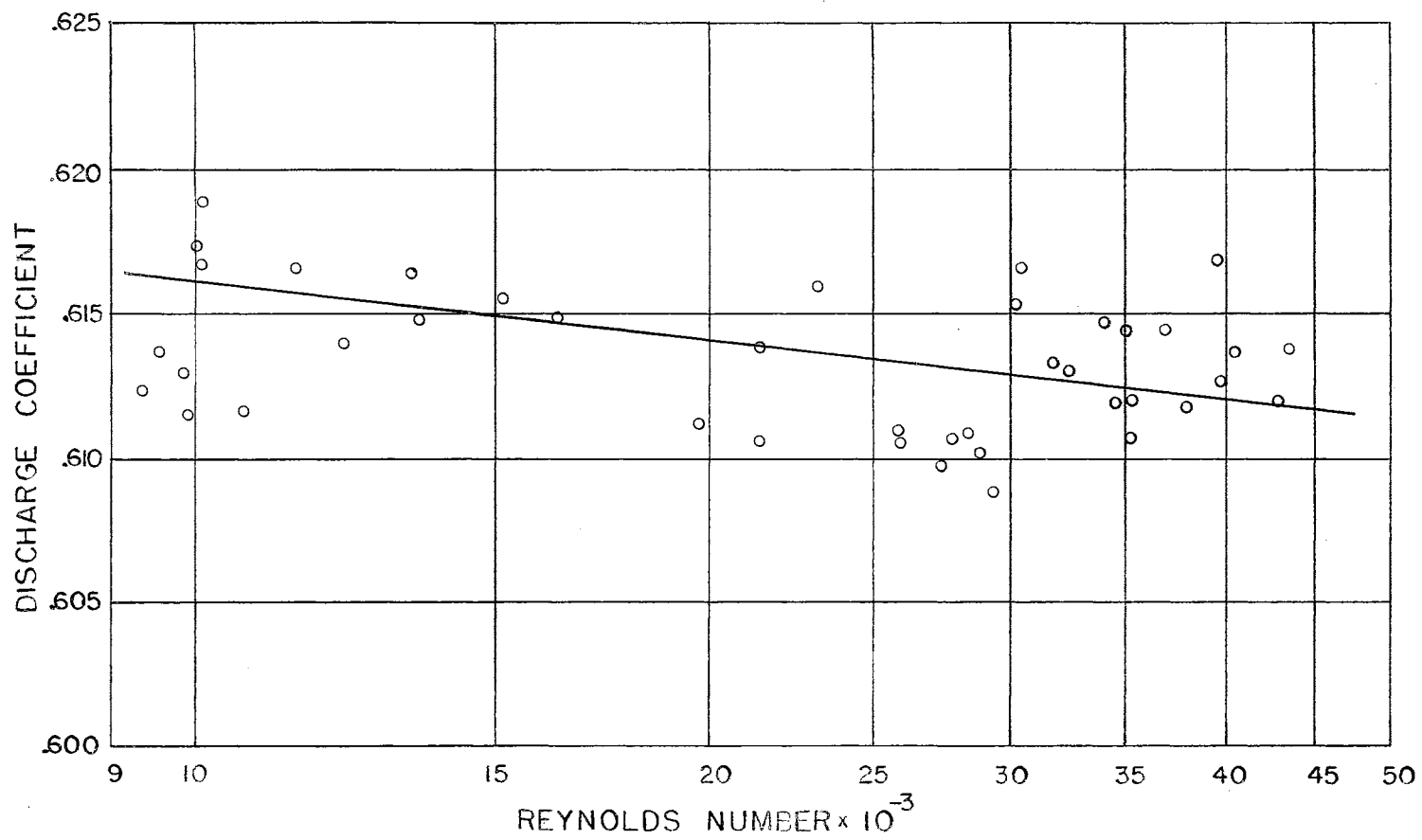


Figure 15. Orifice Calibration Curve

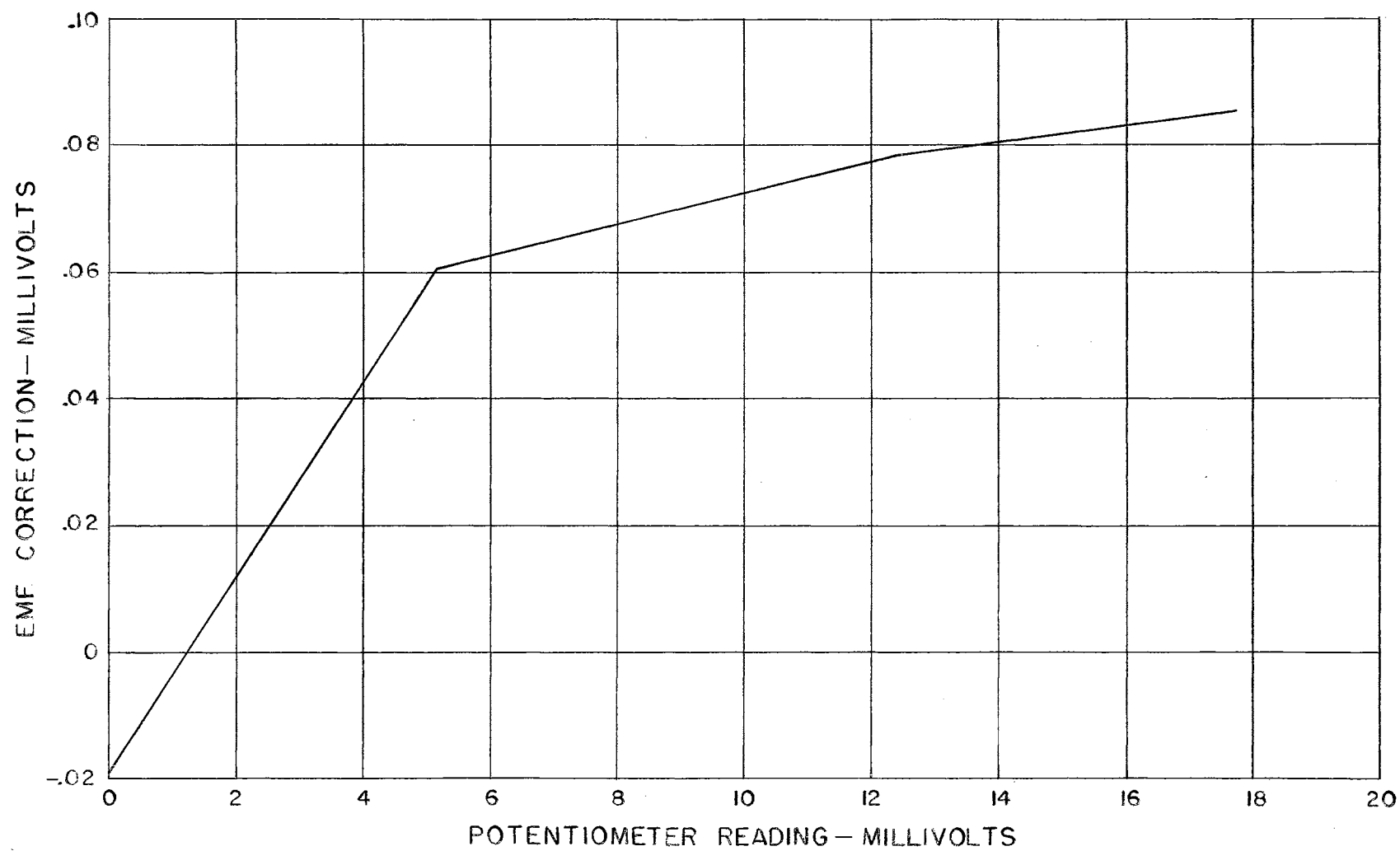


Figure 16. Thermocouple Calibration Curve

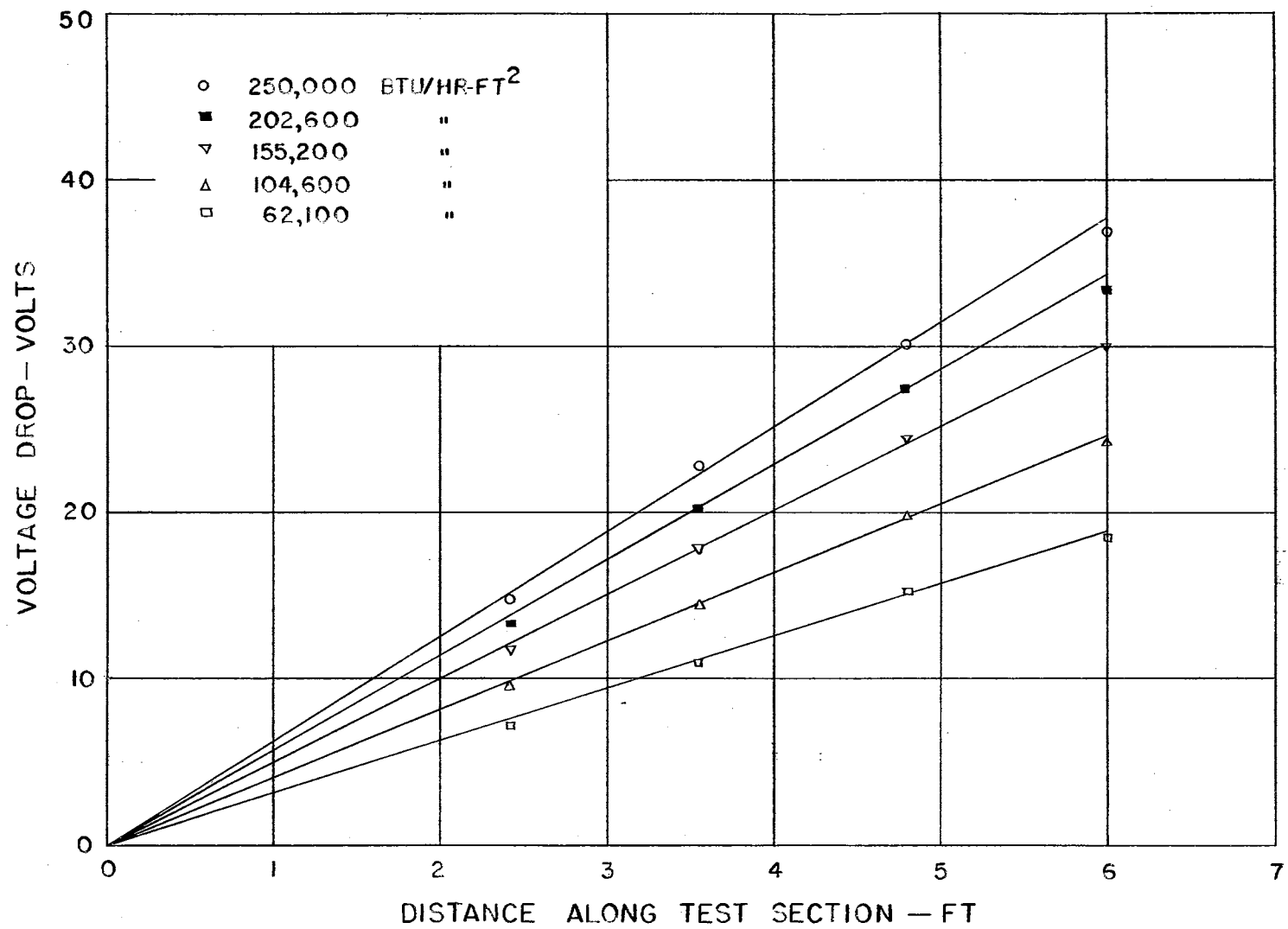


Figure 17. Voltage Drop Along Test Section

APPENDIX B

REPRESENTATIVE PRESSURE PROFILES AND GRADIENTS

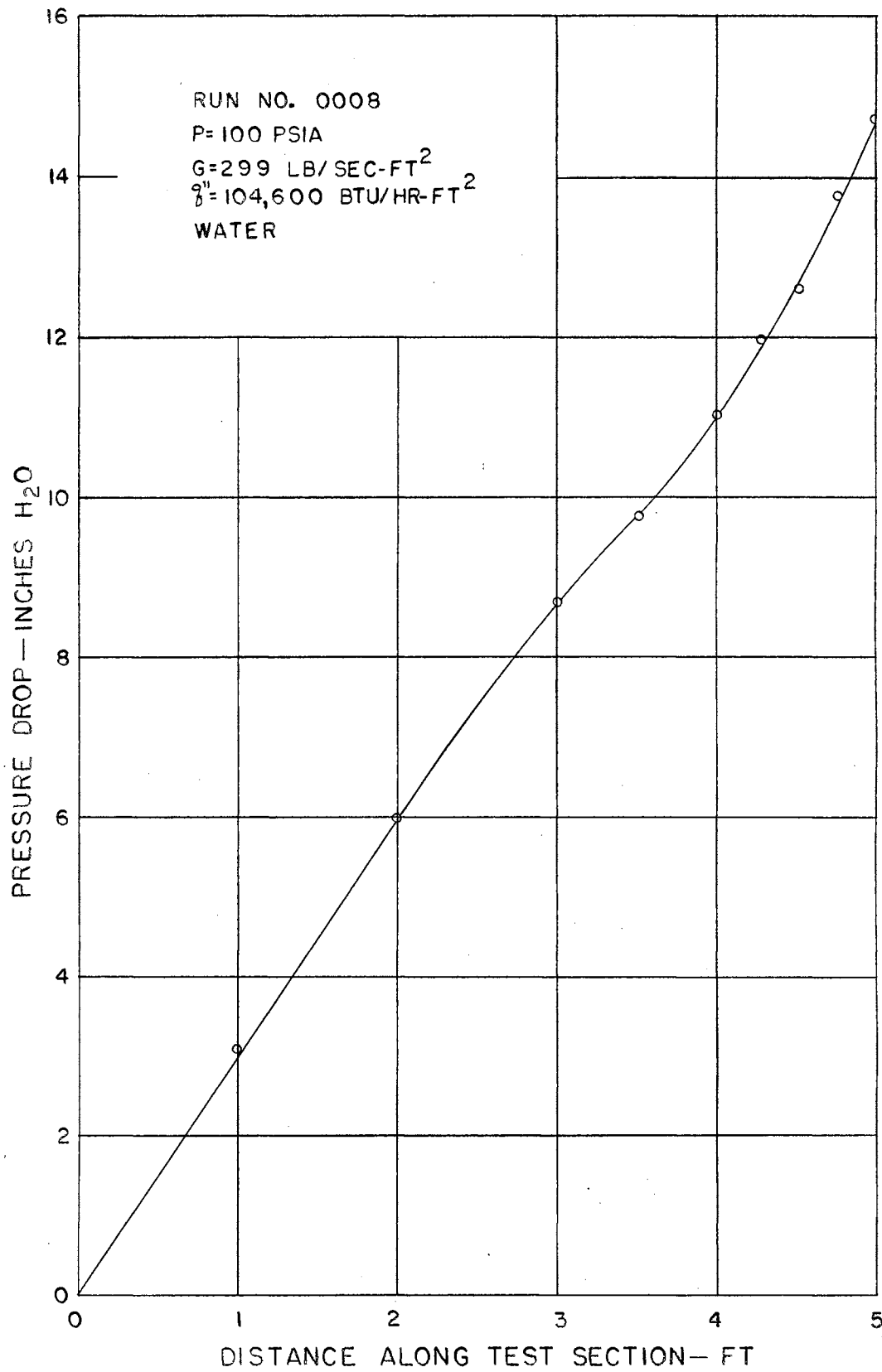


Figure 18. Experimental Pressure Profile --- Run No. 0008

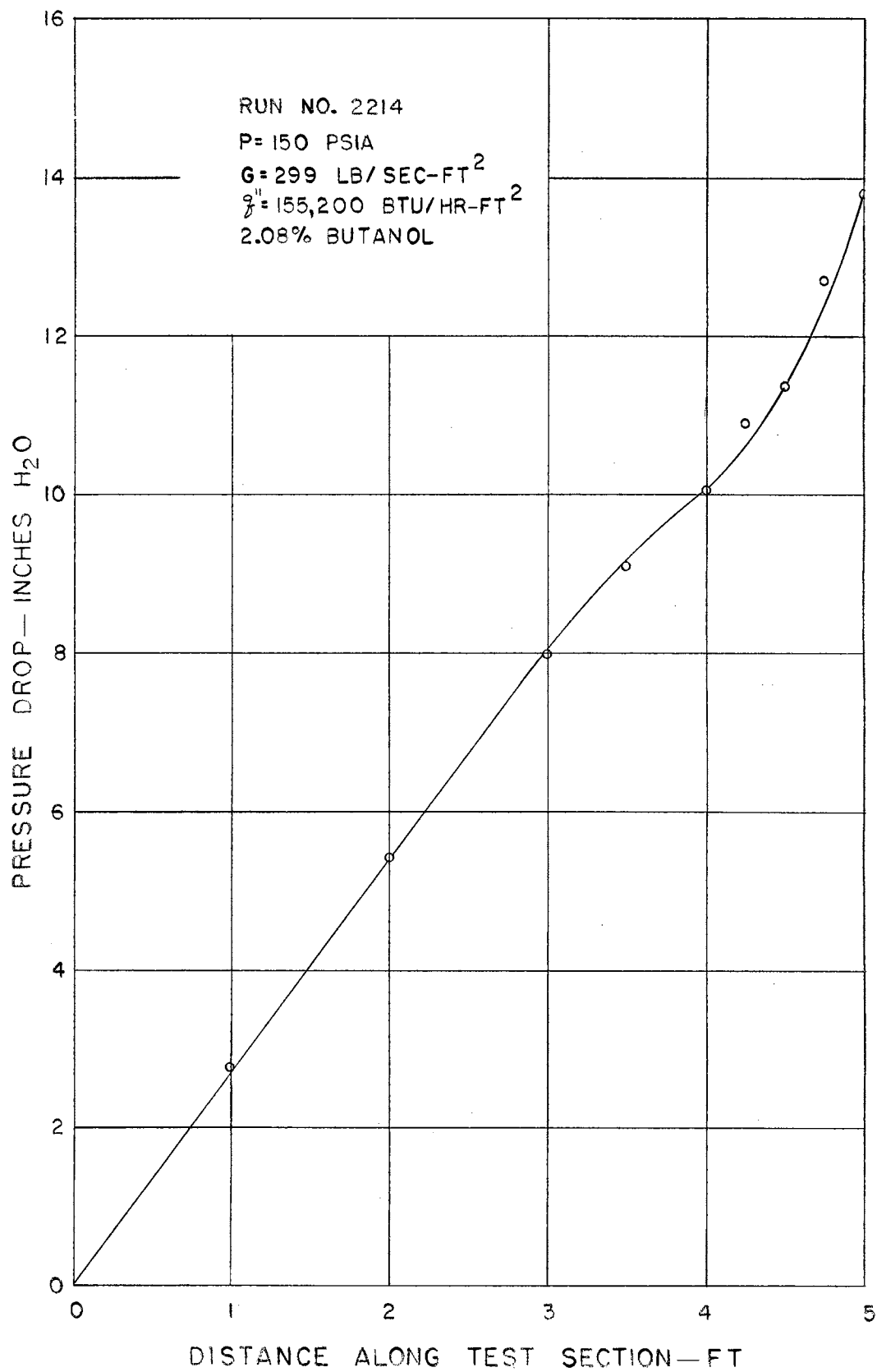


Figure 19. Experimental Pressure Profile --- Run No. 2214

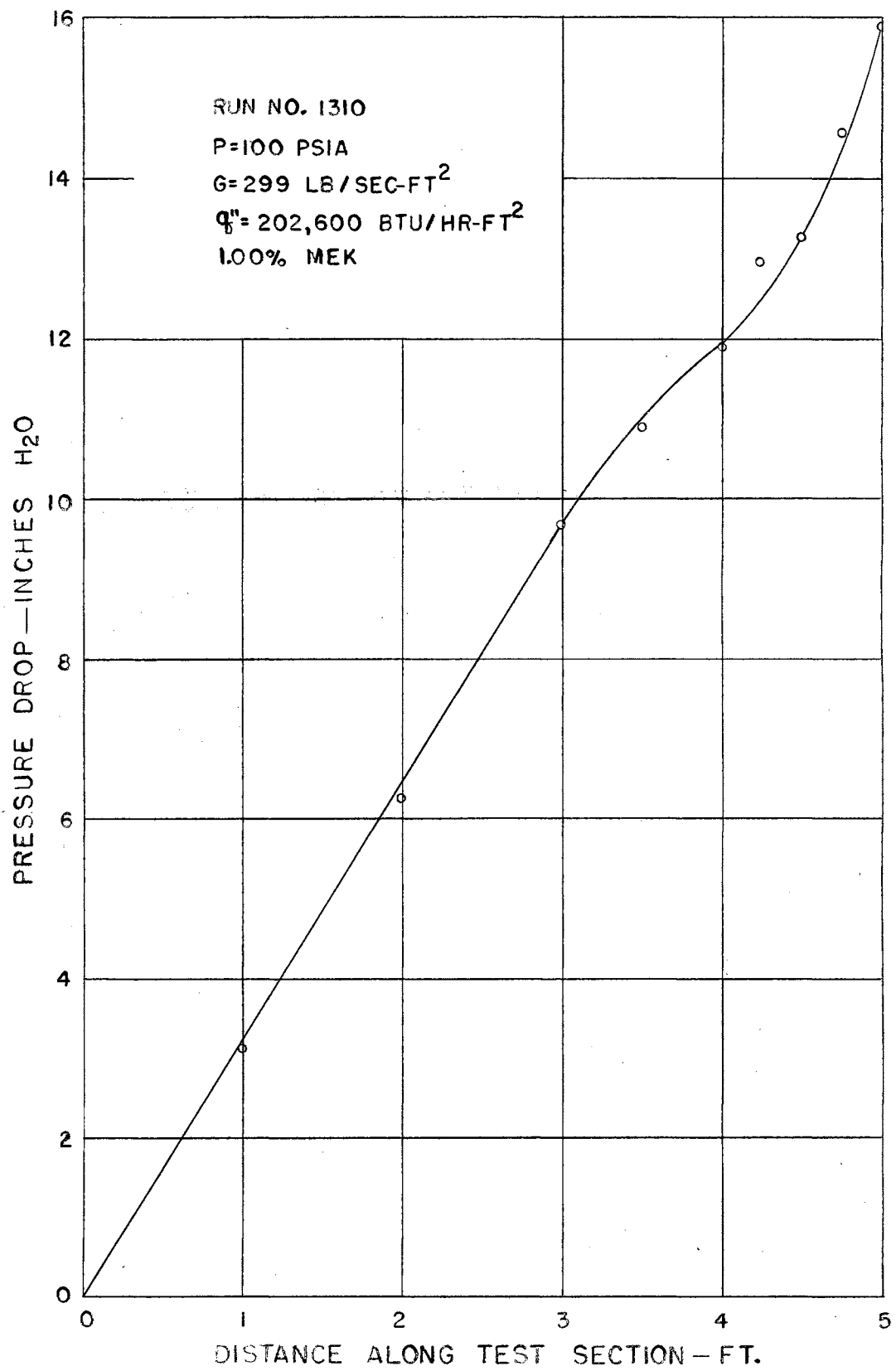


Figure 20. Experimental Pressure Profile --- Run No. 1310

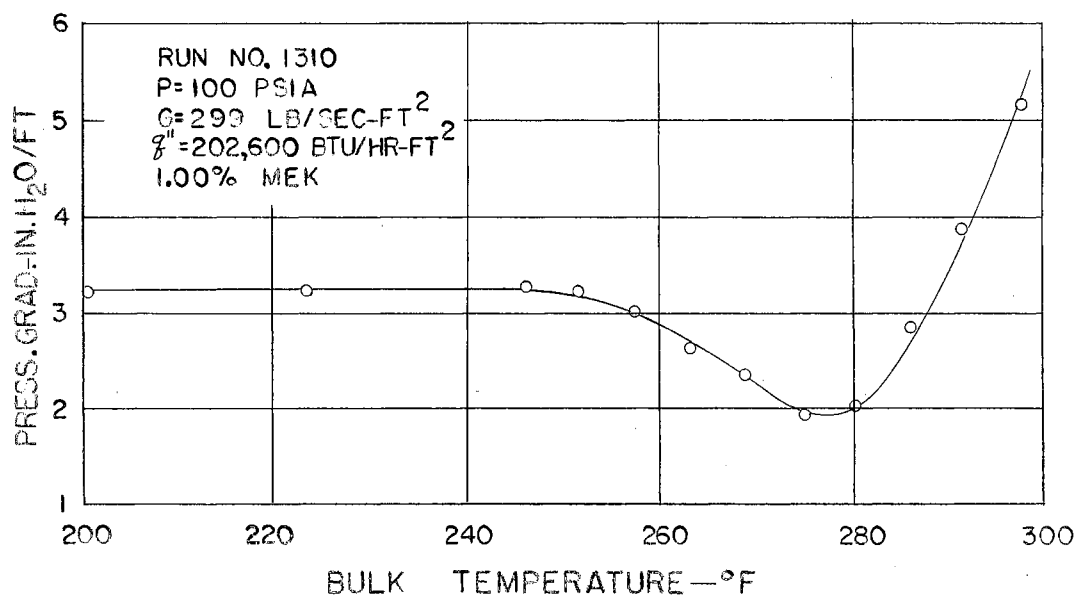
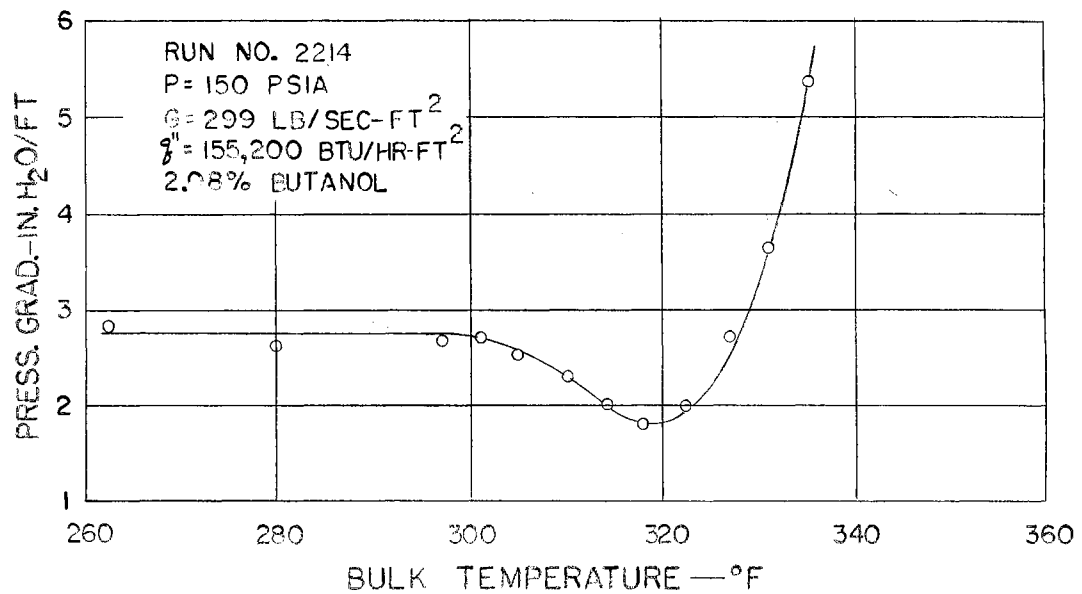
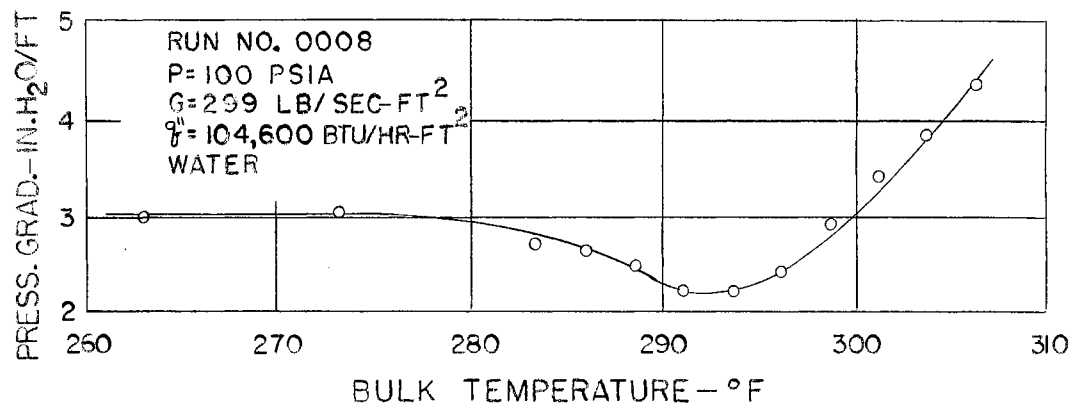


Figure 21. Experimental Pressure Gradients

APPENDIX C

PROPERTIES OF MIXTURES

Knowledge of the thermophysical properties of the mixtures used was necessary for analysis of the data. The procedures followed in determining viscosity, thermal conductivity, density, and heat capacity as functions of temperature will be discussed in this appendix. The method used to determine the variation of saturation temperature with pressure will be described.

Only a limited amount of property data was found for the pure additives, and the data available was, in most cases, restricted to temperatures of less than 200°F. Since temperatures of over 400°F were encountered in the study, it was necessary to extrapolate published data. These were difficulties present in determining property values over a sufficient temperature range for the pure additives. Determining the properties of mixtures presented further problems. The changes in property values from those of water were small; for this reason, ratios defined as the ratio of the property value of the mixture to that of water were plotted as functions of temperature.

Viscosity

The viscosity of the mixtures was determined in the manner prescribed in Reference (22). An Ostwald viscosimeter with a capillary diameter of 0.4 mm was used to measure kinematic viscosity. The basic equation for

the test is

$$\nu = ct$$

C-1

where

ν = the kinematic viscosity, centistokes;

c = the calibration constant for the instrument at a particular temperature;

t = the efflux time, seconds.

The viscosimeter was calibrated with distilled water. The constant in Equation C-1 was obtained by substituting the viscosity of water from (23) at the temperature of the test, and the time required for a fixed quantity of water to flow through the capillary. The constant thus obtained was checked by comparing experimental values of viscosity of methanol and butanol with published values (24), (25), (26). A maximum deviation of 3% between experimental and published values was found. Calibration and test runs were made at 100°F and 140°F. The constants for the Ostwald viscosimeter used were 9.939×10^{-3} and 10.07×10^{-3} at 100°F and 140°F, respectively.

Bingham's Equation (7) was used to obtain viscosity as a function of temperature. Bingham's Equation is

$$\frac{1}{\mu} = 2.155 \left[t + a + \sqrt{8078.4 + (t + a)^2} \right] - 120.4 \quad \text{C-2}$$

where

μ = viscosity in poises, gm/cm-sec;

t = temperature, °C;

a = constant, °C.

If the viscosity of a liquid is known at one temperature, the value of the constant in Equation C-2 can be found. Values of viscosity can then be determined for other temperatures. Agreement within $\pm 5\%$ was found between values of viscosity of water calculated from Equation C-2 and published values (23) in the temperature range of 100°F and 400°F. The values of the constant in Equation C-2 for the mixtures and constituents used in this study are tabulated in Table IV. Figures 22 and 23 are plots of dynamic viscosity as functions of temperature for the mixtures and constituents used in this investigation.

Thermal Conductivity

The thermal conductivity of the pure additives was determined by the method recommended by Sakiadis and Coates (27), (28). This method is based on a modified statement of the theory of corresponding states. Families of curves were presented in (27) and (28) with parameters of reduced temperature (the ratio of an absolute temperature to the critical temperature), molecular structure, and thermal conductivity. This method of correlation predicted the thermal conductivity of 124 liquids within an average deviation of less than $\pm 1.5\%$ from experimental observation.

Thermal conductivity of the mixtures was determined by the linear relationship presented by Cecil and Munch (29):

$$k_m = \%A(k_a) + \%B(k_b) \quad \text{C-3}$$

where

k_m = the thermal conductivity of the mixture;

k_a = the thermal conductivity of constituent A;

k_b = the thermal conductivity of constituent B;

$\%A$ = percent by weight of A in the mixture;

$\%B$ = percent by weight of B in the mixture.

TABLE IV
SUMMARY OF CONSTANTS IN BINGHAM'S EQUATION

Substance A	Substance B	Percent by Weight Of A in Mixture	Constant, a
Water	-----	100	-8.435
Butanol	-----	100	-53.9
Methanol	-----	100	+12.0
Methyl Ethyl Ketone	-----	100	+30.00
Butanol	Water	1.00	-10.9
Butanol	Water	2.08	-12.4
Butanol	Water	3.12	-13.2
Methanol	Water	1.00	-11.2
Methanol	Water	2.00	-12.2
Methanol	Water	2.99	-12.77
Methyl Ethyl Ketone	Water	1.00	-10.9
Methyl Ethyl Ketone	Water	2.03	-12.2
Methyl Ethyl Ketone	Water	3.00	-13.4

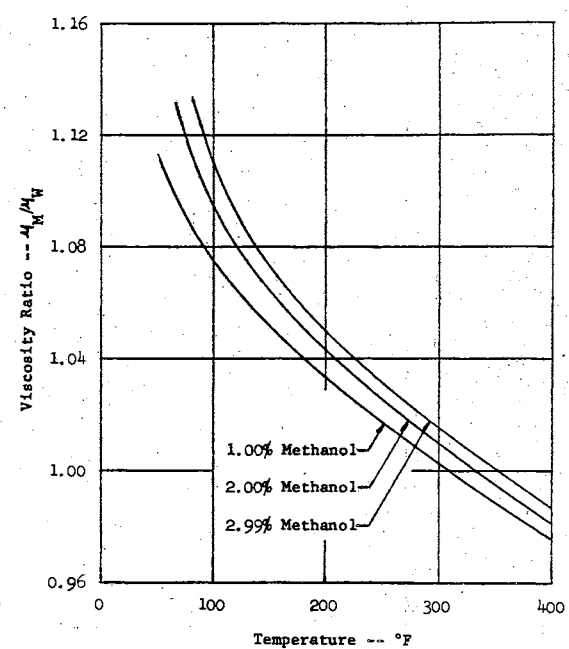
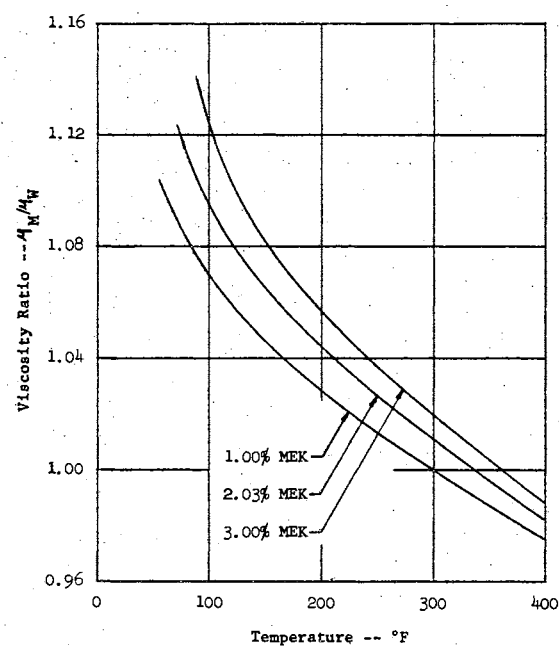
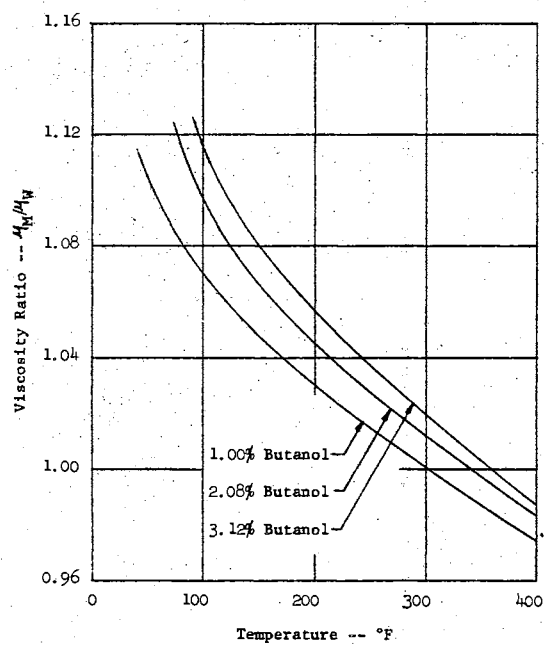


Figure 22. Viscosity Ratio For Mixtures

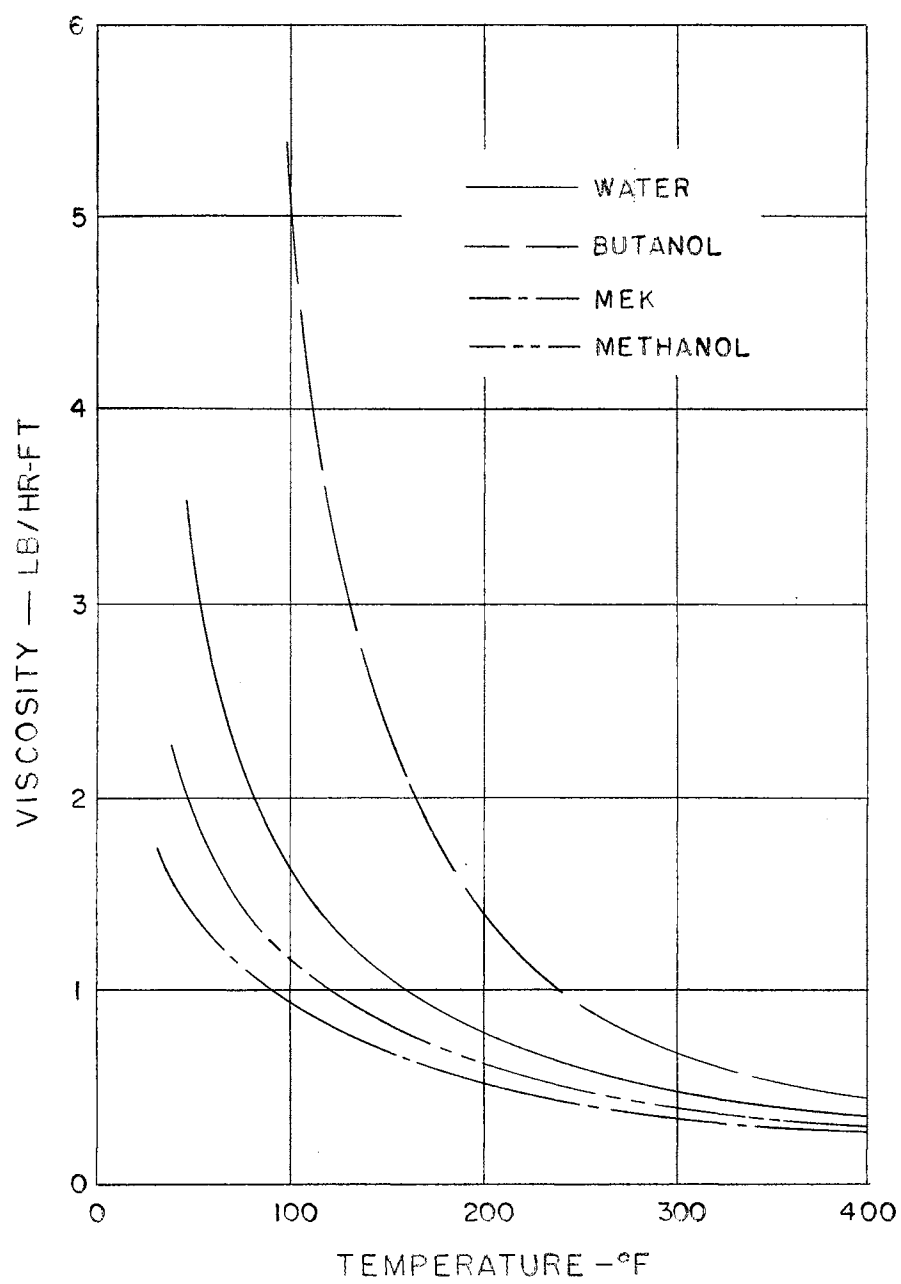


Figure 23. Viscosity of Pure Liquids

It was not expected that such a relationship would predict the thermal conductivity of mixtures. The following is quoted from (29).

A series of formulations of water and methanol was prepared and their thermal conductivities were measured. It was not expected that the above equation [Equation C-3] would be valid for such a mixture, but the results agreed very closely with those of other workers.

Although the authors have no theoretical explanation for the equation used to calculate the thermal conductivity of the mixture, they have found it to be a very valuable and time-saving tool.

The above approach is not recommended in situations requiring precise values of thermal conductivity of mixtures. It was thought to be adequate for purposes of this investigation, particularly in view of the small concentrations of additives which were used. Since the thermal conductivity curves for butanol and methyl ethyl ketone were of the same shape as that of methanol, it was felt that the procedure successfully used for water-methanol mixtures could be extended to butanol-water and methyl ethyl ketone-water mixtures. The thermal conductivity of water was taken from Reference (23). The thermal conductivities of the mixtures and the constituents are presented in Figures 24 and 25.

Density and Heat Capacity

The density and heat capacity of a mixture may be determined from a relation of the form of Equation C-3 in which thermal conductivity is replaced by density or heat capacity. The data found on the additive properties were in general restricted to lower temperatures. Property values were taken from References (23), (24), (25), (26), (30), and (31). The density and heat capacity of the mixtures and constituents are shown in

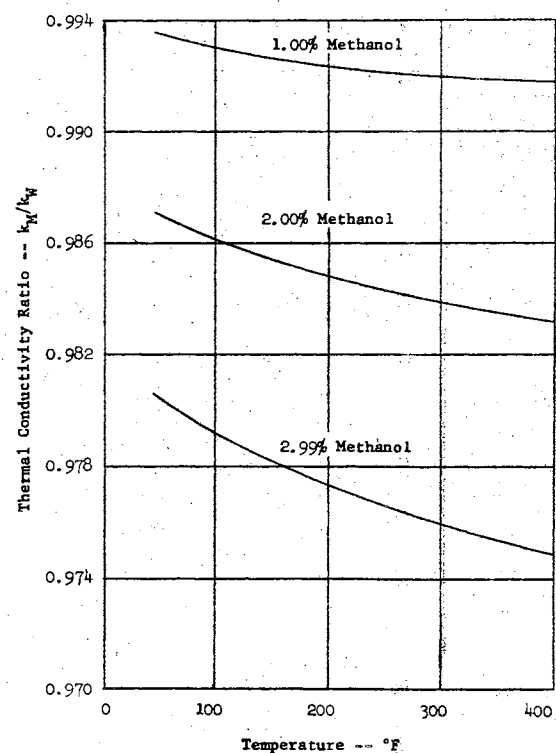
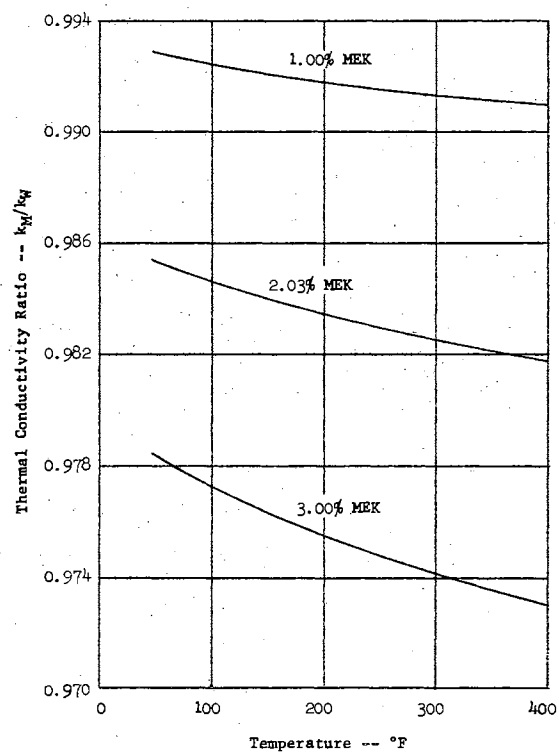
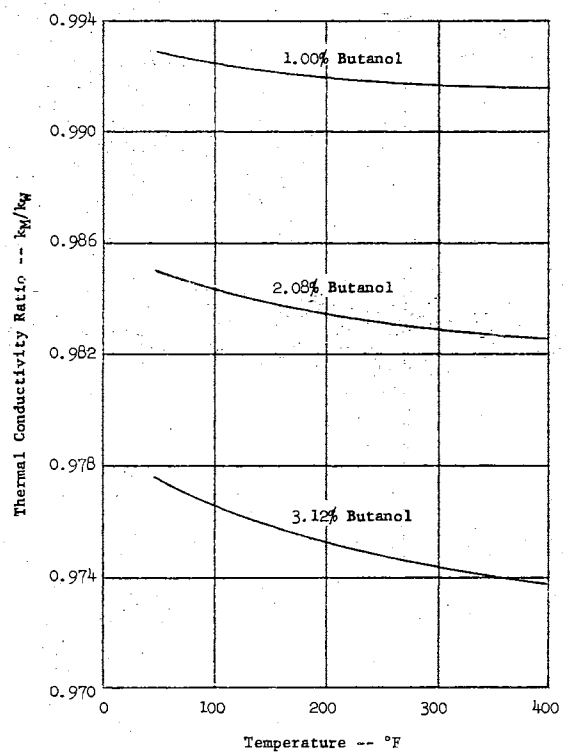


Figure 24. Thermal Conductivity Ratio for Mixtures

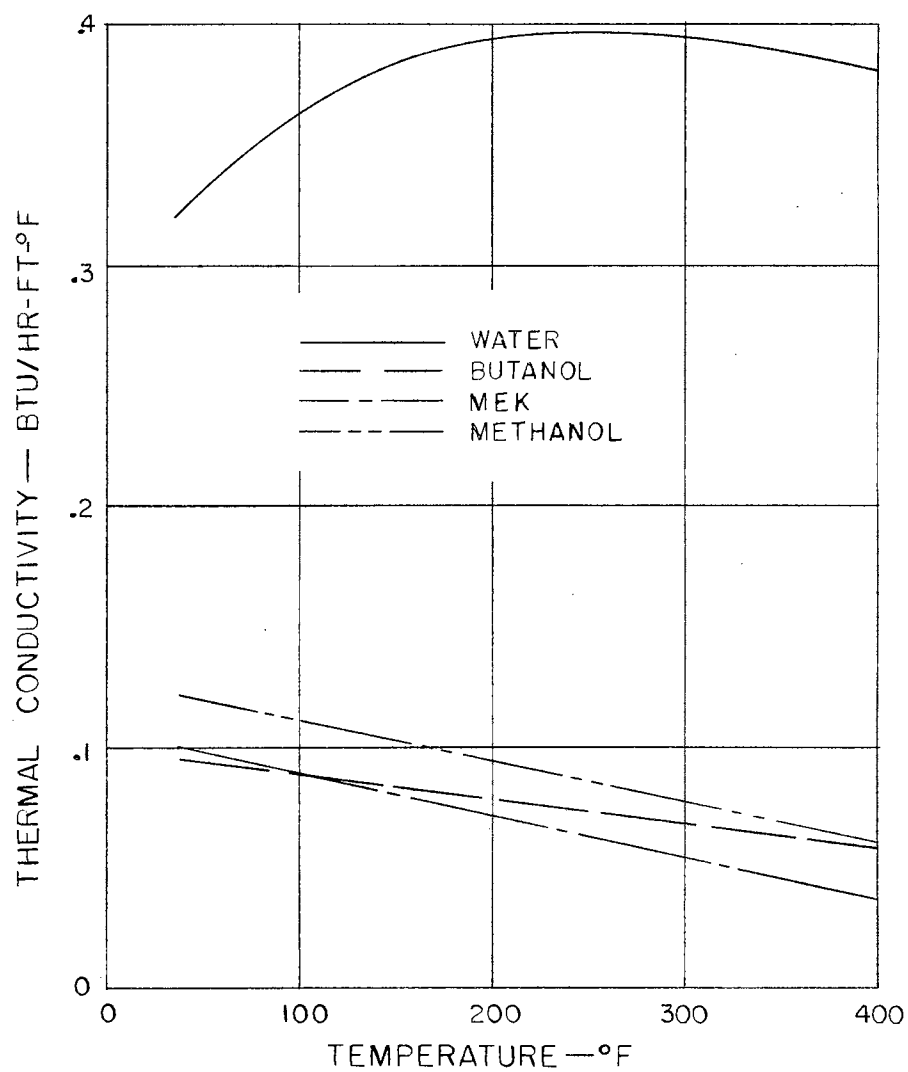


Figure 25. Thermal Conductivity of Pure Liquids

Figures 26 through 29. Due to the small concentrations of additives used in this experiment, an error of the order of 100% in these additive property values will result in an error of the order of only 1% in the mixture property values.

Saturation Temperature

The saturation temperatures at a pressure of 1 atmosphere for the mixtures used were available from the literature (24), (30). Use was made of Dühring's Rule and a modified version of Clapeyron's Equation to determine saturation temperatures at pressures higher than 1 atmosphere (24).

Clapeyron's Equation may be written as

$$\frac{dP}{dT} = \frac{L_v}{T \Delta v}$$

where

L_v = the molal heat of vaporization at atmospheric pressure;

T = absolute temperature;

v = the molal specific volume of the vapor minus the molal specific volume of the liquid.

Since the specific volume of the liquid is much smaller than the specific volume of the vapor, Clapeyron's Equation may be approximated by

$$\Delta T = \Delta P \left(\frac{T}{L_v} \right) v_{\text{vapor}} .$$

Since $Pv = RT$ for a vapor, where R is the universal gas constant and v is the molal specific volume,

$$\Delta T = \Delta P \left(\frac{T}{L_v} \right) \frac{RT}{P} .$$

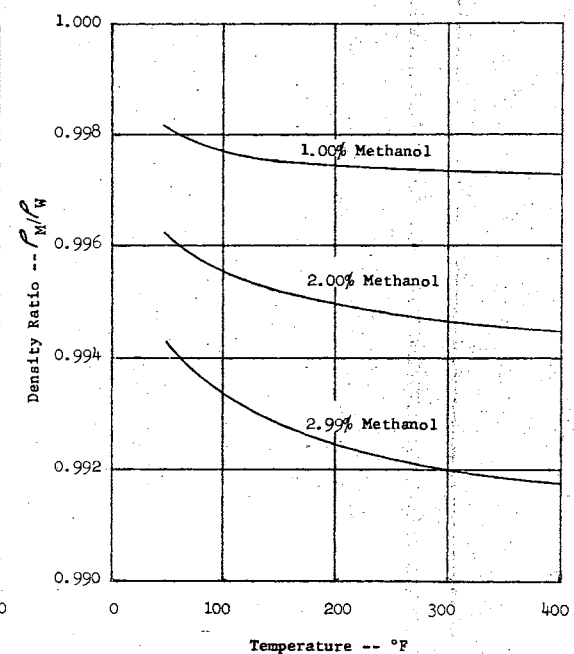
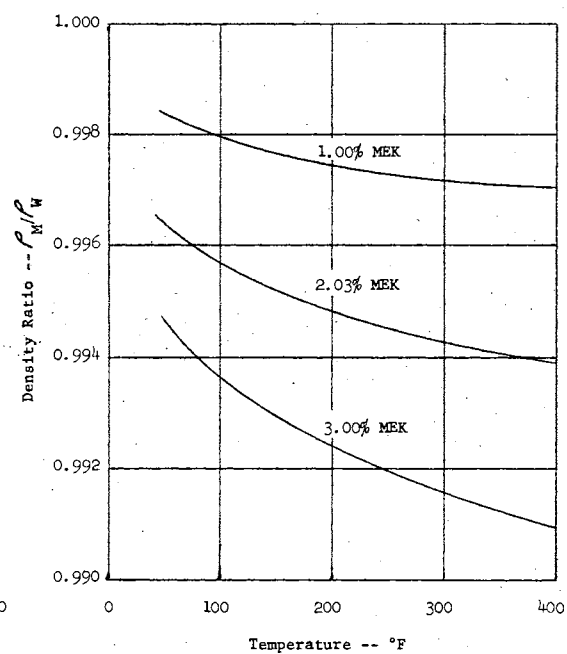
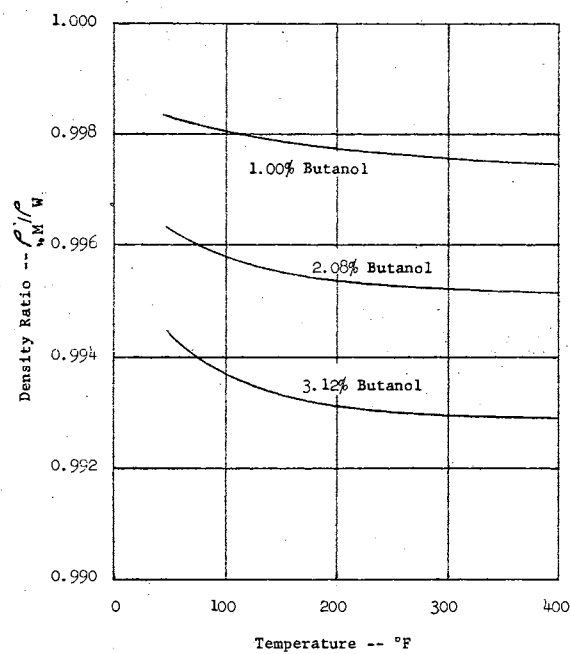


Figure 26. Density Ratio for Mixtures

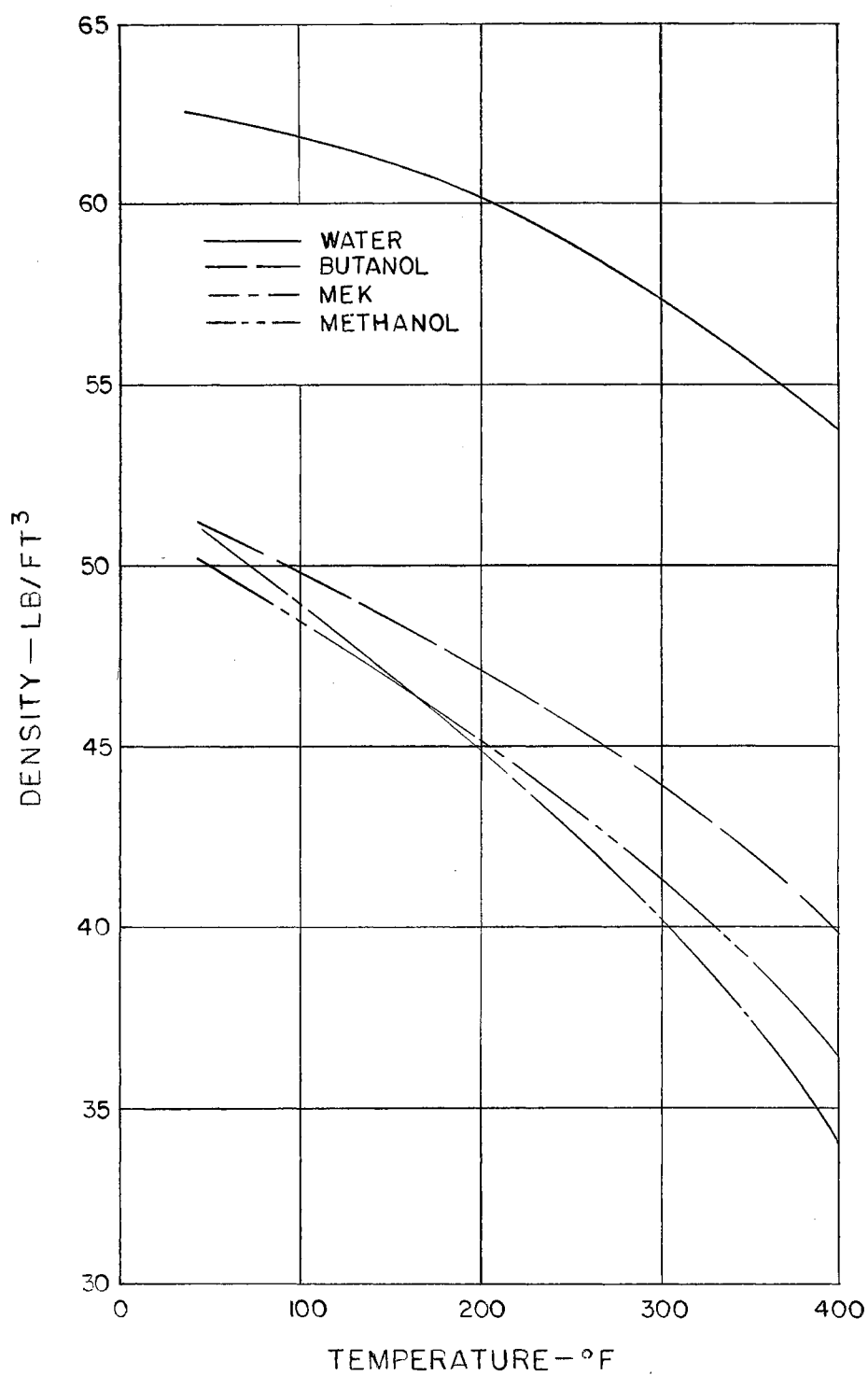


Figure 27. Density of Pure Liquids

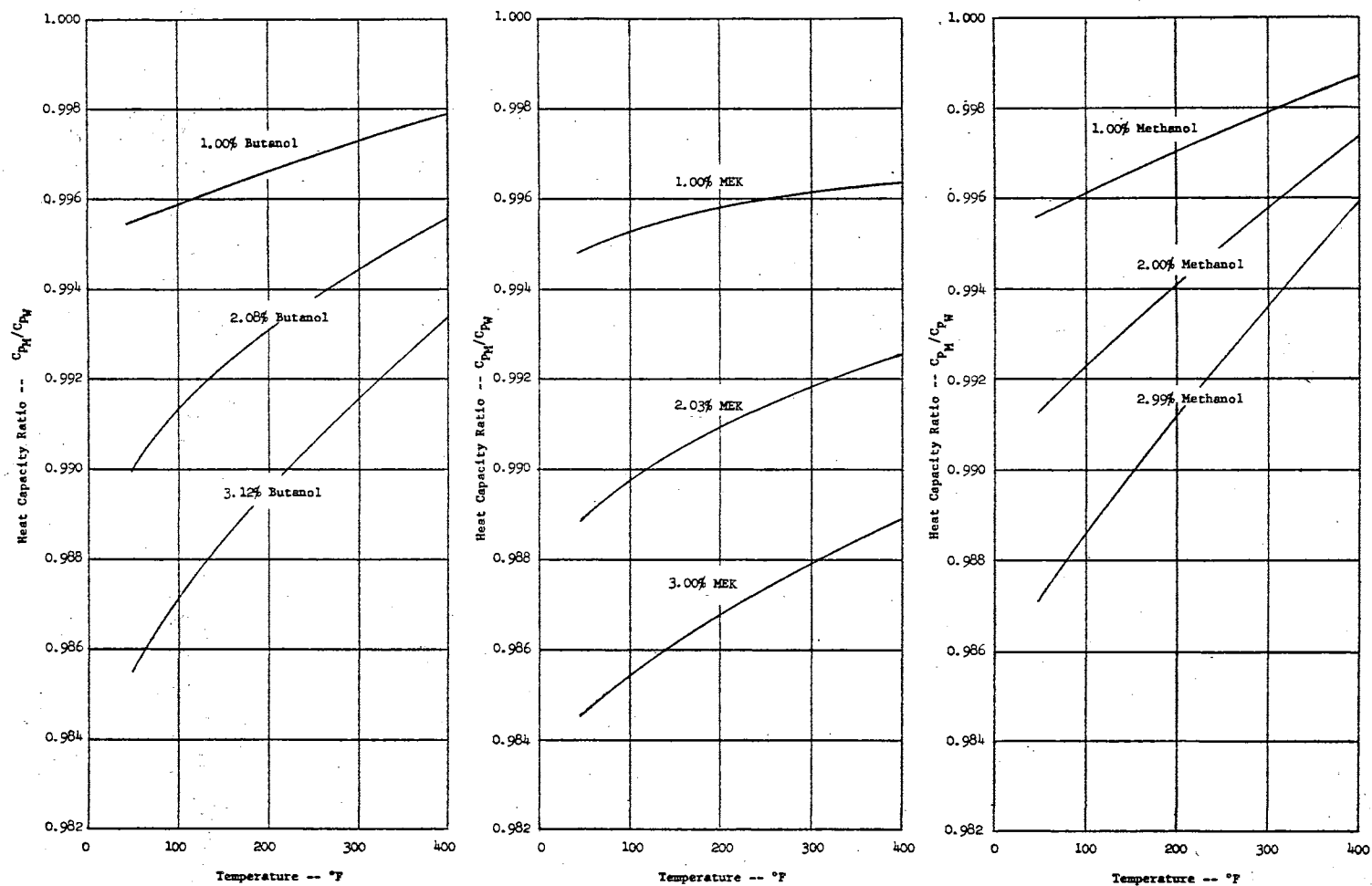


Figure 28. Heat Capacity Ratio for Mixtures

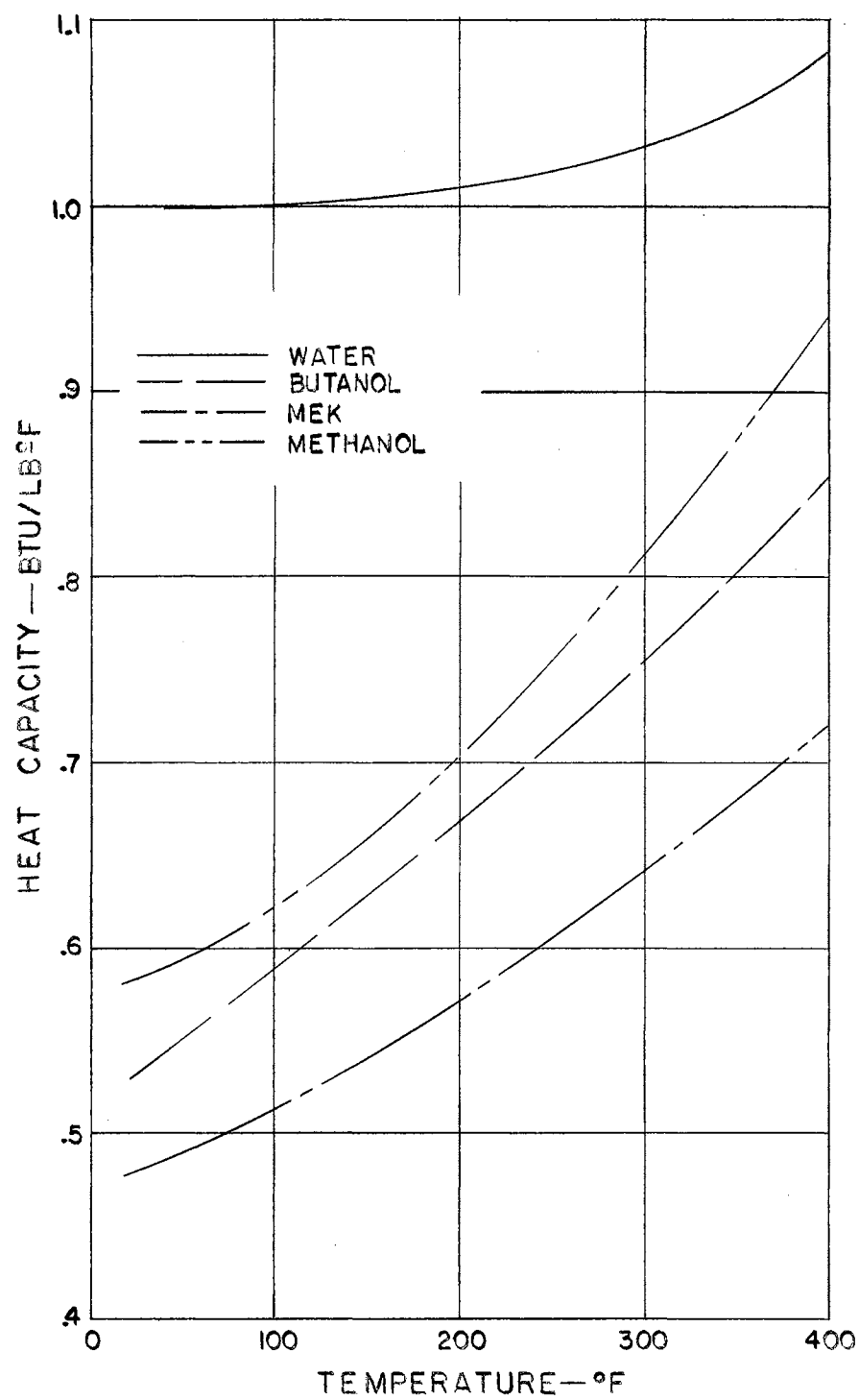


Figure 29. Heat Capacity of Pure Liquids

Equation C-4 may be written for water and a mixture and the following ratio may be formed.

$$\frac{(\Delta T)_M}{(\Delta T)_W} = \frac{\left[\Delta P \left(\frac{T}{L_v} \right) \frac{RT}{P} \right]_M}{\left[\Delta P \left(\frac{T}{L_v} \right) \frac{RT}{P} \right]_W} \quad \text{C-5}$$

Trouton's Rule states that the molal heat of vaporization of normal liquids at the boiling point under atmospheric pressure divided by the absolute boiling temperature is approximately a constant (24). Thus, by cancelling common terms in Equation C-5,

$$(\Delta T)_M = (\Delta T)_W \left(\frac{T_M}{T_W} \right)$$

where

ΔT_M = the change in the boiling point of the mixture produced by a change in pressure ΔP ;

ΔT_W = the change in the boiling point of water produced by the same change in pressure;

T_M and T_W = the boiling points of the mixture and of water, respectively, at atmospheric pressure.

If a small change in pressure is assumed, the corresponding change in the saturation temperature may be calculated. Sufficient information is thus available to apply Dühring's Rule and find the variation of saturation temperature with pressure for the mixture. Figures 30 and 31 are plots of saturation temperature as functions of pressure for the mixtures and the constituents.

No great degree of accuracy is claimed for property values calculated by the methods outlined in this appendix. It was thought, however, that the degree of accuracy was sufficiently high to permit analysis of the data.

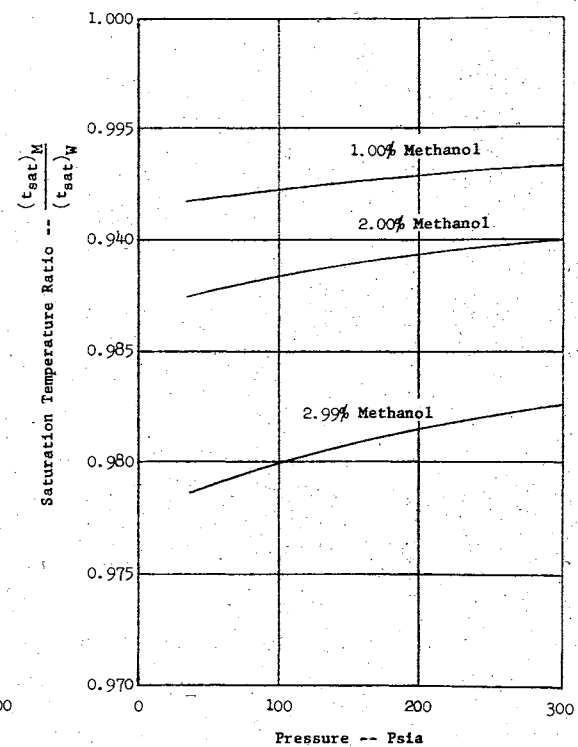
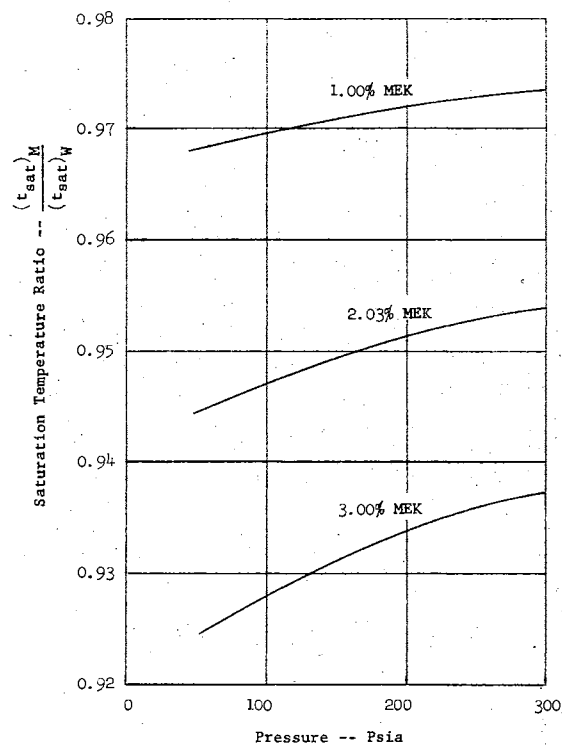
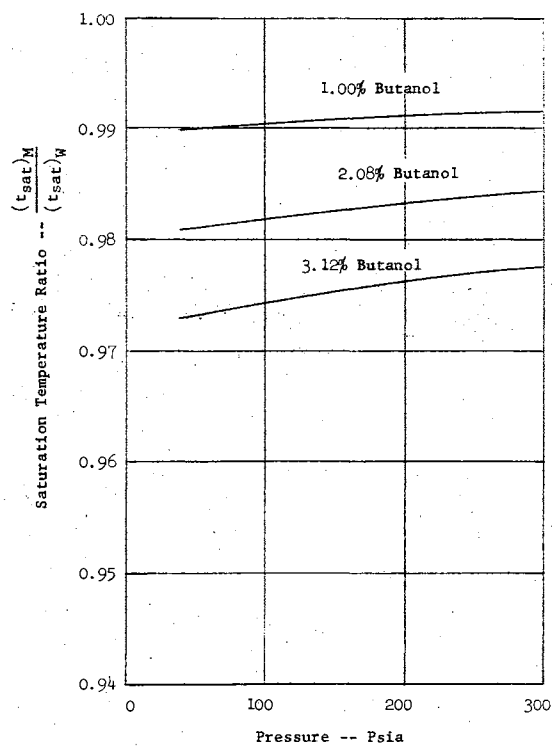


Figure 30. Saturation Temperature Ratio for Mixtures

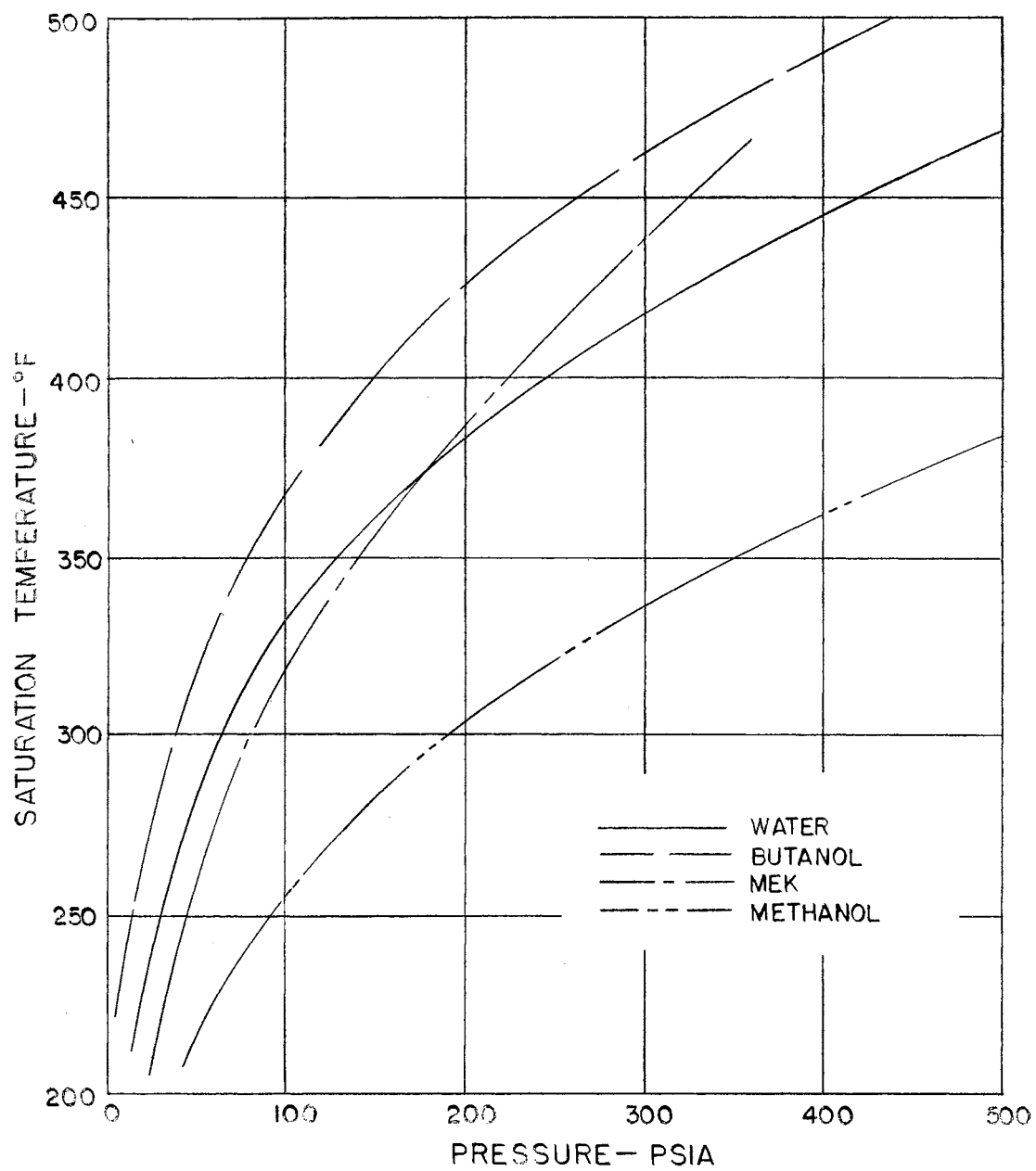


Figure 31. Variation of Saturation Temperature With Pressure for Pure Liquids

APPENDIX D

GENERALIZED LEAST SQUARES METHOD OF CORRELATING EXPERIMENTAL DATA

The experimental data were correlated using the method of least squares described by Scarborough (32). Although the method described in Reference (32) considers only a dependent variable and one independent variable, it was found possible to extend the method for application in cases of more than one independent variable. A brief description of the method and the resulting IBM 650 computer program will be given in this appendix.

Consider a function,

$$y = f(u, v, w, a, b, c, d) \quad \text{D-1}$$

where y is a dependent variable, u , v , and w are independent variables, and a , b , c , and d are coefficients to be determined.

If a_0 , b_0 , c_0 , and d_0 are approximate values of a , b , c and d respectively, and α , β , γ , and δ are corrections which are to be applied to a_0 , b_0 , c_0 , and d_0 respectively, then

$$\begin{aligned} a &= a_0 + \alpha \\ b &= b_0 + \beta \\ c &= c_0 + \gamma \\ d &= d_0 + \delta. \end{aligned} \quad \text{D-2}$$

An approximate value of the function is given by

$$y' = f(u, v, w, a_0, b_0, c_0, d_0).$$

For several sets of observed values of y , u , v , w , the following approximate values of the function may be written:

$$\begin{aligned} y'_1 &= f(u_1, v_1, w_1, a_0, b_0, c_0, d_0) \\ y'_2 &= f(u_2, v_2, w_2, a_0, b_0, c_0, d_0) \\ &\dots \dots \dots \\ y'_n &= f(u_n, v_n, w_n, a_0, b_0, c_0, d_0). \end{aligned} \quad D-3$$

A residual is defined as the difference between the dependent variable calculated according to Equation D-1 and the observed value of the dependent variable. Thus, denoting the residuals by s ,

$$\begin{aligned} s_1 &= f(u_1, v_1, w_1, a, b, c, d) - y_1 \\ s_2 &= f(u_2, v_2, w_2, a, b, c, d) - y_2 \\ &\dots \dots \dots \\ s_n &= f(u_n, v_n, w_n, a, b, c, d) - y_n. \end{aligned} \quad D-4$$

where y_1, y_2, \dots, y_n are observed y 's corresponding to observed values of $(u_1, v_1, w_1), (u_2, v_2, w_2), \dots, (u_n, v_n, w_n)$ respectively.

Substituting the values of a, b, c, d from Equation D-2 in Equation D-4 and transposing yields, for the first residual,

$$s_1 + y_1 = f(u_1, v_1, w_1, a_0 + \alpha, b_0 + \beta, c_0 + \gamma, d_0 + \delta). \quad D-5$$

The right-hand side of Equation D-5 may be expanded by Taylor's formula for several variables. The result, neglecting products of the corrections α, β, γ , and δ , is:

$$\begin{aligned} s_1 + y_1 &= f(u_1, v_1, w_1, a_0, b_0, c_0, d_0) + \alpha \left(\frac{\partial f_1}{\partial a} \right)_0 + \\ &\quad \beta \left(\frac{\partial f_1}{\partial b} \right)_0 + \gamma \left(\frac{\partial f_1}{\partial c} \right)_0 + \delta \left(\frac{\partial f_1}{\partial d} \right)_0. \end{aligned} \quad D-6$$

where, for example, $\left(\frac{\partial f_1}{\partial a} \right)_0$ indicates evaluation of the partial with values of $u_1, v_1, w_1, a_0, b_0, c_0$, and d_0 substituted for u, v, w, a, b, c , and d , respectively.

Since $y_1' = f(u_1, v_1, w_1, a_o, b_o, c_o, d_o)$, Equation D-6 may be written as

$$s_1 = \alpha \left(\frac{\partial f_1}{\partial a} \right)_o + \beta \left(\frac{\partial f_1}{\partial b} \right)_o + \gamma \left(\frac{\partial f_1}{\partial c} \right)_o + \delta \left(\frac{\partial f_1}{\partial d} \right)_o + y_1' - y_1.$$

Let $r_1 = y_1' - y_1$, $r_2 = y_2' - y_2$, . . . , $r_n = y_n' - y_n$.

The residual equations may be written as

$$\begin{aligned} s_1 &= \alpha \left(\frac{\partial f_1}{\partial a} \right)_o + \beta \left(\frac{\partial f_1}{\partial b} \right)_o + \gamma \left(\frac{\partial f_1}{\partial c} \right)_o + \delta \left(\frac{\partial f_1}{\partial d} \right)_o + r_1 \\ s_2 &= \alpha \left(\frac{\partial f_2}{\partial a} \right)_o + \beta \left(\frac{\partial f_2}{\partial b} \right)_o + \gamma \left(\frac{\partial f_2}{\partial c} \right)_o + \delta \left(\frac{\partial f_2}{\partial d} \right)_o + r_2 \\ &\dots \dots \dots \\ s_n &= \alpha \left(\frac{\partial f_n}{\partial a} \right)_o + \beta \left(\frac{\partial f_n}{\partial b} \right)_o + \gamma \left(\frac{\partial f_n}{\partial c} \right)_o + \delta \left(\frac{\partial f_n}{\partial d} \right)_o + r_n. \end{aligned}$$

These equations are linear in the corrections α , β , γ and δ , and may be solved for the corrections according to the method of least squares.

The principle of least squares states that the best representative curve for a given set of data is that for which the sum of the squares of the residuals is a minimum. The condition that $f(\alpha, \beta, \gamma, \delta)$ be a maximum or minimum is that its partial derivatives with respect to α , β , γ , and δ shall each be zero.

Thus,

$$\frac{\partial f}{\partial \alpha} = \frac{\partial}{\partial \alpha} \left[\sum (s_i)^2 \right] = 0$$

$$\frac{\partial f}{\partial \beta} = \frac{\partial}{\partial \beta} \left[\sum (s_i)^2 \right] = 0$$

$$\frac{\partial f}{\partial \gamma} = \frac{\partial}{\partial \gamma} \left[\sum (s_i)^2 \right] = 0$$

$$\frac{\partial f}{\partial \delta} = \frac{\partial}{\partial \delta} \left[\sum (s_i)^2 \right] = 0.$$

The resulting simultaneous equations may be solved by determinants for α , β , γ and δ . These corrections may be added to a_0 , b_0 , c_0 , and d_0 , respectively, and new values for the coefficients obtained. The process may be repeated until the desired accuracy is achieved.

The procedure outlined above was programmed, for one independent variable, in the For Transit system for the IBM 650 computer. This program was written by Professor William Granet of the Oklahoma State University Computing Center. At the suggestion of Professor Clark Edwards of the Agricultural Economics Department at Oklahoma State University, the program was modified by Professor Granet and the author for cases of more than one independent variable. Table V is a listing of the For Transit statements for the program used in obtaining the coefficients in the correlation equation,

$$R = [a + b(\theta)^c] \left(\frac{\mu_m}{\mu_w} \right)^{d(\text{conc.})}.$$

The following comments may be made regarding the use of such a method.

1. Obviously, the form of the correlation equation must be known or assumed. Several models may be tried with final selection based on the model giving the best fit for a given set of data.
2. Initial estimates of the unknown coefficients must be made.
3. Although considerable latitude is available in both model selection and in initial estimates of the coefficients, it is possible to select models and initial coefficients which yield a near singular determinant for the solution of the corrections α , β , γ , and δ . Results obtained from the computer solution of such a determinant were of no value, and were characterized in this investigation by differing by orders of magnitude from the initial estimates.

TABLE V

FOR TRANSIT STATEMENTS FOR DATA

CORRELATION PROGRAM

```

DIMENSION A(8,8),D(8),P(7)
READ,NP,NO
READ,P(1),P(2),P(3),P(4),P(5),
1 P(6),P(7)
M=NP+1
TEST=9.0E40
ITER=0
7 0 CONTINUE
DO 1 I=1,M
21 0 DO 1 J=1,M
1 0 A(I,J)=0.0
DO 2 K=1,NO
77 0 READ,B,TT,PP,T,V,C,R
R1=C*P(4)
D(1)=V**R1
D(2)=D(1)*(T**P(3))
D(3)=P(2)*D(2)*2.3025851*LOGTF
1 (T)
D(4)=C*P(2)*D(2)*2.3025851*LOG
1 TF(V)
D(5)=R-D(1)*(P(1)+P(2)*(T**P(3)
1 )))
DO 2 I=1,M
23 0 DO 2 J=1,M
2 0 A(I,J)=D(I)*D(J)
2 1 +A(I,J)
M1=NP
DO 3 I=1,M1
24 0 MA=I+1
DO 3 J=MA,M1
3 0 A(J,I)=A(I,J)
M2=M-2
DO 5 I=1,M2
25 0 M3=I+1
DO 4 J=M3,M
4 0 A(I,J)=(A(I,J))/(A(I,I))
DO 5 L=1,M2
26 0 DO 5 K=M3,M
5 0 A(L+1,K)=A(L+1,K)
5 1 -A(L+1,I)*A(I,K)
A(M-1,M)=(A(M-1,M))/(A(M-1,
1 M-1))
L=M2
K=M1
DO 6 J=1,M2
32 0 DO 31 I=1,L
31 0 A(I,M)=A(I,M)-A(I,K)
31 1 *A(K,M)
L=L-1
6 0 K=K-1
ITER=ITER+1
IF(A(M,M)-TEST)8,9,9
8 0 TEST=A(M,M)
DO 10 I=1,M1
10 0 P(I)=A(I,M)+P(I)
PUNCH,P
GO TO 7

```

```

9 0 CONTINUE
IF(ITER-2)11,11,12
12 0 BIGD=0.0
DO 17 K=1,NO
84 0 READ,B,TT,PP,T,V,C,R
R2=C*P(4)
YCAL=(V**R2)*(P(1)+P(2)*(T**P(
1 3)))
YNOW=R
YR=R-YCAL
14 0 PUNCH,YNOW,YCAL,YR
IF(BIGD-ABSF(YR))
1 16,17,17
16 0 BIGD=ABSF(YR)
DYNOW=YNOW
17 0 CONTINUE
15 0 PUNCH,P,ITER
19 0 PUNCH,BIGD,DYNOW
11 0 CONTINUE
20 0 DO 34 I=1,M
33 0 PUNCH,A(I,M)
34 0 CONTINUE
END

```

NOTES

ASSUMED MODEL $R=(P(1)+P(2)*(T)**P(3))*V**P(4)*(CONC)$
 NP=THE NUMBER OF UNKNOWN COEFFICIENTS
 NO=THE NUMBER OF OBSERVATIONS
 P(1),P(2),--,P(N)=INITIAL ESTIMATES OF COEFFICIENTS
 B,TT,PP NOT USED BY PROGRAM
 T,V,C=OBSERVED VALUES OF INDEPENDENT VARIABLES
 R=OBSERVED VALUES OF DEPENDENT VARIABLE
 D(1),D(2),---,D(N)=PARTIAL DERIVATIVES WITH RESPECT TO COEFFICIENTS
 D(N+1)=OBSERVED VALUE OF DEPENDENT VARIABLE-CALCULATED VALUE FROM ASSUMED MODEL
 P=VALUES OF COEFFICIENTS AT END OF EACH ITERATION
 YCAL=CALCULATED VALUE OF DEPENDENT VARIABLE
 ITER=NUMBER OF ITERATIONS REQUIRED
 A(I,M)=FINAL DIFFERENCES IN COEFFICIENTS

APPENDIX E

NOMENCLATURE

Symbols

A	Constituent A
A	Area
A ₂	Area used in Equation II-5
a	Empirical constant in Equation C-2
a	Parameter related to heat flux by $a = 4.6 \times 10^{-6} q'' + 1.2$
a, b, c, d	Coefficients in Correlation Equation VI-4
B	Constituent B
c	Constant in Equation C-1
C'	Constant in Equation II-5
C _f	Skin friction coefficient
conc.	Concentration of additive in mixture
C _p	Heat capacity
D	Diameter
D	Drag force
d	Diameter
E	Area multiplier for thermal expansion of the orifice plate
f	Fanning friction factor
g _c	Gravitational constant
G	Mass velocity

G'	Mass velocity
h	Heat transfer film coefficient
K	Orifice discharge coefficient
k	Thermal conductivity
L	Length
L	Length of test section from start of local boiling to any point in the local boiling region
L_v	Molal heat of vaporization at atmospheric pressure
L_B	Local boiling length
L/L_B	Ratio of length of test section from start of local boiling to local boiling length
MEK	Methyl Ethyl Ketone
\dot{m}	Mass flow rate
P	System pressure
P	Pressure
ΔP	Pressure drop
ΔP	Change in pressure in Clapeyron's Equation
$\frac{dP}{dL}$	Pressure gradient
$\left(\frac{dP}{dL}\right)_h$	Pressure gradient
q	Heat transfer rate
q''	Heat flux
R	Ratio of pressure gradient in local boiling region to reference pressure gradient
R	Universal gas constant
T	Absolute temperature
t	Temperature

t	Time
ΔT	Change in saturation temperature
Δt	Change in temperature
Δt_b	Change in bulk temperature
t_s	Bulk temperature at start of local boiling
t_{sat}	Saturation temperature
Δt_{sat}	Temperature difference between wall and saturation temperatures
Δt_{sub}	Temperature difference between saturation and bulk temperatures
u	Velocity
V	Viscosity ratio defined on p. 51
v	Vapor
v	Specific volume
W	Flow rate
Δx	Increment of distance
θ	Temperature ratio defined by Equation VI-2
ρ	Fluid density
μ	Dynamic viscosity
ν	Kinematic viscosity

Dimensionless Groups

Pr	Prandtl number
Re	Reynolds number
St	Stanton number

Subscripts

a	Constituent A
b	Constituent B
b	Bulk conditions
F	Film conditions
h	Head of fluid
LB	Local boiling conditions
M	Mixture
max	Maximum
NB	Nonboiling conditions
o	Isothermal conditions
o	Reference conditions
s	Conditions at start of local boiling
sat	Saturation conditions
w	Wall conditions
W	Water

VITA

Reid Robinson June

Candidate for the Degree of

Doctor of Philosophy

THESIS: PRESSURE DROP DURING FORCED CONVECTION LOCAL BOILING
OF WATER CONTAINING AN ORGANIC ADDITIVE

MAJOR FIELD: Mechanical Engineering

BIOGRAPHICAL:

Personal Data: The writer was born in Kit Carson, Colorado, December 3, 1931.

Undergraduate Study: The writer graduated from Rocky Ford High School, Rocky Ford, Colorado, in May 1950. He entered Oklahoma State University in September 1950 and received the Bachelor of Science degree in Mechanical Engineering from that institution in May 1954.

Graduate Study: The writer entered the Graduate School of Oklahoma State University in September 1957 and received the Master of Science degree in Nuclear Engineering from that institution in May 1959. He completed the requirements for the Doctor of Philosophy degree at that institution in May 1961.

Professional Experience: The writer was employed as an Inspection Engineer by Standard Oil Company (Indiana) from July 1954 until August 1955. He entered the service in August 1955 as a Second Lieutenant in the U.S. Army Corps of Engineers and served as Assistant Operations Officer and Personnel Officer in an Engineer Battalion until August 1957. He was employed by Boeing Airplane Company as a Junior Engineer during the summer of 1958. He served as a graduate teaching assistant and research assistant in Mechanical Engineering from September 1957 until May 1960. He taught courses or assisted in courses in thermodynamics, heat transfer, steam and gas laboratory, and drafting.

Professional Organizations: The writer is enrolled as an Engineer-in-Training (Oklahoma), and is a member of Pi Tau Sigma and Sigma Tau.